

**REMOTE CONTROL OF CAR T CELL THERAPIES  
BY THERMAL TARGETING**

A Dissertation  
Presented to  
The Academic Faculty

by

Ian Contado Miller

In Partial Fulfillment  
of the Requirements for the Degree  
Doctorate in Biomedical Engineering in the  
Wallace H. Coulter Department of Biomedical Engineering

Georgia Institute of Technology and Emory University  
August 2020

**COPYRIGHT © 2020 BY IAN CONTADO MILLER**

# REMOTE CONTROL OF CAR T CELL THERAPIES BY THERMAL TARGETING

Approved by:

Dr. Gabriel. A. Kwong, Advisor  
Department of Biomedical Engineering  
*Georgia Institute of Technology*

Dr. Koichi Araki  
Division of Infectious Diseases  
*Cincinnati Children's Hospital*

Dr. Erik C. Dreaden  
Department of Biomedical Engineering  
*Georgia Institute of Technology*

Dr. Krishnendu Roy  
Department of Biomedical Engineering  
*Georgia Institute of Technology*

Dr. Susan N. Thomas  
School of Mechanical Engineering  
*Georgia Institute of Technology*

Date Approved: June 23, 2020

# TABLE OF CONTENTS

<b>LIST OF TABLES</b>	<b>v</b>
<b>LIST OF FIGURES</b>	<b>vi</b>
<b>LIST OF SYMBOLS AND ABBREVIATIONS</b>	<b>ix</b>
<b>SUMMARY</b>	<b>xi</b>
<b>Introduction</b>	<b>1</b>
<b>1.1 T cell therapies and their current challenges</b>	<b>3</b>
1.1.1 Tumor recognition and discrimination from healthy tissues	6
1.1.2 Challenges with solid tumor microenvironments	7
1.1.3 Exhaustion and persistence of transferred T cells	10
<b>1.2 Engineering approaches to improve anti-tumor T cell activity</b>	<b>11</b>
1.2.1 Biomaterials approaches	11
1.2.2 Genetic approaches	12
1.2.3 Remote control platforms	13
<b>1.3 Thesis overview</b>	<b>17</b>
<b>Remote control of mammalian cells with heat-triggered gene switches and photothermal pulse trains</b>	<b>19</b>
<b>1.4 Abstract</b>	<b>19</b>
<b>1.5 Introduction: Heat Shock Response</b>	<b>20</b>
<b>1.6 Results</b>	<b>22</b>
1.6.1 Engineering a thermal gene switch	22
1.6.2 Triggering cellular activity with pulses of heat	25
1.6.3 Photothermal targeting of Jurkat T cells	27
1.6.4 Thermal pulse trains for long-term control of Jurkat T cells in vivo	29
<b>1.7 Discussion</b>	<b>33</b>
<b>1.8 Methods</b>	<b>35</b>
<b>Remote control of CAR T cell therapies by thermal targeting</b>	<b>38</b>
<b>1.9 Abstract</b>	<b>38</b>
<b>1.10 Introduction</b>	<b>39</b>
<b>1.11 Results</b>	<b>41</b>
1.11.1 Engineering thermal-specific gene switches	41
1.11.2 Primary T cells maintain key functions after thermal treatments	48
1.11.3 Thermal control of CAR T cell functions	52
1.11.4 Photothermal targeting of CAR T cells enhances anti-tumor therapy	59
<b>1.12 Discussion</b>	<b>64</b>
<b>1.13 Methods</b>	<b>65</b>
<b>Conclusions</b>	<b>72</b>
<b>1.14 Summary of advancements</b>	<b>72</b>

<b>1.15</b>	<b>Future directions of the technology</b>	<b>74</b>
1.15.1	Fever-induced switch activity	74
1.15.2	Heat-triggered chemotaxis to a targeted site	75
1.15.3	Expanding T cell specificity in vivo	75
<b>APPENDIX A.</b>	<b>Supporting information</b>	<b>77</b>
<b>A.1</b>	<b>Bolus injections of IL-2 augment adoptive transfer in immunocompetent mice</b>	<b>77</b>
<b>A.2</b>	<b>Endogenous switch activity in primary murine T cells</b>	<b>79</b>
<b>A.3</b>	<b>Thermal tolerance of primary murine T cells</b>	<b>82</b>
<b>A.4</b>	<b>Broader targeting using TS-BiTE T cells</b>	<b>84</b>
<b>A.5</b>	<b>Adoptive transfer of constitutive CAR T cells in a leukemia model</b>	<b>88</b>
<b>A.6</b>	<b>Synthetic thermal gene switch sequences</b>	<b>90</b>
<b>A.7</b>	<b>Core promoter sequences</b>	<b>91</b>
<b>A.8</b>	<b>Immunostimulatory gene sequences</b>	<b>92</b>
<b>References</b>		<b>96</b>

## LIST OF TABLES

Table 1	Table 1: Active clinical trials with engineered T cells	4
Table 2	Synthetic thermal gene switch sequences.	90
Table 3	Core promoter sequences.	91
Table 4	Immunostimulatory gene sequences.	92

## LIST OF FIGURES

Figure 1	The Cancer-Immunity Cycle	2
Figure 2	Adoptive transfer of genetically engineered T cells.	3
Figure 3	TCR and CAR architecture	6
Figure 4	Local control of engineered T cell activity	14
Figure 5	Thermal medicine enables targeted heating of tumors	16
Figure 6	Remote control of engineered T cell therapies with pulses of heat	17
Figure 7	Heat-triggered gene switches in Jurkat T cells.	23
Figure 8	Heat actuation of thermal gene switches in Jurkat T cells	24
Figure 9	Thermal pulse trains augment switch activity and enhance Jurkat thermal tolerance	26
Figure 10	Mild hyperthermia is well-tolerated by Jurkat T cells	27
Figure 11	Remote control of engineered Jurkats	28
Figure 12	Spatially selective activation of thermal switches	29
Figure 13	Photothermal control of mammalian cells in vivo	30
Figure 14	In vivo pulsatile heating enables long-term control of mammalian cell activity	32
Figure 15	Schematic of Synthetic thermal gene switches	41
Figure 16	qPCR of screen of HSPs in primary murine T cells	42
Figure 17	Synthetic thermal gene switches respond to mild hyperthermia	43
Figure 18	Synthetic thermal switches do not respond to orthogonal cellular stresses	44
Figure 19	Core promoters tune the activity of synthetic thermal gene switches in primary T cells	46
Figure 20	Prolonged heat treatments do not trigger thermal switches at lower temperatures	47

Figure 21	Pulsed heating regimens increase thermal switch activity in primary T cells	49
Figure 22	Continuous heat treatments are well-tolerated by primary human T cells	50
Figure 23	T cells maintain critical functions after thermal treatments	51
Figure 24	Schematic of a heat-inducible TS-CAR and constitutive EF1 $\alpha$ CAR construct	52
Figure 25	Thermal control of CAR T cell cytotoxicity	53
Figure 26	Thermal control of T cell proliferation	54
Figure 27	Targeting NKG2DL+ cells with heat-triggered BiTEs	55
Figure 28	Detection of BiTEs and targeted NKG2DLs	56
Figure 29	TS-BiTE T cells primarily activate via paracrine pathways	57
Figure 30	Heat-triggered BiTEs control cytokine release and cytotoxicity	58
Figure 31	Photothermal control of engineered T cell activity	59
Figure 32	CAR antigen expression on cell lines	60
Figure 33	Remote control of intratumoral T cell activity	61
Figure 34	Repeated photothermal heating and TIL quantification	62
Figure 35	Photothermal targeting of CAR T cells improves anti-tumor responses	63
Figure 36	IL-2 augments adoptive transfer of Pmel T cells	77
Figure 37	Thermal switch activity in primary murine T cells	80
Figure 38	Heterogeneous switch activity in primary murine T cells	81
Figure 39	Thermal tolerance of primary murine T cells	82
Figure 40	NKG2DL expression on breast cancer lines and in vitro differentiated MDSCs	84
Figure 41	NKG2DL BiTE-mediated killing of MDSCs	85
Figure 42	NKG2DL BiTE-mediated killing of K562s	86



## LIST OF SYMBOLS AND ABBREVIATIONS

ACT	Adoptive Cell Transfer
APC	Antigen Presenting Cell
AuNR	Gold Nanorod
BiTE	Bispecific T cell Engager
CAR	Chimeric Antigen Receptor
CD19	Cluster of Differentiation 19
CRS	Cytokine Release Syndrome
CTV	CellTrace Violet
DC	Dendritic Cell
EF1 $\alpha$	Elongation Factor 1 $\alpha$
Fluc	Firefly Luciferase
FUS	Focused Ultrasound
GBM	Glioblastoma
GFP	Green Fluorescent Protein
Gluc	Gaussia Luciferase
HIPEC	Hyperthermic Intraperitoneal Chemotherapy
HSE	Heat Shock Element
HSF	Heat Shock Factor
HSP	Heat Shock Protein
IL	Interleukin
LITT	Laser Interstitial Thermal Therapy
MDSC	Myeloid Derived Suppressor Cell

NIR	Near Infrared
NKG2D	Natural-Killer Group 2, member D
ORF	Open Reading Frame
PBMCs	Peripheral Blood Mononuclear Cells
PD-1	Programmed Death-1
pMHC	peptide Major Histocompatibility Complex
scFv	single chain variable Fragment
TAA	Tumor-associated antigen
TAM	Tumor Associated Macrophage
TCR	T Cell Receptor
TDLN	Tumor Draining Lymph Node
TGF- $\beta$	Transforming Growth Factor $\beta$
TME	Tumor microenvironment
T <sub>reg</sub>	Regulatory T cell
T <sub>ex</sub>	Exhausted T cell
UTD	Untransduced
$\lambda$	Wavelength

## SUMMARY

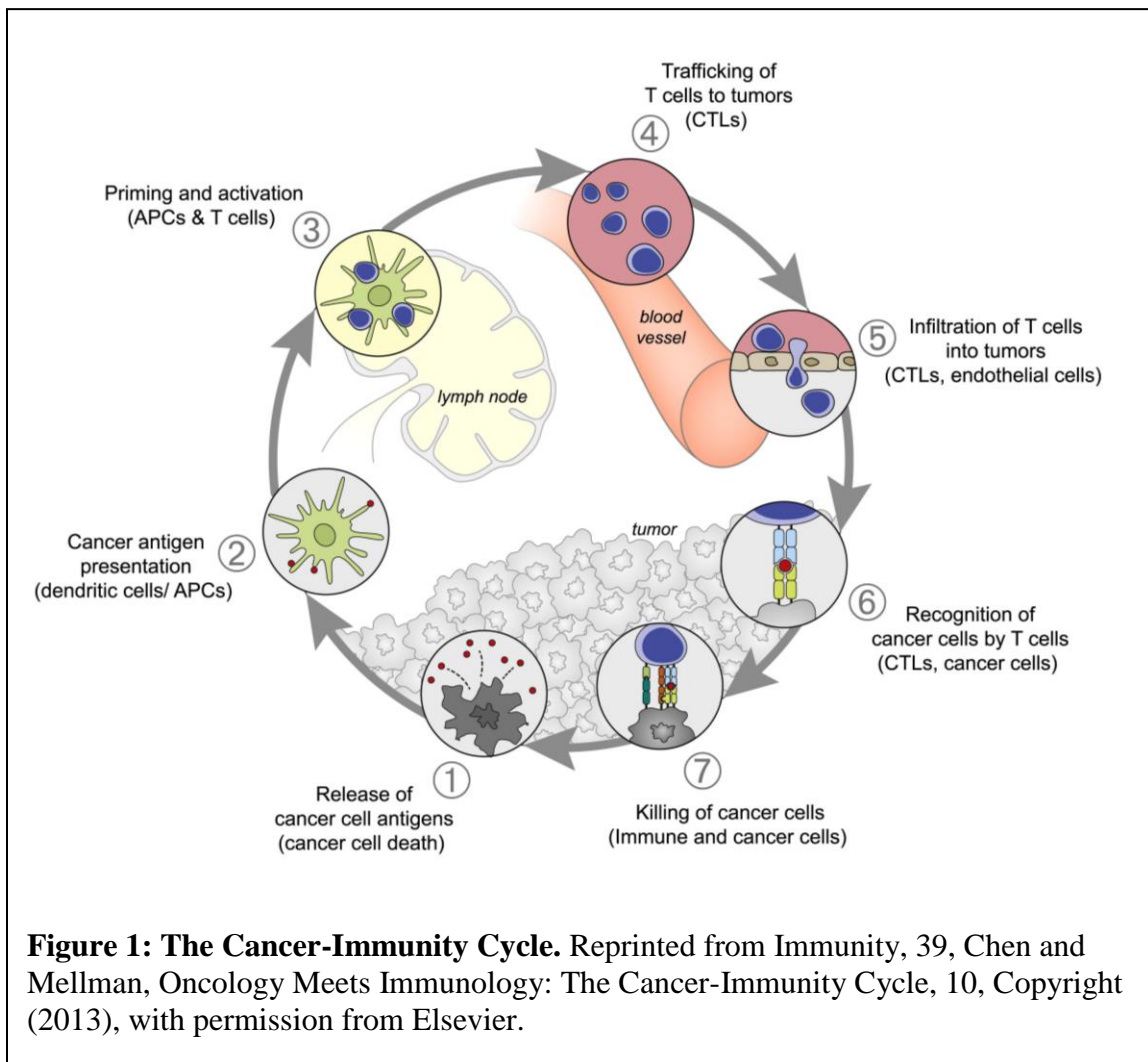
In 2017, the FDA approved two T cell therapies – Kymriah and Yescarta – for multiple relapsed or refractory hematological malignancies. In addition to providing new treatment options for patients with few viable alternatives, these approvals served as a watershed moment in the development of a new class of cellular therapies based on T cells. As the use of these ‘living drugs’ grows, scientists, engineers, and clinicians continue to improve their therapeutic and safety profiles by developing new mechanisms to control immune cell activity in the body. This thesis presents a remote control platform that enables localized control of engineered T cell activity via targeted thermal treatments. The following chapters describe the development of this platform as well as its first applications in mouse models of cancer and illustrate its potential to improve anti-tumor responses and advance the larger field of cellular immunotherapies. The introduction provides an overview of the history of the field of T cell therapies, identifies current challenges facing these treatments, and summarizes ongoing efforts in this area. In the future, thermal control of engineered T cells could provide finer control of their *in vivo* activity and improve the safety and efficacy of future cellular therapies.

## INTRODUCTION

For the majority of the 20<sup>th</sup> century, oncology was largely dependent on physical and chemical interventions intended to preferentially excise, irradiate, or poison malignant cells in the body<sup>1</sup>. These methods can eradicate cancer cells although clinicians constantly balance their therapeutic benefits with off-target effects on normal tissues. These off-target effects are evident in the large surgical margins taken during tumor resection or the rapid hair loss observed during chemotherapy; yet milder treatments increase the risk of cancer relapse as small numbers of surviving cells can cause treatment failure. Thus, the need to preserve healthy tissue while targeting pathogenic cells at a cellular level has emerged as a fundamental goal of modern oncology. Because the immune system constantly performs these exact tasks when protecting the body from foreign pathogens, many strategies have emerged that seek to harness its precision and potency to improve cancer treatment<sup>2</sup>. Thus, cancer immunotherapy is joining conventional therapies as a new staple in the clinical toolkit as it offers new ways to treat disease.

The extent to which the immune system can be directed towards cancer cells is critically dependent on the efficient progression of the cancer immunity cycle (Figure 1)<sup>3</sup>. Central to this process is the generation of T cell responses through the presentation of neoantigens by antigen presenting cells (APCs), efficient trafficking and infiltration of effector cells into the TME, and release of cytotoxic granules to kill malignant cells. Although this process does not function optimally in cancer patients, several classes of biologic drugs are designed to augment specific steps in this cycle. These include checkpoint blockade antibodies to overcome immunosuppression in the TME<sup>4</sup>, bispecific

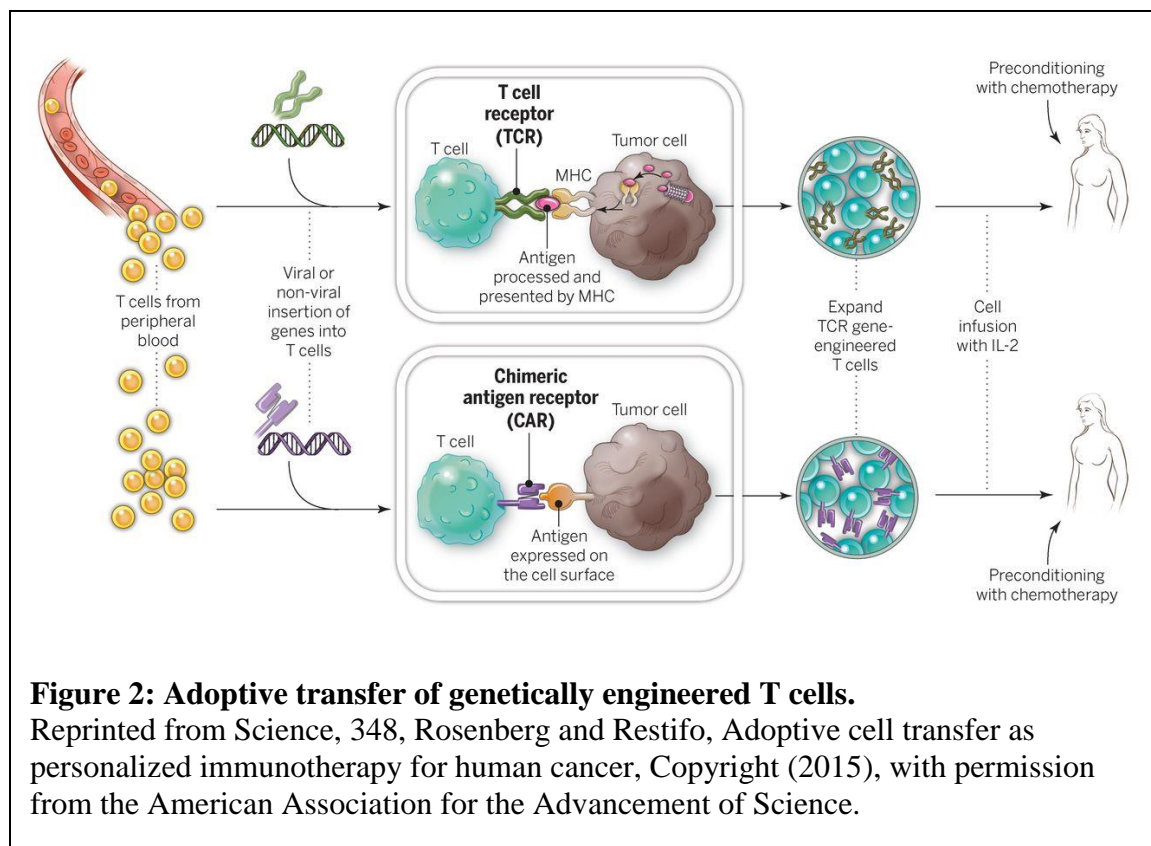
T cell engagers (BiTEs) to enable recognition of tumor epitopes<sup>5</sup> or cytokines to expand and stimulate T cells<sup>6</sup>. Although these have advanced disease treatment, such biologic drugs have pharmacokinetic and pharmacodynamics properties that can lead to harmful off-target effects in healthy tissues and limit delivery to tumors<sup>7-9</sup>. As a deeper mechanistic understanding of T cell biology has developed, the possibility of using T cells themselves as a therapeutic agent has gained momentum. This strategy presents the prospect of programming therapeutic immune cells to autonomously sense and respond to complex arrays of signals allowing them to adapt their migration, proliferation, and cell killing as



needed<sup>10</sup>. This enormous potential to increase treatment efficacy and safety has motivated the development of T cell therapies.

### 1.1 T cell therapies and their current challenges

Starting in the 1980s, studies at the NIH demonstrated that T cells themselves could be used as a therapeutic agent. In these seminal studies, autologous infusions of tumor-specific T cells harvested from patient tumors and expanded *ex vivo* mediated durable anti-



tumor responses in melanoma patients<sup>11, 12</sup>. These discoveries coincided with significant improvements in genetic engineering technologies<sup>13</sup> and spurred the development of a host of strategies to improve anti-tumor responses. For example, identification of tumor-specific TCR sequences in tumor-infiltrating lymphocyte (TIL) populations enabled the cloning of TCR genes into T cells prior to infusion as a cellular therapy<sup>14-16</sup> (Figure 2). In this manner,

populations of T cells could be genetically engineered to recognize tumor associated antigens (TAAs) and effector populations expanded without endogenous recognition of tumor cells. To enhance TCR recognition of cancer cells and improve anti-tumor responses, directed evolution of TCR sequences using phage display platforms enabled affinity enhancement of tumor-reactive TCR sequences<sup>17-19</sup>. Equipped with transgenic TCRs, engineered T cells mediated sustained clinical responses in multiple forms of leukemia<sup>18, 20, 21</sup>, and this success motivated hundreds of ongoing clinical trials targeting dozens of TAAs with adoptively transferred cells (Table 1).

While transgenic TCRs enable targeting of tumor antigens, this process is contingent on the epitope's presentation in the context of the patient's HLA haplotype<sup>22</sup>.

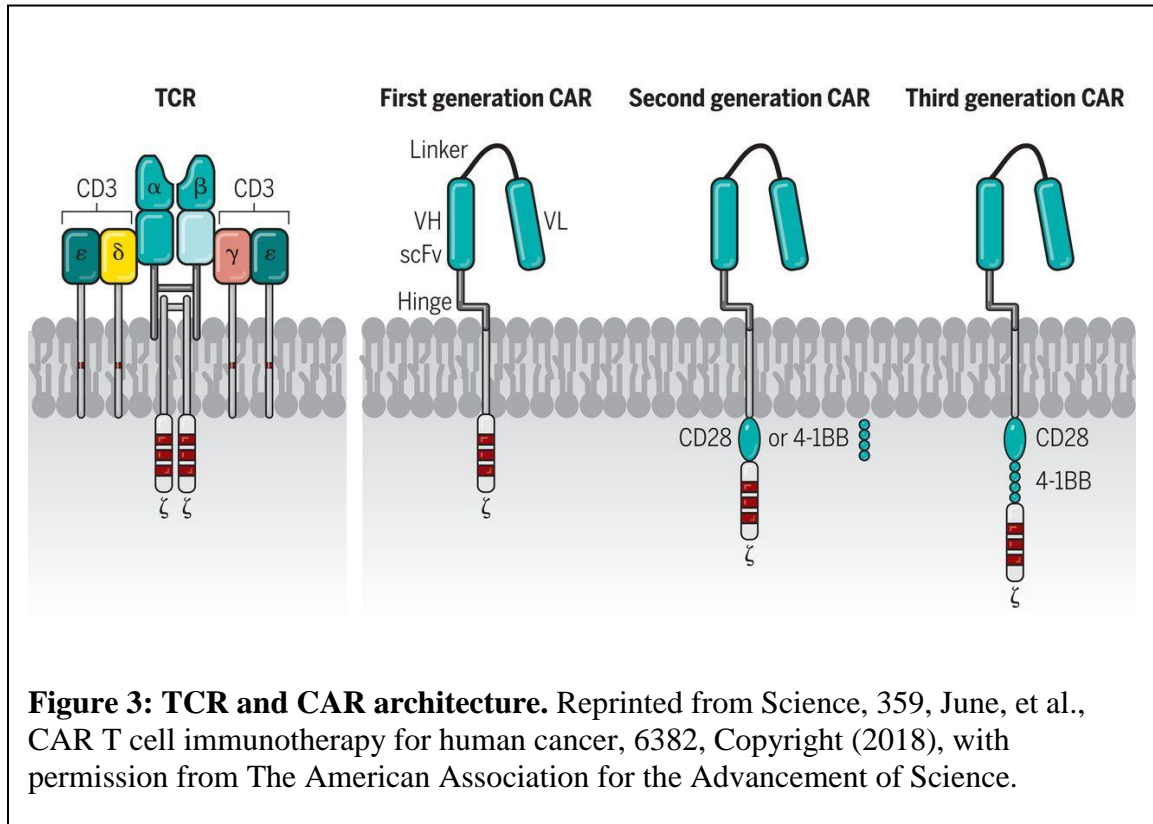
**Table 1: Active clinical trials with engineered T cells.** Data taken from clinicaltrials.gov on May 23, 2020.

Target antigen	Targeting molecule	Cancer	Sponsor	NCT number
MCPyV	TCR	Merkel Cell	Fred Hutchinson Cancer Research Center	NCT03747484
MAGE-A3	TCR	Various solid tumors	National Cancer Institute	NCT02111850
NY-ESO-1	TCR	Multiple Myeloma	GlaxoSmithKline	NCT03168438
BCMA	CAR (scFv)	Multiple Myeloma	Celgene	NCT03651128
CD19 and CD22	CAR (scFv)	Various leukemias	M.D. Anderson Cancer Center	NCT04029038
CD33	CAR (scFv)	Acute Myelogenous Leukemia	Center for International Blood and Marrow Transplant Research	NCT03971799
Her2	CAR (scFv)	CNS tumors	Seattle Children's Hospital	NCT03500991
IL13R $\alpha$ 2	CAR (scFv)	Glioblastoma	City of Hope	NCT04003649
CD70	CAR (CD27)	Various solid tumors	National Cancer Institute	NCT02830724

Because MHC genes are highly polymorphic in the general population, this requirement effectively precludes the use of a single TCR in all patients. Furthermore, loss of MHC expression is a common mechanism of immune escape in malignant cells that allows

evasion of TCR recognition<sup>23</sup>. Thus, targeting cells through MHC-independent axes has been pursued along multiple pathways. For example, T cells that recognize target cells via the monomorphic protein MR1 have recently been demonstrated to kill a wide range of cancerous cells without harming noncancerous cells<sup>24</sup>. This process is hypothesized to be specific for cancer-associated metabolites presented by the MR1 molecule and illustrates one of many non-MHC restricted targeting pathways. Other examples include stress-inducible NKG2D ligands which are widely expressed by cells in the TME and recognized by the NKG2D receptor<sup>25</sup>. Fusing the extracellular domain of this receptor to intracellular signaling domains of TCRs (e.g.  $\zeta$ -chain) produces Chimeric Antigen Receptors (CARs) capable of recognizing TAA's and triggering effector functions in the engineered cell. Using such CARs, NKG2DLs have been targeted by engineered cells without relying on MHC presentation by the target cells<sup>26,27</sup>. Furthermore, a wide variety of targeting moieties have been incorporated into CAR designs including hybridizing DNA<sup>28</sup> or chlorotoxin derived from scorpion venom<sup>29</sup> allowing broad recognition of malignant cells without MHC restriction. In addition to tumor recognition domains and  $\zeta$ -chains, second and third generation CARs incorporate costimulatory molecules such as the endodomains of CD28 or 4-1BB to facilitate downstream signaling and effector functions in engineered T cells (Figure 3)<sup>30</sup>. CAR T cells containing each of these domains have demonstrated sustained clinical efficacy with CD28 CARs generally exhibiting higher peak expansion levels and cytokine secretion and 4-1BB CARs demonstrating improved persistence and resistance to exhaustion<sup>31</sup>. The most common of these architectures are CARs comprised of scFv domains targeting surface antigens expressed by cancer cells (Figure 3). Indeed, the two FDA-approved T cell therapies are scFv-based CAR T cells specific for CD19 – a lineage

marker widely expressed by malignant B cells in several forms of leukemia. The majority of clinical stage cellular therapy candidates target cancer cells with CARs containing scFv domains and hundreds of clinical trials targeting dozens of surface antigens are ongoing (Table 1). Despite these advances, the field faces several challenges that must be overcome to enable wider use of this transformative class of therapies.



### 1.1.1 Tumor recognition and discrimination from healthy tissues

One of the major challenges facing immunotherapies is identifying tumor-associated antigen targets that allow discrimination from healthy tissues. For example, CAR T cells targeting CD19 and BCMA are the most clinically advanced cellular therapies yet they also deplete non-malignant B cells or plasma cells that express the target antigen in addition to cancer cells<sup>32</sup>. In these cases, the loss of normal cells can be tolerated and mitigated by

intravenous infusions of immunoglobulin to replace the antibodies typically produced by the healthy cells<sup>33,34</sup>. However, the killing of healthy cells which express the target antigen has also led to potentially fatal off-tumor, on-target toxicity following administration of engineered T cells<sup>35,36</sup>. These effects can occur even when healthy cells express low levels of the target antigen (e.g. Her2 by lung epithelial cells<sup>37</sup>) or epitopes that are stereochemically similar to the tumor target (e.g. MAGE-A12 or titin in the brain or heart<sup>38-40</sup>). Collectively, these examples illustrate the challenges presented by CAR and TCR target expression on healthy cells and motivate efforts to carefully tune receptor affinities to enable killing of tumor cells as well as tolerance of normal tissues<sup>41,42</sup>.

When TAAs for engineered T cell therapies can be identified, efforts to target these epitopes have encountered challenges as tumors evolve to cope with this new selective pressure. For example, the constitutively active EGFRvIII variant is not expressed on healthy cells<sup>43</sup>, but infusions of EGFRvIII-specific CAR T cells in glioblastoma (GBM) patients led to outgrowth of EGFRvIII-negative tumor cells<sup>44</sup>. It is now understood that antigen escape occurs through several mechanisms including heterogeneous expression of the target antigen at treatment<sup>44,45</sup>, alternative splicing of the target molecule to prevent surface expression or recognition<sup>46</sup>, and lineage switching by tumor cells leading to complete loss of target expression<sup>47</sup>. Thus, simultaneously targeting multiple epitopes using bispecific CARs (also called OR-gated CARs) is under development to broaden T cell specificity and prevent outgrowth of antigen-negative cells<sup>48,49</sup>.

### *1.1.2 Challenges with solid tumor microenvironments*

While engineered T cells consistently demonstrate durable responses in multiple forms of leukemia, these success rates have not reliably translated into solid tumors which develop many mechanisms to impair effective cancer immunity<sup>50</sup>. For example, solid tumors require additional trafficking steps prior to T cell-mediated killing of cancer cells and intratumoral cells inhibit many steps of this process including T cell homing to the tumor site and rolling or adhesion on tumor vasculature<sup>3</sup>. This disruption is accomplished, in part, by the reduced expression or aberrant post-translational modification of chemokines<sup>51, 52</sup> and inhibition of adhesion molecules (e.g. ICAM-1 and VCAM-1) on the tumor vascular endothelium<sup>53, 54</sup>. To mitigate these effects, regional delivery of engineered T cells has improved trafficking and therapeutic outcome compared to intravenous infusions, especially in CNS tumors<sup>55-58</sup>. Furthermore, intratumoral injections of therapeutic agents such as oncolytic viruses induce selective destruction of tumor cells and improve recruitment of neoantigen-specific T cells to the site. The ability to activate the immune system appears to be critical to the success of these therapies<sup>59</sup> and efforts to incorporate GM-CSF into the platform resulted in an FDA approval for advanced melanoma.

When T cells successfully infiltrate tumors, they encounter microenvironments containing high levels of suppressive cytokines (e.g. TGF- $\beta$  and IL-10)<sup>60, 61</sup> or depleted of critical metabolic substrates by upregulation of enzymes such as indoleamine 2,3-dioxygenase (IDO) and arginase<sup>62</sup>. These immunosuppressive microenvironments are generated by the cancer cells themselves as well as non-malignant cells such as tumor associated macrophages (TAMs), regulatory T cells (T<sub>regs</sub>), and myeloid derived suppressor cells (MDSCs) which are recruited to the site<sup>2, 63</sup>. These cells also express surface molecules which suppress or kill T cells such as PD-L1, PD-L2, FasL, and TRAIL and aid

immune evasion<sup>64-67</sup>. Thus, in addition to cancer cells themselves, non-malignant cells in the TME also contribute to disease progression making them important targets for immunotherapies. However, these cells also mediate normal peripheral tolerance and targeting them without deleterious off-tumor effects remains difficult<sup>26, 68-70</sup>. These soluble and cellular factors are also present in the tumor draining lymph node (TDLN) where they inhibit anti-tumor immunity by preventing effective presentation of TAAs to cytotoxic CD8 T cells as well as polarization of CD4 cells to a T helper 1 (T<sub>h</sub>1) phenotype<sup>71, 72</sup>.

To counteract immunosuppression in the TME and TDLNs, several classes of biological drugs have emerged that prevent immunosuppressive signaling or provide immunostimulatory cues. For example, checkpoint blockade using monoclonal antibodies specific for proteins in the CTLA-4 or PD-1 axes have transformed clinical practice for many types of cancer including Merkel cell carcinoma, melanoma, and hepatocellular carcinoma<sup>73</sup>. Additionally, infusions of recombinant cytokines such as IL-2 and IL-15 can support the proliferation of T cells and stimulate the generation of cytotoxic T cell populations<sup>74</sup>. In fact, IL-2 immunotherapies were among the first to demonstrate clinical efficacy<sup>75, 76</sup> and different forms of IL-15 are being tested in trials seeking to proliferate and maintain memory CD8 T cells<sup>9, 77, 78</sup>. These checkpoint blockade and cytokine approaches are most effective in cancers characterized by high mutational burdens such as melanoma or colorectal cancer<sup>79, 80</sup> suggesting that existing T cell specificity for neoantigens is critical for treatment success. When endogenous tumor recognition does not occur efficiently, biologics such as Bispecific T cell Engagers (BiTEs) can redirect T cell specificity to tumor-associated antigens by binding the molecular target as well as CD3 on the surface of T cells<sup>5, 81</sup>. However, the systemic administration of all these biologic drugs

can lead to significant off-tumor effects that narrow their therapeutic window<sup>7-9</sup>. Thus, localizing the activity of adjuvant drugs and cytotoxicity of T cells to the TME represents an important goal for future immunotherapies.

### *1.1.3 Exhaustion and persistence of transferred T cells*

In addition to suppressing T cells with soluble or ligand-bound signals, prolonged antigen stimulation can give rise to populations of exhausted T cells ( $T_{\text{ex}}$ )<sup>82</sup>. Originally described in chronic viral infections,  $T_{\text{ex}}$  also present in many forms of cancer and are characterized by high expression of inhibitory receptors (e.g. PD-1, TIM-3, LAG-3), reduced secretion of immunostimulatory cytokines, attenuated proliferation, and diminished ability to kill target cells<sup>83-86</sup>. Although biologic interventions such as checkpoint blockade can transiently reinvigorate  $T_{\text{ex}}$ , the epigenetic profiles of  $T_{\text{ex}}$  play important roles in maintaining this exhausted phenotype and are largely unaffected by treatments such as PD-1 blockade<sup>87, 88</sup>. To prevent differentiation of exhausted T cell populations and improve therapeutic outcome, many efforts have sought to leverage or generate stable populations of effector T cells ( $T_{\text{eff}}$ ) or memory T cells ( $T_{\text{mem}}$ ) for adoptively transferred cells<sup>89</sup>. These approaches include preselection of memory T cells for genetic manipulation<sup>90, 91</sup>, *in vitro* differentiation of transduced T cells into  $T_{\text{mem}}$  prior to adoptive transfer<sup>92, 93</sup>, and the transient disruption of CAR signalling to prevent exhaustion<sup>94, 95</sup>. Still, more studies are required to identify the optimal populations for durable anti-tumor responses as well as efficient methods for generating these cells at a clinical scale. Given the breadth of these challenges, numerous strategies to stimulate T cells and augment their anti-tumor activity have emerged.

## 1.2 Engineering approaches to improve anti-tumor T cell activity

### 1.2.1 Biomaterials approaches

Due to difficulties in establishing endogenous niches of functional immune cells, biomaterials approaches seek to establish immunostimulatory environments or provide targeted delivery of adjuvant drugs that support anti-tumor immune activity. For example, cancer vaccines focus on priming tumor-specific responses through the administration of mutated peptides or neoepitope-encoding RNA or DNA although they have historically demonstrated low objective response rates<sup>96, 97</sup>. Because the kinetics of neoepitope presentation and colocalization of immunostimulatory adjuvants are critical to eliciting robust immune responses, biomaterial architectures have emerged which allow greater control of these factors<sup>98, 99</sup>. For example, scaffold-based cancer vaccines containing components such as neoantigens, GM-CSF to recruit endogenous DCs, siRNA to inhibit expression of immunosuppressive cytokines, and adjuvants such as CpG are constructed from numerous biomaterials to ensure that DCs take up antigen in a sustained, pro-inflammatory environment<sup>100-103</sup>. These synthetic microenvironments contrast with immunosuppressive TDLNs which generate tolerance to TAAs if presentation by APCs occurs without the proper costimulatory signals<sup>71</sup>.

In addition to recruiting APCs, biomaterials scaffolds decorated with immunostimulatory agents also encapsulate APCs or effector T cells to provide ideal delivery vehicles for adoptive transfer protocols<sup>104, 105</sup>. In this manner, transferred cells are exposed to high concentrations of factors such as IL-15 superagonists<sup>103</sup>, and antibodies for CD3 and CD28<sup>106, 107</sup>. Such scaffolds are injected near tumors or implanted at surgical

sites to improve postoperative responses following tumor resection. Additional biomaterials approaches also load immunostimulatory agents directly on effector T cells themselves to provide T cell-localized sources of adjuvants. For example, nanoparticle ‘backpacks’ tethered to the surface of tumor-specific T cells allow infiltrating T cells to carry a one-time dose of drug into tumor sites<sup>108</sup>. These nanoparticle backpacks are engineered so they release their cargo within tumors following TCR-recognition of tumor antigen ensuring targeted delivery of these agents<sup>109</sup>. Collectively, these examples illustrate a wide range of biomaterials-based approaches to improve anti-tumor T cell responses.

### 1.2.2 Genetic approaches

In addition to redirecting antigen specificity by introducing CARs or transgenic TCRs, genetic editing platforms can also disrupt endogenous genes to improve the *in vivo* activity of engineered cells. For example, the nuclease CRISPR-Cas9 (clustered regularly interspaced short palindromic repeats associated with Cas9 endonuclease) allows RNA-directed changes to the genome with single-base pair precision<sup>110</sup>. Thus, addition of the tumor-targeting receptor can be coupled with targeted deletions of specific genes in engineered cells. Using this strategy, disruption of genes encoding immunosuppressive ligands such as PD-1 improve anti-tumor responses and have motivated ongoing clinical trials using transferred cells containing multiple genetic edits<sup>111-114</sup>. Furthermore, the  $\alpha$  or  $\beta$  chains of the endogenous TCR can pair with those of the transgenic, tumor-targeting TCR resulting in self-reactive T cells<sup>115-117</sup>. Accordingly, the genes encoding the endogenous TCR (*TRAC* and *TRBC*) are also attractive targets for deletion in engineered T cells<sup>114</sup>. Many studies have identified additional gene targets whose disruption in transferred T cells enhance therapeutic responses such as Tet2<sup>118</sup>, Ppp2r2d<sup>119</sup>, or mTOR<sup>120</sup>.

These examples all demonstrate that inhibition of many cellular processes could improve future T cell therapies.

In addition to deleting endogenous genes, genetic editing also allows T cells to produce biologics to overcome immunosuppression or target antigens after tumor infiltration. For example, ‘armored CARs’ constitutively express tumor-specific CAR as well as biologics such as IL-12<sup>121</sup>,  $\alpha$ PD-1 scFvs<sup>122</sup>, and BiTEs<sup>123</sup> to improve anti-tumor activity. To limit gene expression outside of tumors, T cells engineered with sense-and-respond biocircuits exhibit conditional activation in the presence of specific input signals. Input signals include T cell recognition of a tumor-associated antigen using NFAT-inducible cassettes<sup>124-126</sup> or the presence of soluble molecules upregulated in the TME such as the immunosuppressive cytokine TGF- $\beta$ <sup>127</sup>. To further increase specificity, T cells have been engineered to target unique combinations of epitopes expressed in the TME to allow discrimination from healthy cells expressing a single epitope<sup>128</sup>. Such approaches require the presence of both target antigens for T cell activation to occur and have demonstrated efficacy in multiple models of focal tumors<sup>129, 130</sup>. Other examples based on Boolean logic include the development of NOT-gated circuits which spare cells from cytotoxic activity following detection of a healthy epitope<sup>131</sup>. Collectively, these strategies allow T cells to exhibit emergent therapeutic responses after encountering cues naturally found in their environment.

### *1.2.3 Remote control platforms*

In addition to molecular cues intrinsic to the TME, external cues such as small molecules or light have been used to control engineered T cell activity<sup>132</sup> (Figure 4). These

strategies are especially useful for regulating or tuning engineered T cell activity which is critical for limiting off-tumor toxicity as observed in Cytokine Release Syndrome (CRS) – a potentially fatal inflammatory response observed in patients receiving CAR T cell therapies<sup>133, 134</sup>. To control CRS, “suicide switches” allow rapid induction of apoptosis in transduced cells via drug-induced dimerization of caspase molecules allowing all CAR T cells to be eliminated by a single infusion of a small molecule trigger<sup>135</sup>. This safety mechanism illustrates one method of remote control of T cell activity (i.e. drug-induced suicide) and has been validated in several different CAR circuits<sup>136-138</sup>. Additionally, small-molecule control of CAR expression or signaling can link CAR activity to the presence of a drug allowing tighter control of cytotoxicity and the potential to ameliorate exhaustion from prolonged exposure to antigen<sup>95, 139</sup>. This strategy also has the added benefit of not killing the therapeutic T cells after administration of the drug trigger.

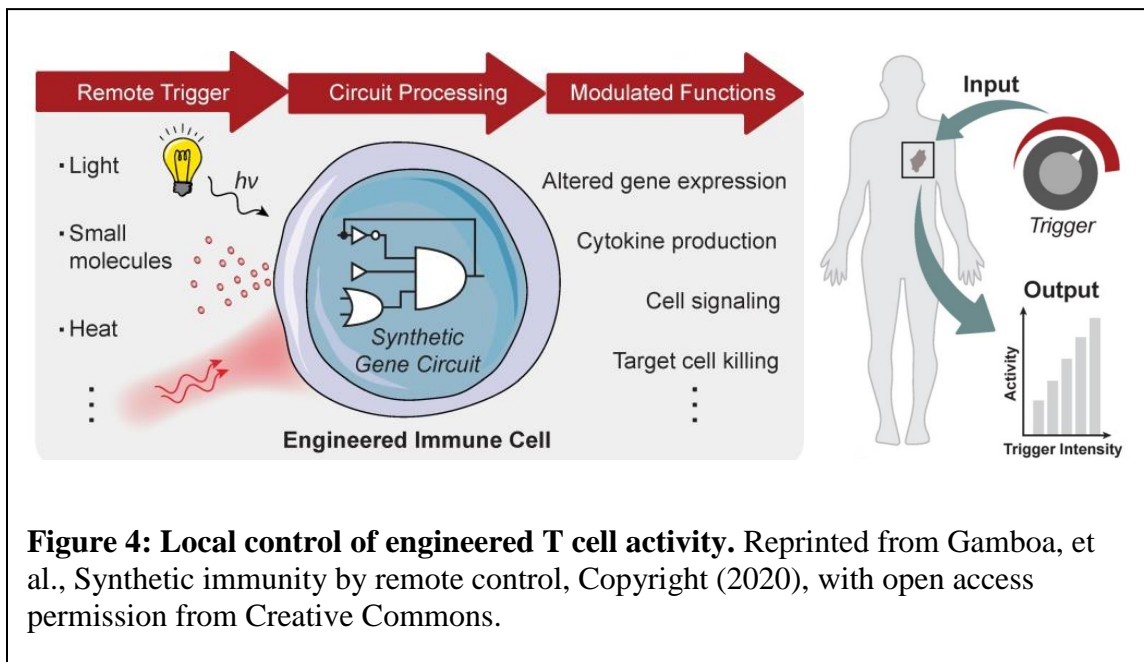
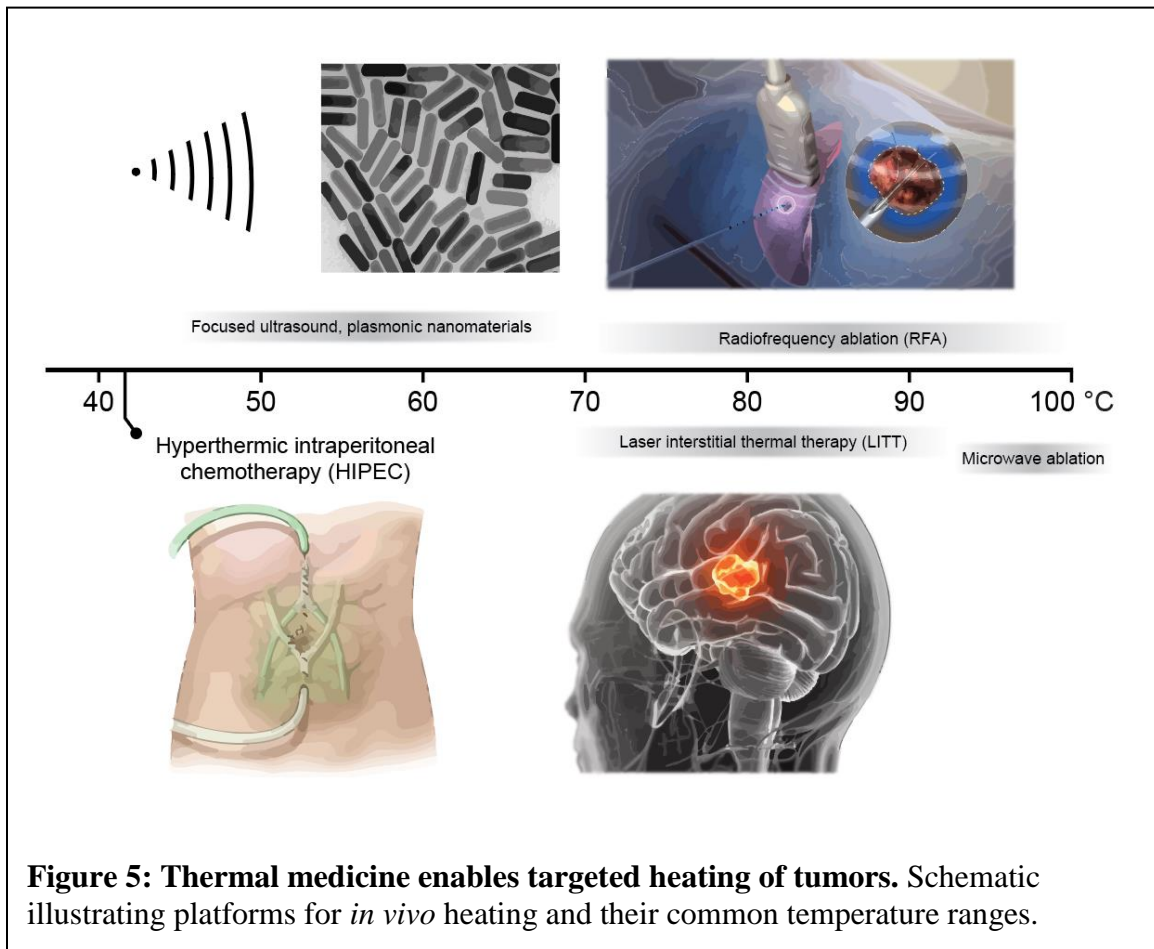


**Figure 4: Local control of engineered T cell activity.** Reprinted from Gamboa, et al., Synthetic immunity by remote control, Copyright (2020), with open access permission from Creative Commons.

Because small molecules are administered systemically and affect all engineered cells in the body, spatially targeted triggers such as light or heat have also been explored

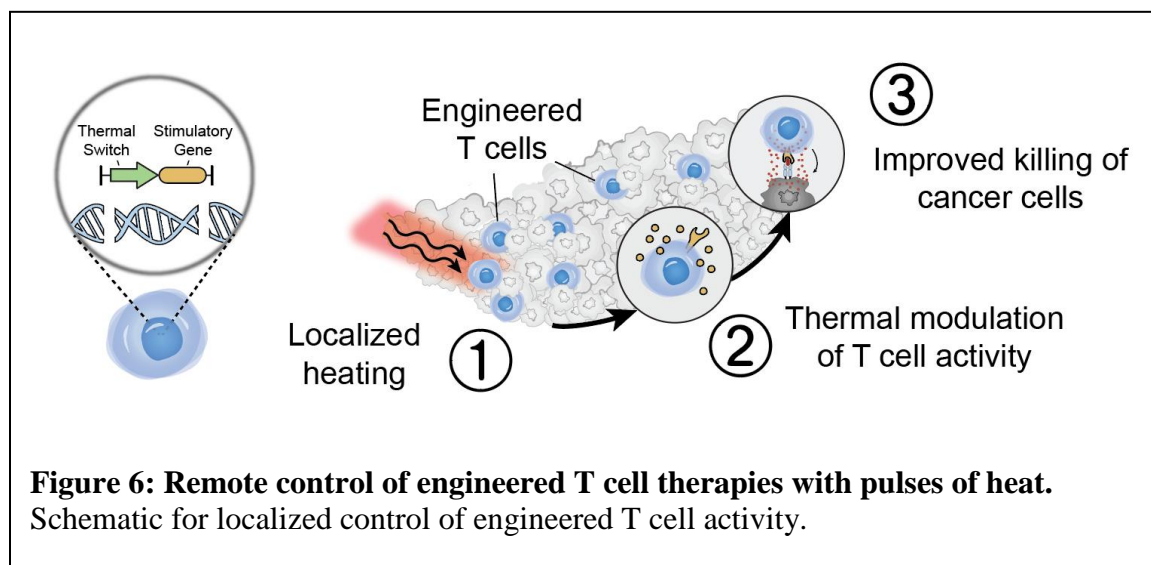
for localized control over engineered T cell activity (Figure 4). Spatial control over immune activity would allow confinement of potent immunostimulatory activity to the TME thereby minimizing concerns with off-tumor toxicity in healthy tissues. Examples of targeted optical systems include light-based control over T cell migration by re-engineering the chemokine receptor CXCR4 to include domains of the light-sensitive protein rhodopsin<sup>140</sup>. Using this photoactivatable chemokine receptor, T cell chemotaxis could be directed with targeted light both *in vitro* and *in vivo*<sup>141</sup>. Light can also control T cell gene expression by several mechanisms such as triggering dimerization of split recombinases<sup>142</sup> or via optically triggered calcium signaling which leads to expression of NFAT-responsive genes<sup>143, 144</sup>. While these systems enable precise spatial control, the limited penetration of activating light limits their use to superficial tissues<sup>145</sup>.

To enable localized control of immune cell activity in deep tissues, heat can also trigger engineered cellular activity. One advantage of this strategy is the existing suite of medical platforms engineered for precision heating in the body<sup>146</sup> (Figure 5). For example, Hyperthermic Intraperitoneal Chemotherapy (HIPEC) uses heated infusions of chemotherapy to sensitize cancer cells to small molecule agents and enhance their diffusion into tumors<sup>147</sup>. Furthermore, technologies such as high intensity focused ultrasound (HIFU)<sup>146, 148</sup>, intracranial laser heating<sup>149, 150</sup>, and microwave ablation<sup>151</sup> all use localized hyperthermia to directly target tumors within different temperature ranges (Figure 5). Several mechanisms can convert thermal signals into immunological activity by initiating gene expression following heat treatments<sup>132</sup>. These include temperature sensitive



transcriptional suppressors which lose the ability to inhibit transcription at defined temperatures<sup>152, 153</sup>, and RNA thermometers that are translated following heat-induced conformational changes which expose ribosome binding sites<sup>154</sup>. The evolutionarily conserved heat shock response also upregulates the transcription of protective chaperones, collectively called heat shock proteins (HSPs), at levels comparable to the strongest known viral promoters<sup>155, 156</sup>. Heat-inducible systems based on HSP promoters have incorporated the HSP70 promoter due to its strong inducibility<sup>157, 158</sup>. Such platforms used localized heating to trigger immunostimulatory cytokine expression following intratumoral injections of recombinant adenovirus vectors<sup>159, 160</sup>. Thus, thermal cues can also be leveraged for remote control of engineered T cell therapies.

### 1.3 Thesis overview



In this context, this thesis describes the development of a platform enabling thermal control of engineered T cell therapies as well as its first applications in mouse models of cancer (Figure 6). Chapter 2 describes efforts to construct thermal gene switches using truncated sections of an endogenous heat shock promoter. It also introduces a photothermal method

for targeted *in vivo* heating as well as pulsatile heating regimens to improve thermal tolerance and enhance switch activity in engineered cells. Chapter 3 describes the design of synthetic thermal gene switches which exhibit lower basal activity and enhanced specificity for thermal cues compared to genomic sequences. Using these synthetic thermal gene switches, we demonstrate control of potent immunostimulatory genes and T cell effector functions such as proliferation and cytotoxicity. Using models of adoptive cell transfer in murine models of cancer, we demonstrate that photothermal control of engineered T cells improves their anti-tumor activity and treatment outcome. Finally, the appendices catalog several unpublished studies that guided the experimental design of the previous chapters. These include experiments with primary murine cells which ultimately led to the selection of human T cells and xenograft models as the initial testbed for the thermal control platform. The thesis ends with exploratory studies that use *in vitro* differentiated MDSCs to recapitulate immunosuppressive niches in the TME and provide a roadmap for future applications of remote thermal control of T cell therapies.

# REMOTE CONTROL OF MAMMALIAN CELLS WITH HEAT-TRIGGERED GENE SWITCHES AND PHOTOTHERMAL PULSE TRAINS

Adapted from Miller, I.C., Castro, M.G., Maenza, J., Weis, J.P. & Kwong, G.A. Remote Control of Mammalian Cells with Heat-Triggered Gene Switches and Photothermal Pulse Trains. *Acs Synth Biol* 7, 1167-1173 (2018) with permission from the American Chemical Society.

## 1.4 Abstract

Engineered T cells are transforming broad fields in biomedicine, yet our ability to control cellular activity at specific anatomical sites remains limited. Here we engineer thermal gene switches to allow spatial and remote control of transcriptional activity using pulses of heat. These gene switches are constructed from the heat shock protein HSP70B' (HSPA6) promoter, show negligible basal transcriptional activity, and activate within an elevated temperature window of 40–45°C. Using engineered Jurkat T cells implanted in vivo, we use plasmonic photothermal heating to trigger gene expression at specific sites to levels greater than 200-fold. We show that delivery of heat as thermal pulse trains significantly increases cellular thermal tolerance compared to continuous heating curves with identical area-under-the-curve (AUC), enabling long-term control of gene expression in Jurkat T cells. This approach expands the toolkit of remotely controlled genetic devices for basic and translational applications in synthetic immunology.

## 1.5 Introduction: Heat Shock Response

Recent developments in mammalian synthetic biology are providing new approaches to control complex cellular activity, such as cell signaling, communication, and differentiation using orthogonal cues including small-molecules, proteins, or light<sup>161-163</sup>. These advances are leading to numerous applications for synthetic immunology; in particular, the design of engineered T cells with entirely new abilities<sup>164</sup> such as the capacity to migrate toward synthetic chemical cues<sup>165</sup>, deliver drugs to tumors<sup>166</sup>, employ logic-gates to sense antigens<sup>128</sup>, and target cancer with chimeric receptors<sup>167</sup>. Despite these advances, our ability to precisely control T cell gene expression at specific anatomical sites *in vivo* remains limited. This is particularly important for therapeutic applications of engineered T cells. Clinically used methods to control T cells that involve systemic administration of potent immune-modulating drugs<sup>168</sup> or biologics<sup>4, 74</sup> lack spatial and temporal precision and can be associated with significant adverse effects<sup>169</sup>. Engineered T cells capable of being locally activated at desired locations in the body by externally applied cues – such as light<sup>145, 163</sup> or radio waves<sup>170</sup> – will increase the precision of engineered T cell applications for use in humans.

Inspired by the precision with which pulses of heat can be delivered to sites located both superficially and at depth inside the body (e.g., by laser heating<sup>171</sup>, induction heating<sup>151</sup>, or focused ultrasound<sup>172</sup>), we engineer Jurkat T cells with heat-triggered gene switches for remote control of transcriptional activity by plasmonic photothermal heating. Temperature control has a rich and longstanding clinical history such as the use of freezing temperatures for cryoablation<sup>173</sup> and hyperthermia to increase radiosensitivity<sup>174</sup> or enhance drug delivery<sup>146</sup>. Despite this, few engineered genetic systems have been designed

that leverage temperature triggers to regulate cellular activity. Past work on mammalian gene switches include transcriptional activity triggered by small molecules, protein ligands, and light<sup>161</sup>. Genetically encoded thermal switches such as RNA thermometers<sup>154</sup> or temperature-sensitive transcriptional regulators<sup>152, 153</sup> have been developed for bacterial systems, but the prokaryotic origin of these approaches raises concerns with immunogenicity in T cells and potentially limits their use for cellular control in mammalian systems. By contrast, our thermal gene switches are constructed from endogenous promoters that drive the heat shock (HS) response – a highly conserved reactive mechanism to transient elevations in temperature (~3–5°C above basal temperature) that triggers expression of protective HS proteins at levels comparable to the strongest known viral promoters<sup>175</sup>. The ubiquity of the HS response has driven past work on thermal gene regulatory systems in mammals, worms, fish and other organisms<sup>176</sup>, including the use of plasmonic nanomaterials to remotely activate engineered cells<sup>157, 177-179</sup>. However, these approaches activated wild-type promoters with continuous heating methods that result in low cellular viability<sup>180</sup> and preclude their use for longitudinal control of cells.

Here we show that Jurkat T cells engineered with thermal gene switches constructed from the heat shock protein 70B' (HSPA6) promoter have negligible activity at basal body temperatures but trigger gene expression to levels greater than 200-fold following exposure to elevated temperatures within a narrow transition window (40–42°C). We spatially control Jurkat T cell activity with heat delivered by the photothermal effect using the precision of near infrared (NIR) laser light for targeting and plasmonic gold nanorods as transducers to convert incident NIR light into localized heat<sup>171</sup>. We also demonstrate that the use of thermal pulse trains compared to heat delivered at a constant

temperature significantly increases thermal tolerance to allow long-term control of Jurkat T cells for weeks in a living host.

## 1.6 Results

### 1.6.1 *Engineering a thermal gene switch*

Within the mammalian family of HS promoters, heat responsiveness is primarily mediated by Heat Shock Factor 1 (HSF1) – a transcription factor that is normally present as an inactive monomer under basal conditions. During hyperthermia, HSF1 is converted to a homotrimer that then binds to heat shock response elements (HSEs) arrayed upstream of the transcription start site<sup>156, 181</sup>. These HSEs, together with putative negative regulatory regions, dictate the heat response characteristics of a promoter. Therefore, we sought to perform truncation analysis on the HSPA6 locus to characterize different regions of the wild-type promoter sequence to identify constructs with low basal activity and high fold-induction<sup>182, 183</sup>. We cloned 8 candidate constructs (labelled i–viii, Figure 7a) into HEK 293T cells starting at four upstream sites at –2964, –1231, –648, and –71 bp relative to the transcriptional start site, and ending at two downstream sites at +48 and +119 bp – the latter corresponding to the beginning of the open reading frame (ORF) of the HSPA6 gene. From our library, we selected construct ii for use in further studies based on several considerations: it had a high fold-induction, absolute level of activity, and small base pair footprint to allow larger gene inserts into viral vectors.

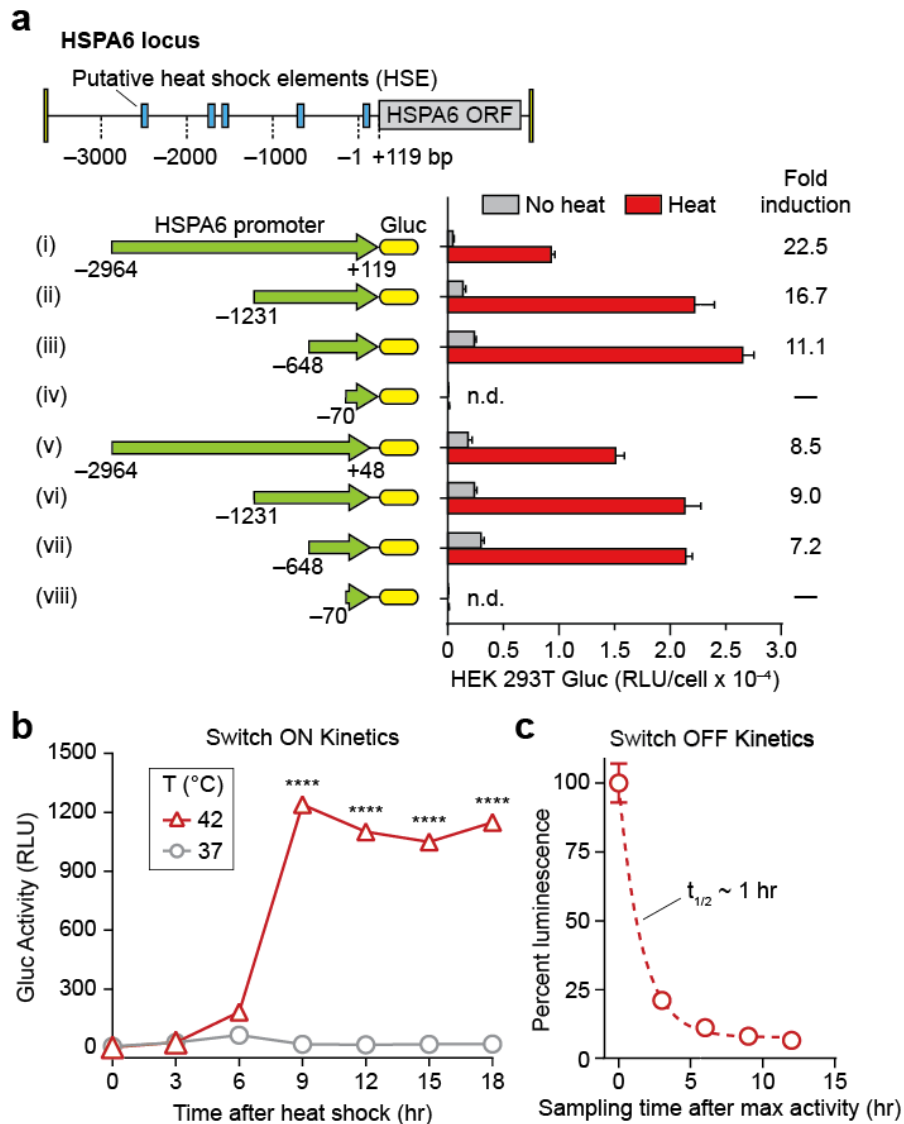
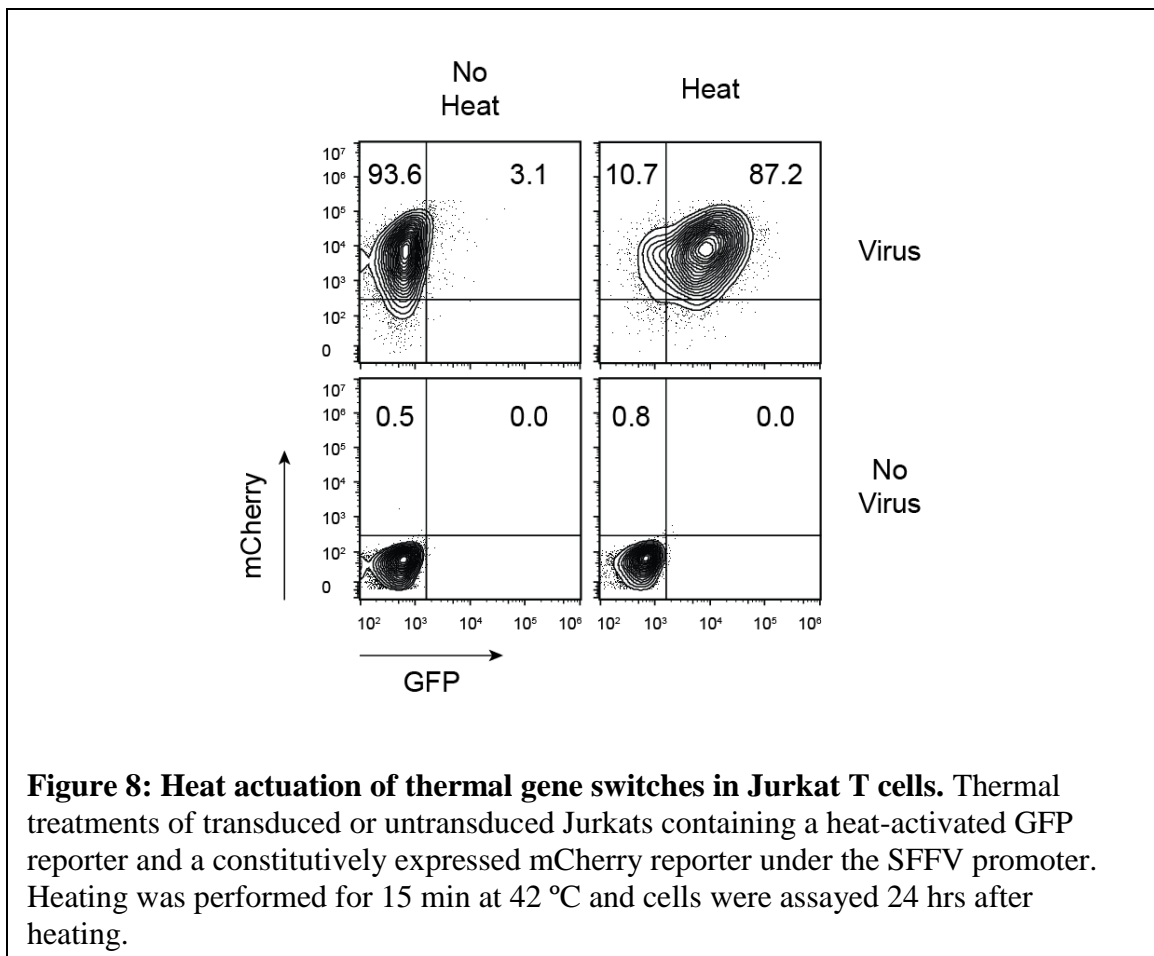


**Figure 7: Heat-triggered gene switches in Jurkat T cells.** (a) Eight constructs (i-viii) cloned from the heat shock protein HSPA6 locus used to evaluate sensitivity to thermal activation in HEK 293T cells. Constructs i-iv extend to +119 bp beyond transcriptional start site while constructs v-viii terminate at +48 bp. Fold inductions of normalized luminescence (Heat/No heat) are listed to the right of each construct. RLU: Relative Luminescence Units, n = 3, error bars = SEM. (b) Kinetic trace of cumulative switch activity at 42 °C in Jurkat T cells following 1 hr heating, n = 3, error bars show SEM and are smaller than the displayed data points, \*\*\*\* P < 0.0001, one-way ANOVA and Dunnett's multiple comparison test. (c) Decay kinetics of switch activation after 1 hr heating at 42 °C. Luminescent values were determined by sampling and replacing supernatant after maximum activity was reached, n = 3, error bars = SEM.

We next evaluated thermal switch activity in Jurkat T cells which showed a sharp

switch-on transition 6 hours after heat treatment (42 °C) that resulted in a ~70-fold increase in luminescent signals (Figure 7b). At time points greater than 9 hours, no appreciable decrease in signals were observed that would indicate a switch-off transition. We attributed this result to the Gluc reporter we used because it is naturally secreted and not subject to intracellular degradation pathways such as ubiquitination. Therefore, to measure our thermal switch-off kinetics, we repeatedly sampled and replaced the cellular supernatant after maximum Gluc activity was attained at 9 hours and determined a decay constant half-life of ~1 hour (Figure 7c). Additionally, incorporation of a GFP reporter revealed that ~90% of transduced Jurkats were actuated by heat treatments (Figure 8). These results

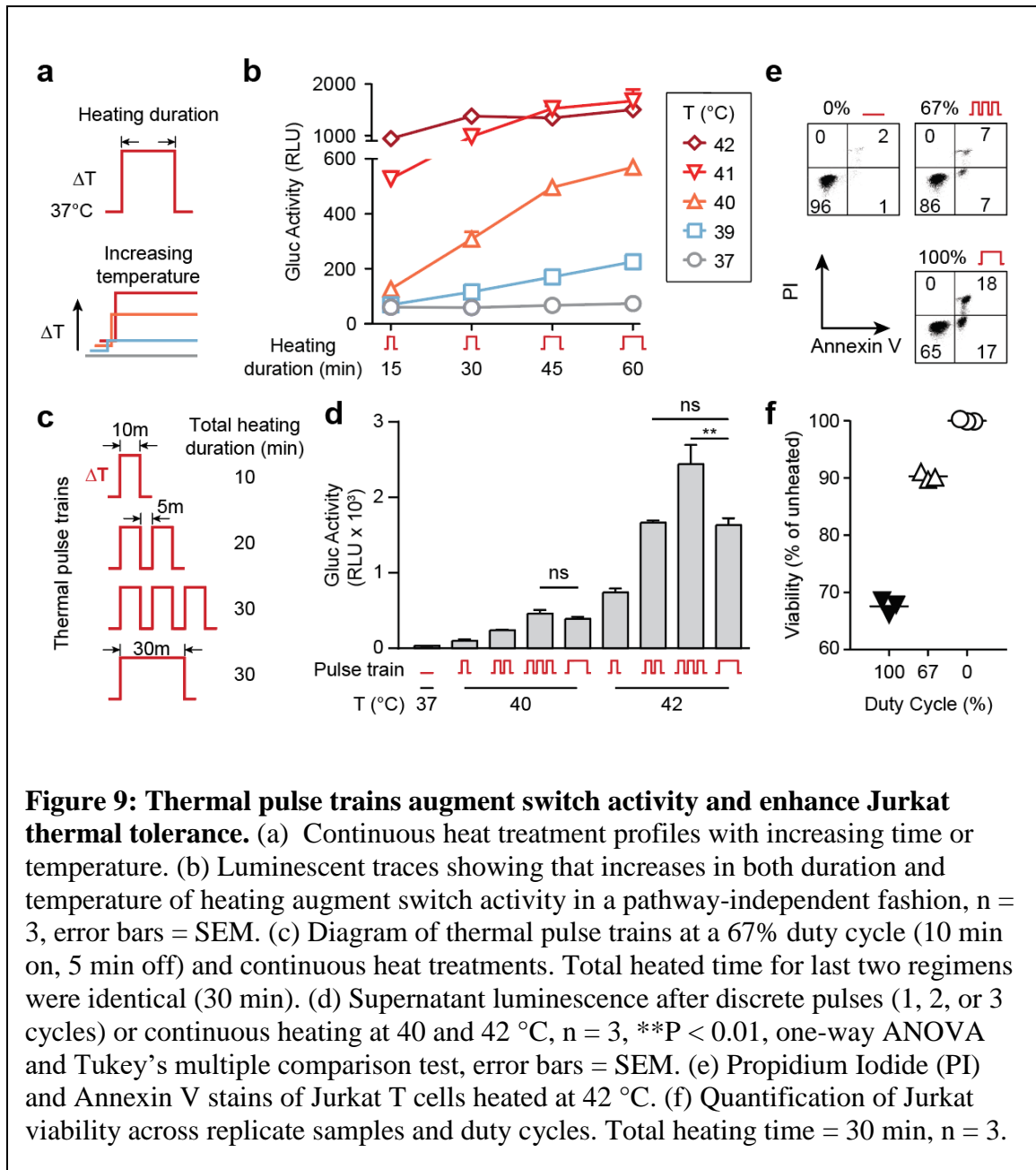


show that thermal switches constructed from the HSPA6 promoter exhibit sharp switch-on and switch-off kinetics in transduced Jurkat T cells.

### *1.6.2 Triggering cellular activity with pulses of heat*

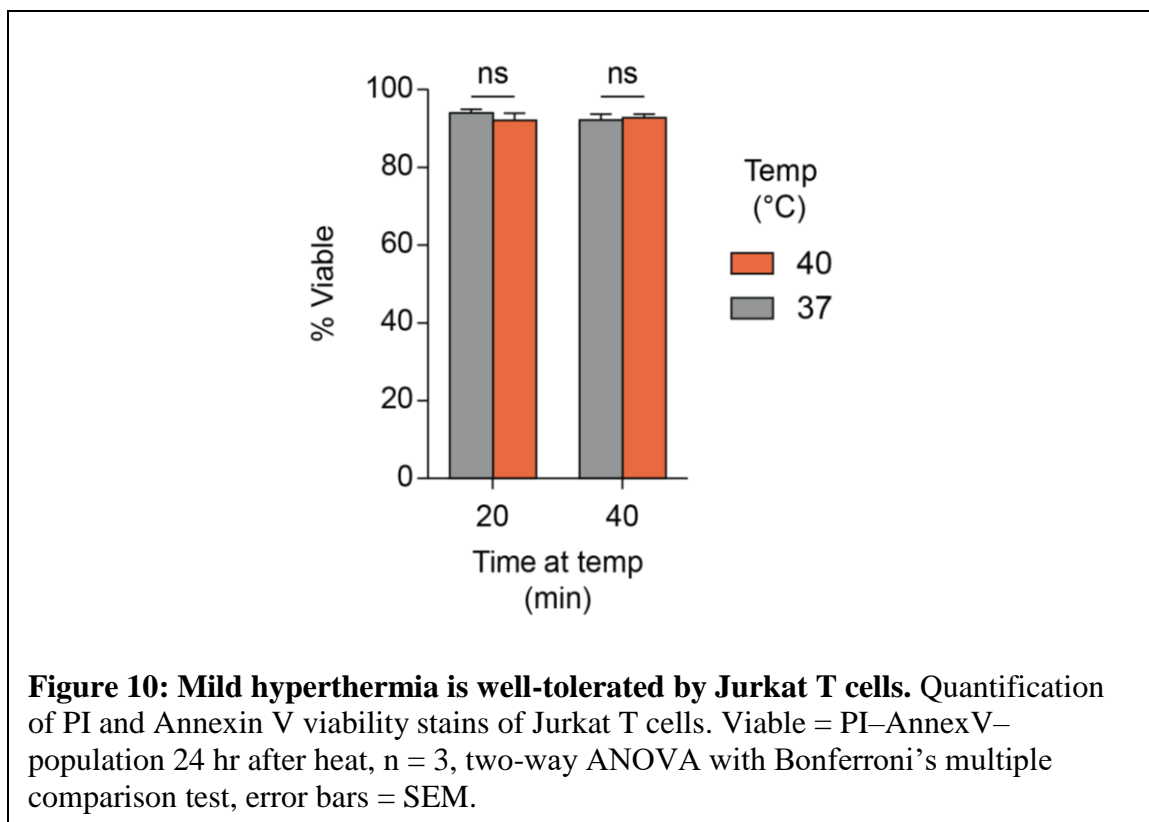
To determine the relationship between heating duration, temperature, and thermal switch activity using continuous temperature inputs, we heated transduced Jurkat T cells for 15 – 60 minutes at temperatures ranging between 37 and 42 °C (Figure 9a, b). Elevations in temperature as low as 39 °C ( $\Delta T = 2$  °C) were sufficient to induce switch activity, and either higher temperatures or extended heating durations increased output activity, with maximal levels occurring at 41–42 °C. Moreover, our data showed that the level of thermal switch activity was independent of path; therefore, we hypothesized that milder heating conditions using discrete pulses of heat could be used to increase T cell thermal tolerance yet achieve similar levels of thermal switch activity.

To test this, we compared the efficacy of delivering heat using pulse train or constant temperature profiles (Figure 9c). Under a 67% duty cycle comprised of a 10 minute heat step at 42 °C and 5 minute rest period at 37 °C, each additional thermal pulse progressively increased cell output activity such that the cumulative effect from three pulses was ~50% higher compared to the intensity obtained using a constant temperature



profile (i.e., 100% duty cycle) with an identical area under the curve (AUC) (Figure 9d).

We observed a similar trend where output activity increased with the number of pulses at a lower activating temperature of 40 °C; however, the level of activity between three pulses and continually heated samples was statistically identical. We attributed this difference between 40 and 42 °C to the ability of Jurkats to better tolerate smaller elevations in temperature. To test this, we analyzed Jurkat viability by Annexin V and propidium iodide



(PI) stains for apoptosis and cell death respectively, and found that at 42 °C, a 67% duty cycle significantly reduced double positive cells by over 70% compared to continuous heating, and maintained a cell viability of ~90% relative to that of unheated cells (Figure 9e, f). Conversely, no significant differences in cell death and viability were observed at 40 °C even after 40 minutes of constant heating (Figure 10). Collectively, our data showed that the number of pulses in a thermal train controls the level of output activity and significantly increases thermal tolerance of Jurkat T cells compared to constant temperature inputs.

### 1.6.3 Photothermal targeting of Jurkat T cells

We next set out to demonstrate temperature control of Jurkat T cells using externally applied triggers. Spatially targeted heating in human patients can be achieved in deep

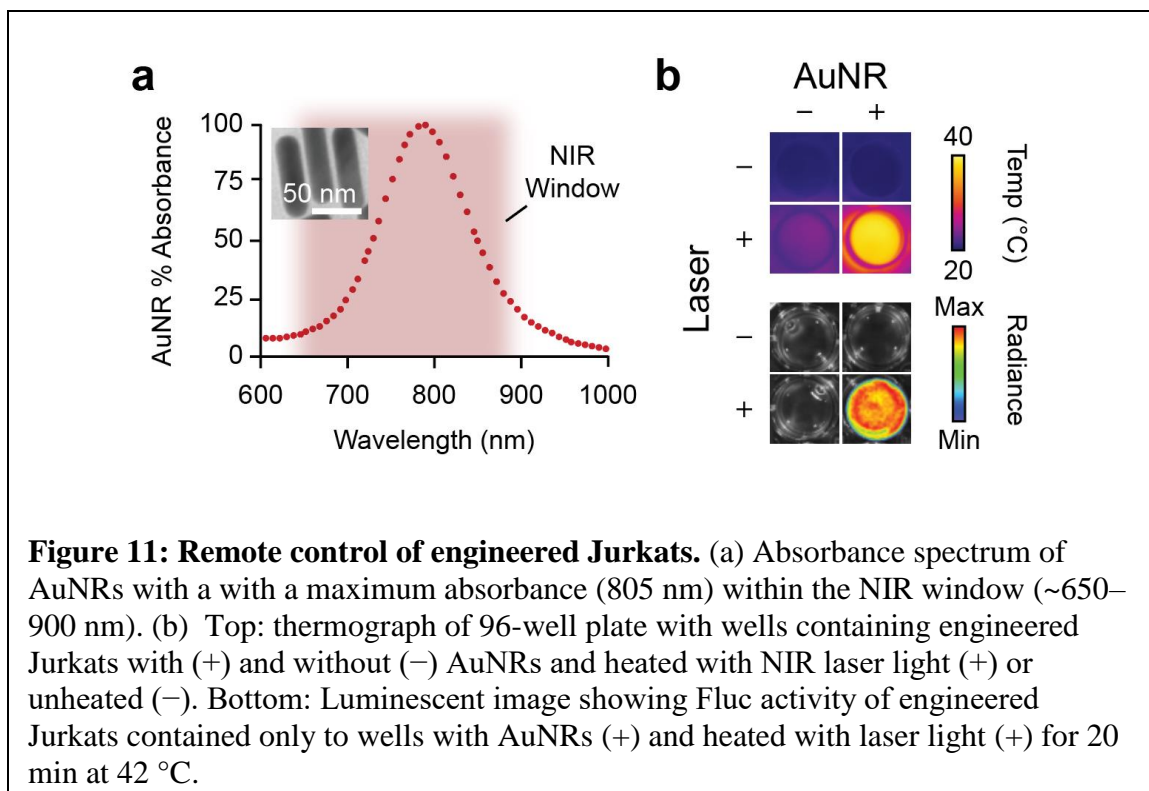
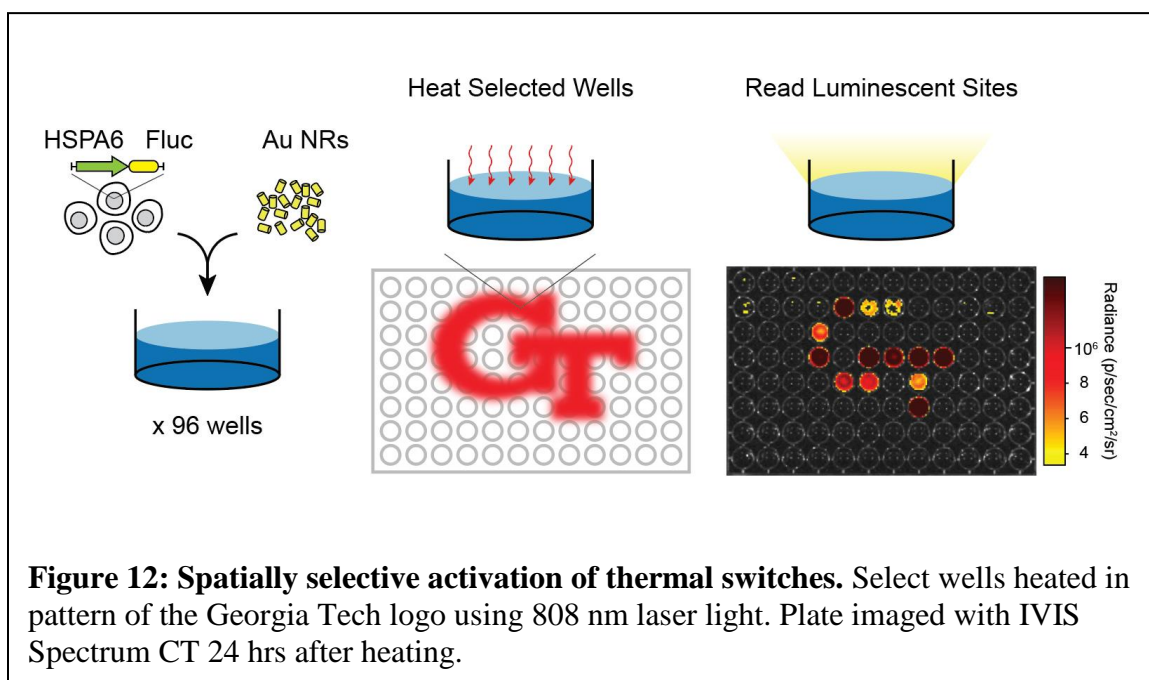


**Figure 11: Remote control of engineered Jurkats.** (a) Absorbance spectrum of AuNRs with a maximum absorbance (805 nm) within the NIR window (~650–900 nm). (b) Top: thermograph of 96-well plate with wells containing engineered Jurkats with (+) and without (–) AuNRs and heated with NIR laser light (+) or unheated (–). Bottom: Luminescent image showing Fluc activity of engineered Jurkats contained only to wells with AuNRs (+) and heated with laser light (+) for 20 min at 42 °C.

tissues using multiple platforms including focused ultrasound, inductive heating, and microwave heating<sup>146</sup>. Here we chose photothermal heating using near infrared (NIR) laser light ( $\lambda = 808$  nm) irradiation of plasmonic gold nanorods (AuNRs)<sup>171</sup>. AuNRs are long-circulating nanomaterials whose geometry can be precisely tuned to absorb and convert incident NIR light into thermal energy by surface plasmon resonance (SPR) (Figure 11a). Passively targeted AuNRs accumulate in tissue across fenestrated endothelium such as tumors<sup>184, 185</sup> and allow for localized heating when the site is exposed to otherwise benign NIR light. To test this approach, we arrayed mixtures of AuNRs and luciferized Jurkats into a 96-well plate and confirmed coincident increases in both temperature and luciferase activity in wells treated with NIR laser light (Figure 11b), allowing spatial targeting of cellular expression in patterns such as the Georgia Tech logo (Figure 12). We then tested this system *in vivo* by laser heating subcutaneous matrigel implants encapsulated with Jurkat T cells and AuNRs (Figure 13a) under the guidance of a thermal camera to allow



maintenance of target skin temperatures in real time (Figure 13b, c). At implant sites heated to focal skin surface temperatures of 42 °C and 45 °C, we observed over 105-fold and 209-fold increases in luciferase activity respectively compared to unheated sites kept at body temperature (Figure 13d). In contrast to our *in vitro* studies showing maximum cell activation at 42 °C (Figure 9b), a surface skin temperature of 45 °C was required to robustly trigger our thermal switch *in vivo*. We attributed this difference to measuring temperature at the surface of the skin compared to the core of the implant. We did not observe tissue damage to the skin surface at 45 °C and chose to work with this activating temperature for further *in vivo* studies. Taken together, our data showed that photothermal heating using NIR light and AuNRs effectively allows spatial targeting and control of cellular activity *in vivo*.

#### 1.6.4 Thermal pulse trains for long-term control of Jurkat T cells *in vivo*

Based on our *in vitro* studies which showed the benefits of heat delivery using thermal pulse trains, we sought to determine whether this method could be used to control Jurkat T cells over several weeks without significant reductions in cell viability and function. Serial

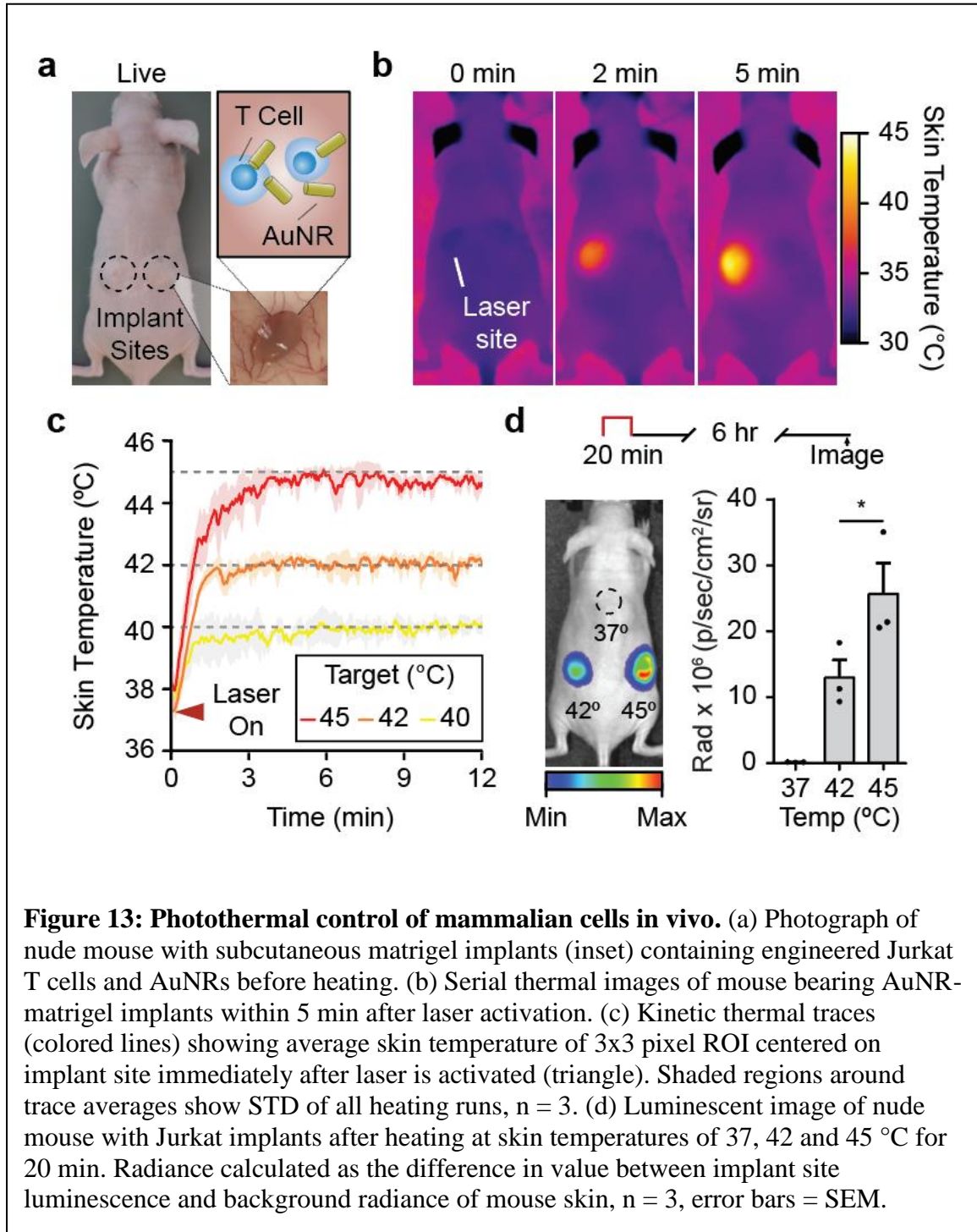
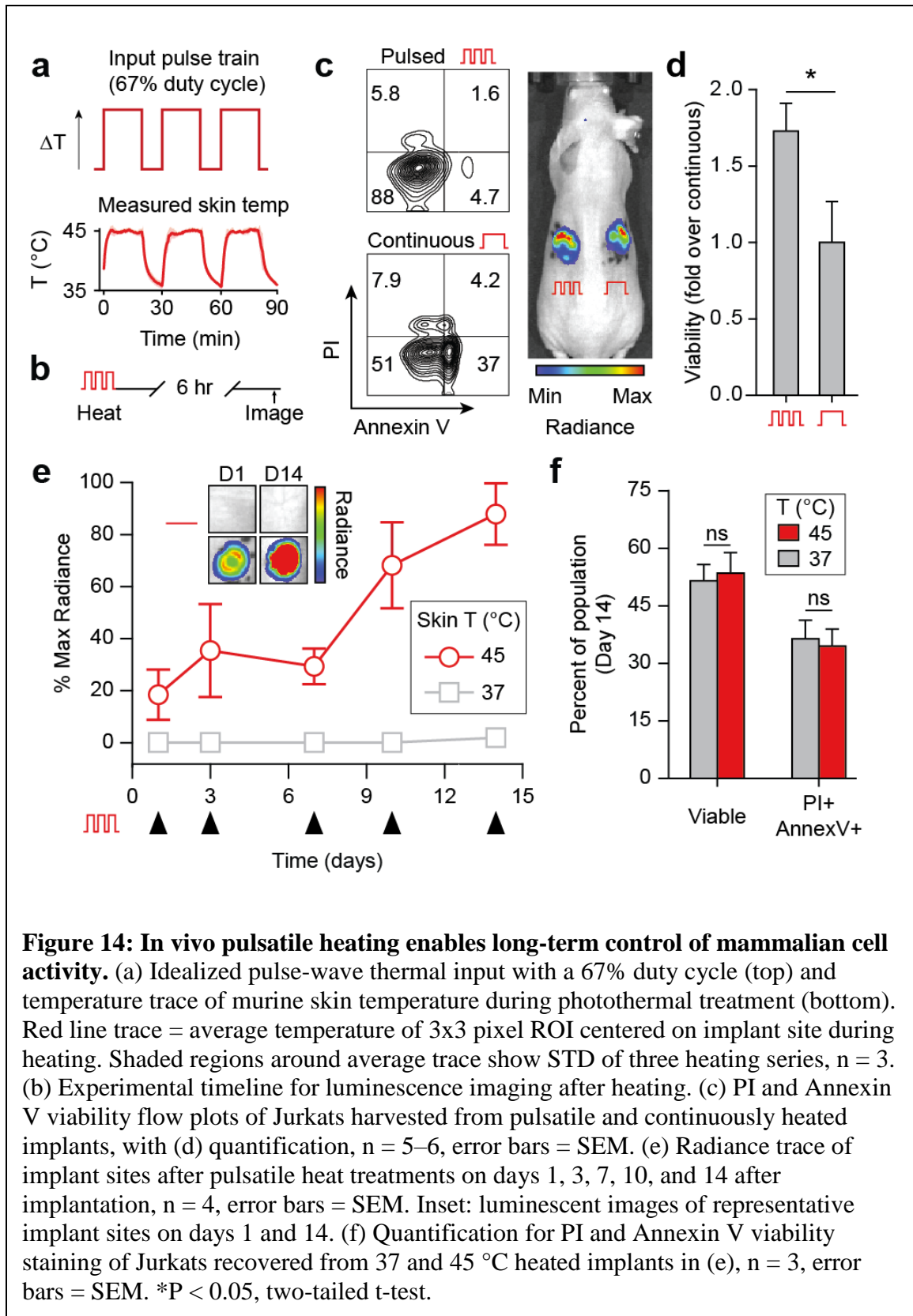


**Figure 13: Photothermal control of mammalian cells in vivo.** (a) Photograph of nude mouse with subcutaneous matrigel implants (inset) containing engineered Jurkat T cells and AuNRs before heating. (b) Serial thermal images of mouse bearing AuNR-matrigel implants within 5 min after laser activation. (c) Kinetic thermal traces (colored lines) showing average skin temperature of 3x3 pixel ROI centered on implant site immediately after laser is activated (triangle). Shaded regions around trace averages show STD of all heating runs, n = 3. (d) Luminescent image of nude mouse with Jurkat implants after heating at skin temperatures of 37, 42 and 45 °C for 20 min. Radiance calculated as the difference in value between implant site luminescence and background radiance of mouse skin, n = 3, error bars = SEM.

modulation of T cell phenotype is especially relevant to chronic diseases such as HIV or refractory cancer that produce exhausted or anergic T cell populations<sup>186</sup> and where recovering T cell effector functions requires repeated administration of activating drugs (e.g., cytokines and checkpoint blockade antibodies). To enable localized, extended control over Jurkat T cell behavior while maintaining high cell viability, we applied thermal pulse trains to heat matrigel implant sites serially using NIR laser light and AuNRs. To confirm that the rate of heat transfer *in vivo* would allow on-off cycling of thermal pulses, we irradiated implant sites at a 67% duty cycle which produced discrete skin temperature profiles characterized by a decay half-life of 1.7 minutes between pulses and an area under the curve (AUC) of 1.2 compared to the ideal square wave input (Figure 14a). We then compared the viability of Jurkats recovered from *in vivo* matrigel implants heated with thermal pulse trains to those treated by continuous heating (Figure 14b) and, consistent with *in vitro* studies (Figure 9e, f), found greater than a 1.7-fold increase in viability (Annexin V<sup>-</sup>, PI<sup>-</sup>) within pulsed cells after one day (Figure 14c, d). Because of this significant reduction in viability using a constant temperature profile, we explored long-term control of cell behavior using repeated pulsatile heat treatments. Over the course of 14 days, implanted Jurkats steadily increased switch activity compared to unheated controls such that signals by Day 14 were more than 4-fold higher than on Day 1 (Figure 14e). To confirm long-term pulsatile heating did not adversely affect implanted cells, we analyzed the Jurkat T cells on Day 15 and observed no significant differences in apoptosis and cell death markers (Annexin V and PI) between pulsed and unheated cells kept at body temperature that were implanted concomitantly on Day 0 (Figure 14f). Together our data



shows that heat delivered in discrete pulses preserves cell viability and allows remote

control of Jurkat T cells for weeks *in vivo*.

## 1.7 Discussion

Inspired by remote control of biological systems, we establish a framework for engineering mammalian cells with thermal gene switches for *in vivo* control using pulses of heat. Thermal gene switches constructed from the HSPA6 promoter activate within a narrow temperature window of 40–42 °C and trigger gene expression to hundreds of fold above basal levels while remaining silent at normal body temperature. Here we used wild-type promoter sequences but key thermal switch properties, including thermal activation temperatures and on-off ratios, could be further developed by directed evolution or incorporating similar genetic architectures from a wide range of species that have different temperature thresholds for heat shock activation (e.g., Arabian camel and zebrafish). This could provide orthogonal thermal band-pass circuits that express different genes depending on the temperature of the hyperthermic input as demonstrated recently in bacteria<sup>152</sup>.

In our study, we found that pulsatile heat delivery significantly improved thermal tolerance of Jurkat T cells compared to continuous heating profiles with identical AUCs, which allowed long-term control of cells *in vivo* without reduction in output activity or cellular viability. In past studies, thermal tolerance was achieved by pretreatment of cells with mild heat followed by a rest period to allow expression of protective HSPs before full thermal induction<sup>187</sup>; however, this mechanism is unlikely to explain our results as our off-cycle time (~10 minutes) was short for protein expression. The induction of thermal tolerance under our heating schedule may be related to HSF1's trimerization mechanism in which hydrophobic regions in repeated heptad domains are disrupted and form

intermolecular coiled coils in response to hyperthermic conditions. These interactions allow HSF1 to stably trimerize and bind with high affinity to HSEs to initiate transcription<sup>156, 175, 181</sup>. Our pulsed delivery method may influence the rate at which these hydrophobic domains are exposed, or the population frequency of trimers since higher-order oligomers are formed as well<sup>188, 189</sup>. The exact mechanism may be elucidated by examining the heat-response of substitution or deletion mutations within the hydrophobic domains that govern and regulate HSF1 trimerization<sup>188, 190-193</sup>.

To heat specific sites *in vivo*, we chose to use NIR laser light and plasmonic gold nanorods to induce local hyperthermia in matrigel implants. The well-established bio-distribution of nanoparticles<sup>194</sup> in tissues with porous vessels such as secondary lymphoid organs (e.g., spleen or lymph nodes) or sites of disease (e.g., tumors) could allow engineered cells within these tissues to be remotely controlled. In humans, modalities such as focused ultrasound, radio- or microwaves are routinely used to precisely heat deeper tissues where targeting with optical techniques remains challenging<sup>146</sup>. In a clinical setting, a future application is to incorporate thermal gene switches into engineered T cell therapies for cancer to allow local expression of potent immune-modulating biologics<sup>4, 74</sup> – which are otherwise associated with significant off-target toxicity when administered systemically – to combat tumor immunosuppression. Moreover, local heating may be targeted to sites implanted with biomaterials designed to enhance T cell function, including wafers that expand and disperse tumor-reactive T cells<sup>195</sup>. Looking forward, this framework of activating gene expression by heat provides an orthogonal mechanism to control cellular activity in addition to small-molecule<sup>196</sup> or light-based methods<sup>145</sup>. Such

platforms may be integrated across different immune cell types for remote control of synthetic immunological systems.

## 1.8 Methods

*Plasmid construction and viral production.* The promoter of the HSPA6 gene (Uniprot P17066) was amplified from human genomic DNA (Clontech # 636401) at positions indicated in Fig 1a similar to previous studies<sup>182</sup>. XbaI and XhoI sites were added to the 5' and 3' ends of annealing sequences listed in the Supplementary Methods, digested, and used to insert the promoters into the Lego-C plasmid (Addgene #27348) that contains the reporter mCherry as a selectable marker. This fluorescent reporter was used to sort transduced cells using FACS. Additional reporters including Gluc (LifeTech 16146), emGFP (Imanis DNA1023) and Fluc (Addgene #33307) were added under control of the heat shock promoter via restriction enzyme digestion and ligation. Plasmid DNA was purified using a Plasmid Maxi Kit (Qiagen cat # 12163) and packaged into lentiviral vectors with psPAX2 (Addgene #12260) and pMD2.G (Addgene #12259). Cells were transduced in 10 µg/mL of protamine sulfate (Sigma) before FACS (BD FACS Aria) and downstream use.

*Switch Construction:* HSPA6 promoter sequences had XbaI and XhoI restriction sites added to the 5' and 3' ends respectively during PCR amplification before being digested and ligated into the Lego-C plasmid (Addgene #27348). Annealing sequences for the primers are listed below here. Forward: tcattctgaattcccacaacacatgg (Constructs i and iv); gatctgaatggaatgttctggattgaaga (Constructs ii and vi); aattctaccactgaaccaccaatgc (Construct

iii and vii); cgaaagttcgcggcgg (Constructs iv and viii). Reverse ggctgaagcttctgtcgga (Constructs i – iv); agtgaggctctcctgcggttctct (Constructs v – viii).

*Preparation of AuNRs.* AuNRs were purchased from Nanopartz (item # A12-10-808-CTAB-500) and pegylated (Laysam Bio cat #MPEG-SH-5000-5g) to replace the CTAB coating before being resuspended in DI at 0.5 mg/mL. This solution was used in a 1:100 dilution for all laser mediated heating experiments in mice and 96-well plates.

*Viability studies.* Jurkats were heated in a thermal cycler (Biorad) in HEPES buffered RPMI (25 mM) at a density of  $10^6$  cells/mL and incubated at 37 °C and 5% CO<sub>2</sub>. After 24 hours, cells were assayed for viability using the Apoptosis Detection Kit (BD cat # 556547). For cells recovered from implant sites, matrigel was excised from mice, physically dissociated and incubated in Cell Recovery Solution (Corning) according to manufacturer's instructions before analysis with Apoptosis Detection Kit 24 hours after conclusion of heating. All samples were analyzed with FlowJo, Version 10 (FlowJo LLC).

*In vitro heating assays.* Cells were heated in a thermal cycler and immediately transferred to a 96-well plate and incubated until assayed. Unless otherwise indicated, cellular supernatant was sampled for reporter activity 24 hrs after heating. Density inside PCR tubes was  $10^6$  cells / mL. Luminescent activity was measured using a Cytation 5 plate reader (BioTek) and Gaussia Luciferase Assay Kit (New England Biolabs) according to manufacturer's instructions.

*In vivo laser heating.* 0.5 µg AuNRs and  $2 \times 10^6$  engineered cells per 100 µL matrigel were used for laser heating with *in vivo* implants after subcutaneous injection into nude mice (Jackson Labs). Mice were anesthetized with isoflurane gas and implant sites were heated

using an 808 nm laser (Coherent) at a power density of  $\sim 9.5 \text{ A} / \text{cm}^2$ . All *in vivo* pulsatile heating profiles were performed for a total of 30 min of heat with a 67% duty cycle. Surface temperature was continually measured using a thermal camera (FLIR model 450sc). Rest periods during cyclic heating began when measured skin temperature reached  $37 \pm 1$  °C.

*In vivo bioluminescence and imaging.* Fluc activity was measured using an IVIS Spectrum CT (Perkin Elmer) after i.p. injections of luciferin (Gold Bio) administered 4.5 hr after conclusion of activating heat shock. Integration time was set to automatic and imaging was conducted for up to 1.5 hr after injection. ROIs were defined within the Living Image software package (Perkin Elmer) and measured as average radiance ( $\text{photons s}^{-1} \text{ cm}^{-1} \text{ sr}^{-1}$ ).

*Statistical Analysis.* All results are presented as mean, and error bars show SEM. Statistical analysis was performed using statistical software (GraphPad Prism 6; GraphPad Software).

\* $p < 0.05$ , \*\* $p < 0.01$ .

# REMOTE CONTROL OF CAR T CELL THERAPIES BY THERMAL TARGETING

Adapted from Miller, I.C., Sun, L., Harris, A. M., Gamboa, L., Zamat, A. & Kwong, G.A. Remote control of CAR T cell therapies by thermal targeting. Pre-print *bioRxiv* doi:10.1101/2020.04.26.0627031167-1173 (2020).

## 1.9 Abstract

The limited ability to control anti-tumor activity within tumor sites contributes to poor CAR T cell responses against solid malignancies. Systemic delivery of biologic drugs such as cytokines can augment CAR T cell activity despite off-target toxicity in healthy tissues that narrows their therapeutic window. Here we develop a platform for remote control of CAR T therapies by thermal targeting. To enable CAR T cells to respond to heat, we construct synthetic thermal gene switches that trigger expression of transgenes in response to mild elevations in local temperature (40–42 °C) but not to orthogonal cellular stresses such as hypoxia. We show that short pulses of heat (15–30 min) lead to more than 60-fold increases in gene expression without affecting key T cell functions including proliferation, migration, and cytotoxicity. We demonstrate thermal control of broad classes of immunostimulatory agents including CARs, Bispecific T cell Engagers (BiTEs), and cytokine superagonists to enhance proliferation and cell targeting. In mouse models of adoptive transfer, photothermal targeting of intratumoral CAR T cells to control the production of an IL-15 superagonist significantly enhances anti-tumor activity and overall survival. We envision that thermal targeting could improve the safety and efficacy of next-generation therapies by allowing remote control of CAR T cell activity.

## 1.10 Introduction

Engineered T cell therapies such as Chimeric Antigen Receptor (CAR) T cells are transforming clinical care for hematological malignancies, spurring numerous efforts to expand their use for different cancer types and applications. However, this success has not reliably translated to solid tumors<sup>197</sup>. The factors that contribute to low response rates are multifaceted and include the paucity of tumor-specific antigens, inefficient persistence and expansion of adoptively transferred T cells, and immunosuppression by the tumor microenvironment (TME)<sup>198</sup>. Promising approaches to improve anti-tumor activity of engineered T cells include systemic administration of potent immunostimulatory agents such as cytokines, checkpoint blockade inhibitor antibodies, and bispecific T cell engagers (BiTEs)<sup>77, 199-201</sup>. However, these biologics lack specificity, activate both engineered and endogenous immune cells, and exhibit toxicity in healthy tissue which limits maximum tolerable doses and narrows their therapeutic windows<sup>4, 7-9</sup>. Thus, expanding current abilities to target and locally augment CAR T cell functions at tumor and disease sites such as draining lymph nodes could improve the safety and efficacy of cell-based therapies.

Emerging strategies to control engineered T cells and augment their anti-tumor activity include the use of biomaterials to co-deliver adjuvants to the TME as well as genetic constructs for autonomous expression of immunostimulatory genes. For example, implantation of biopolymer scaffolds loaded with tumor-specific T cells and immunostimulatory adjuvants at the surgical site improved postoperative responses following primary tumor resection in mouse models<sup>106, 107</sup>. To provide a localized source of adjuvants, T cells tethered on their cell surface to nanoparticle ‘backpacks’ allowed infiltrating T cells to carry cargo<sup>108</sup> and release a one-time dose of drug within tumors<sup>109</sup>.

Increasingly sophisticated genetic circuitry has also allowed T cells to locally produce biologics to overcome immunosuppression or target antigens after tumor infiltration. For example, ‘armored CARs’ leverage constitutive expression of biologics such as IL-12<sup>121</sup>,  $\alpha$ PD-1 scFvs<sup>122</sup>, and BiTEs<sup>123</sup> to improve anti-tumor activity. T cells have also been engineered with sense-and-respond biocircuits that conditionally activate in the presence of specific input signals. These strategies include NFAT-inducible cassettes that upregulate expression of cytokines following T cell recognition of a tumor-associated antigen<sup>124-126</sup>. To further increase specificity, T cells have been engineered to target unique combinations of epitopes expressed in the TME to allow discrimination from healthy cells expressing a single epitope<sup>128</sup>. Such approaches based on Boolean logic require the presence of both target antigens for T cell activation to occur and have demonstrated efficacy in multiple models of focal tumors<sup>129, 130</sup>. Collectively, these approaches illustrate the need to develop strategies to control and improve intratumoral T cell activity.

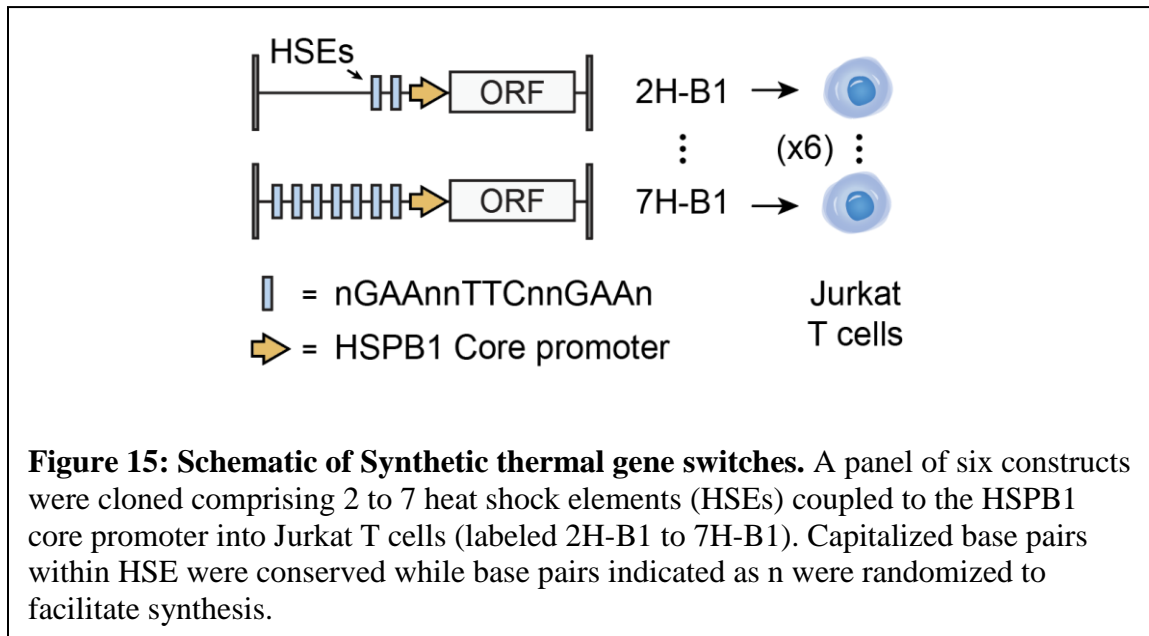
Here we developed a platform for remote thermal control of CAR T cell therapies. Heat treatments are used clinically to sensitize cancer cells to chemotherapy, ablate isolated metastatic nodules, and enhance diffusion of small molecule drugs into tumors<sup>147</sup>. Both superficial and deep-seeded tumors can be targeted for thermal treatment by platforms including high intensity focused ultrasound (HIFU)<sup>146</sup>, laser interstitial thermal therapy (LITT)<sup>149</sup>, and electromagnetic heating<sup>151</sup>. To engineer T cells with the ability to respond to heat, we constructed and screened panels of synthetic thermal gene switches containing combinations of Heat Shock Elements (HSEs) and core promoters to identify an architecture that responds to mild hyperthermia while remaining non-responsive to orthogonal cell stresses. We designed thermal constructs to control broad classes of

immunostimulatory genes including CARs, BiTEs, and a cytokine superagonist to enhance key T cell functions including proliferation and T cell targeting. In an adoptive transfer model of cancer, remote thermal control of an IL-15 superagonist improved anti-tumor CAR T cell activity by reducing tumor burden and improving survival of tumor-bearing animals. Remote control of CAR T cells by thermal targeting could improve the precision of cellular therapies by enabling site-specific control of anti-tumor responses.

## 1.11 Results

### 1.11.1 Engineering thermal-specific gene switches

The cellular response to hyperthermia is mediated by trimerization of the temperature-sensitive transcription factor Heat Shock Factor 1 (HSF1) and its subsequent binding to DNA motifs termed Heat Shock Elements (HSEs). HSEs are comprised of multiple inverted repeats of the consensus sequence 5'-nGAAn-3'<sup>202, 203</sup> and are arrayed upstream of HSPs thereby enabling their upregulation following thermal stress<sup>204</sup>. The response of



endogenous HSP genes is selective, but not specific, for heat as their promoters contain additional regulatory elements (e.g., hypoxia response elements<sup>205</sup>, metal-responsive elements<sup>206</sup>) that mediate transcription following exposure to a diverse set of cues including hypoxia<sup>207</sup>, heavy metals<sup>208</sup>, and mechanical force<sup>209</sup>. Moreover, differences in the core promoter (e.g., initiator elements, TATA box) influence the composition of the pre-initiation complex (PIC) and its interactions with transcriptional enhancers including HSF1, providing an additional mechanism whereby transcriptional responses to heat are regulated differently across tissues and types of cells<sup>210, 211</sup>. Due to this complexity and

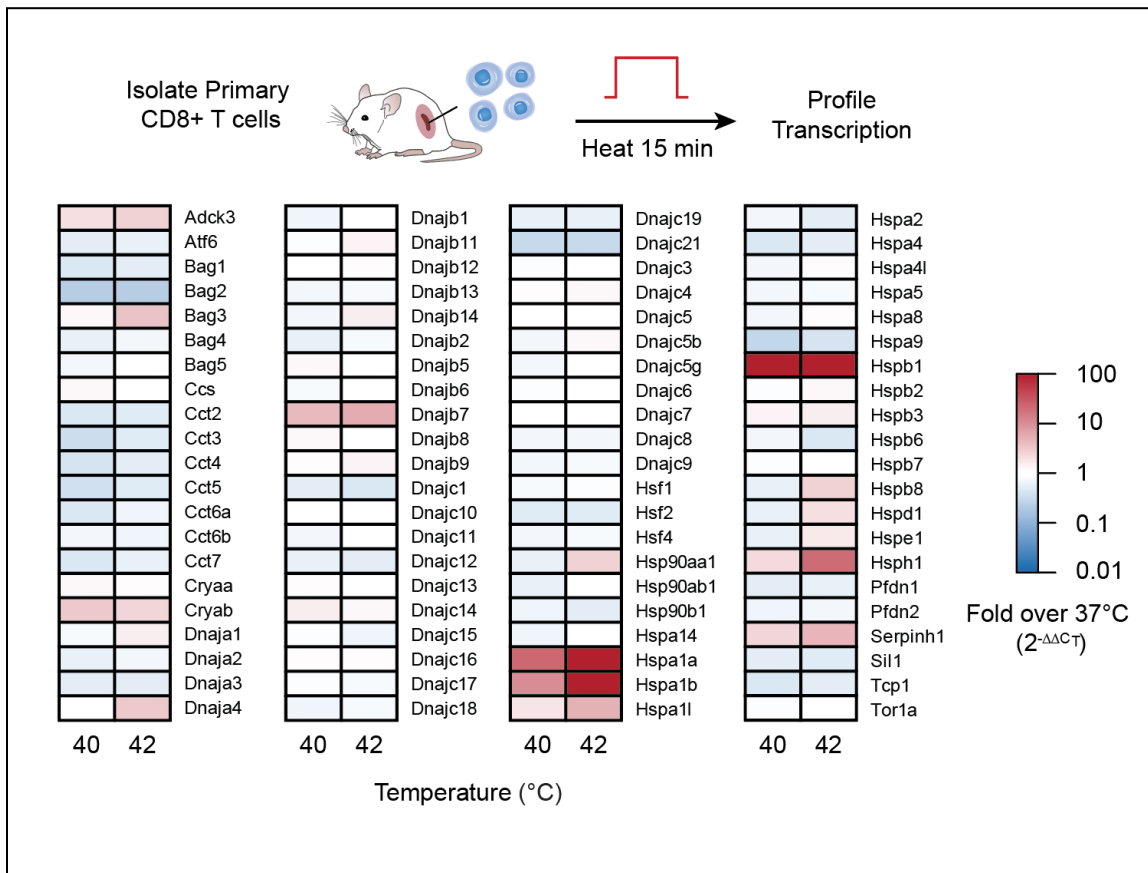
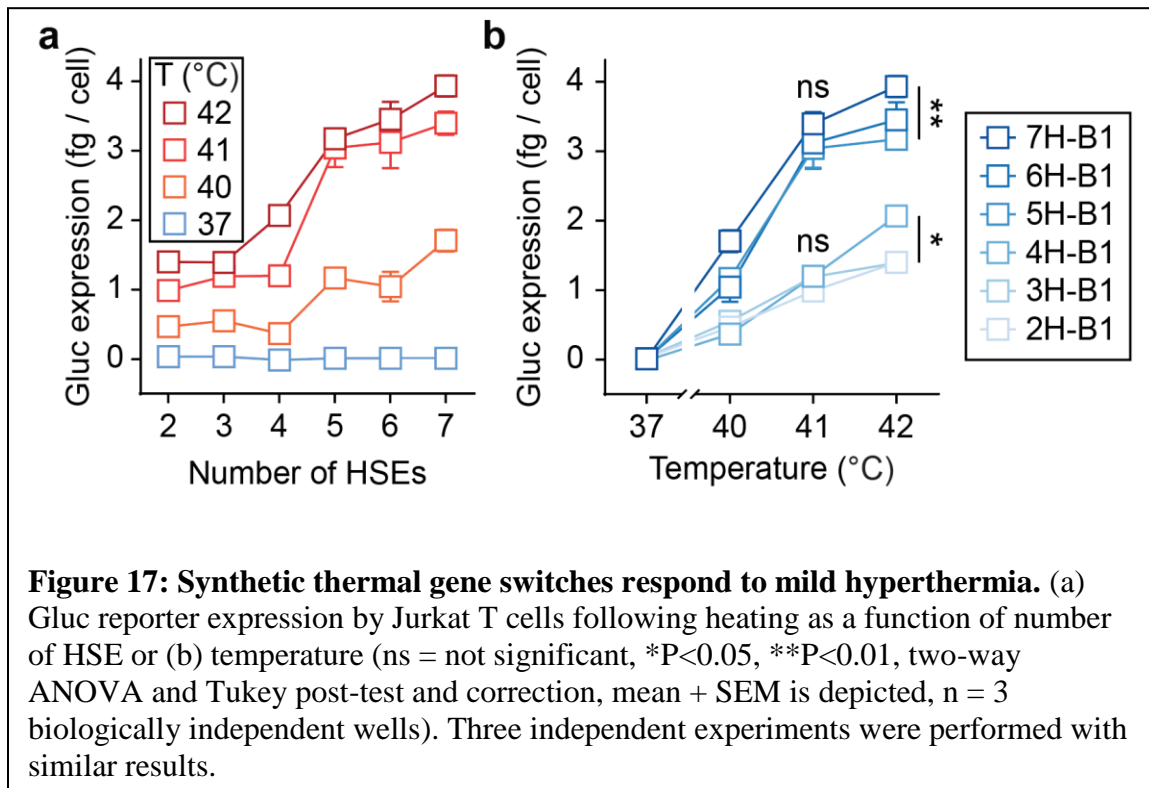


**Figure 16: qPCR of screen of HSPs in primary murine T cells.** Splenic CD8+ T cells were isolated using the CD8+ T cell isolation kit according to (Miltenyi 130-104-075). 6 hours after indicated heat treatments, mRNA was harvested and quantified using the Mouse HSP profiler kit (Qiagen PAMM-076Z) according to manufacturer instructions. Data are displayed relative to unheated controls.

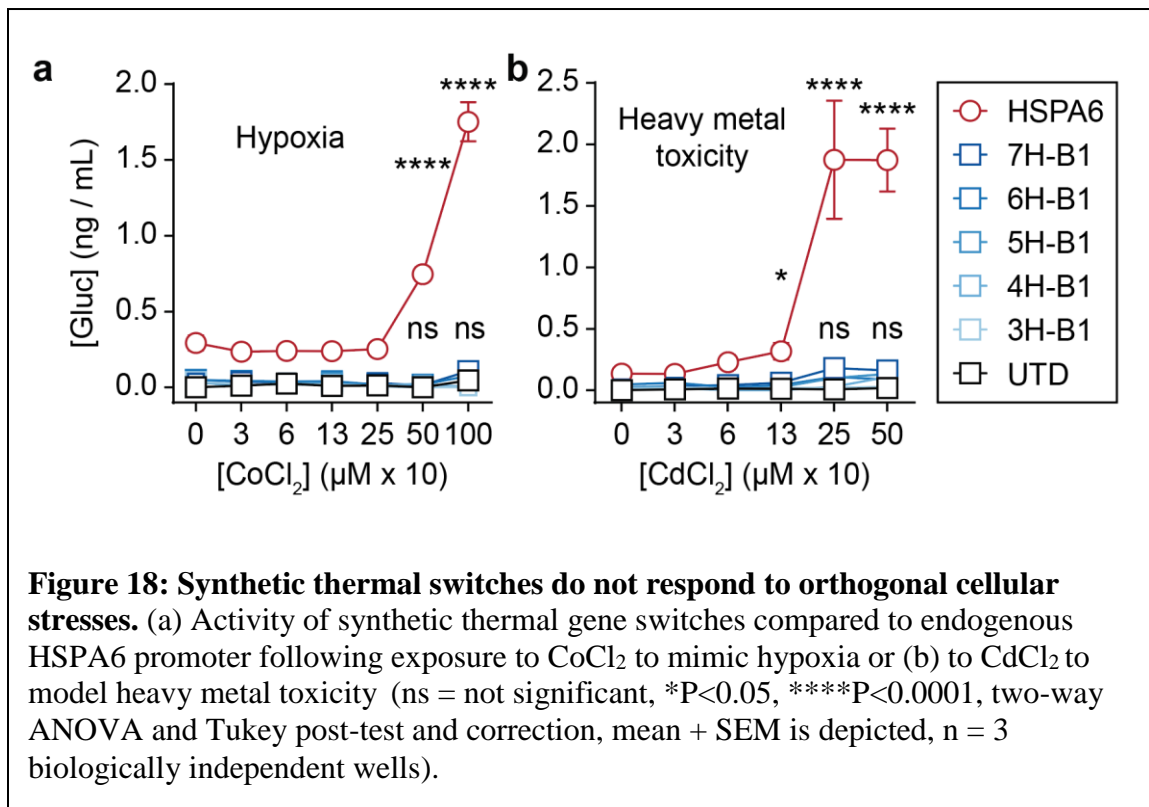
cross-activation of HSP promoters by non-thermal response pathways, we sought to build synthetic gene switches that are activated by heat but not by other sources of stress.

To design thermal-specific gene switches, we cloned 6 candidate constructs comprised of 2 to 7 repeats of the HSE motif 5'-nGAAnnTTCnnGAAn-3' upstream of the Hspb1 core promoter into Jurkat T cells (labeled 2H-B1 to 7H-B1, Figure 15). We initially selected the Hspb1 core promoter as its parent gene was one of two that were upregulated by more than 20-fold at 42 °C in primary murine T cells in contrast to more than 80 HSP and HSP-related genes that did not respond to heat treatment (Figure 16). We reasoned that by selecting a core promoter from an endogenous gene with a high thermal response, it would facilitate transcriptional activity when integrated with HSE repeats. To quantify responses of our thermal switches, transduced Jurkat T cells were transiently heated to 3–5 °C above body temperature (i.e., 40–42 °C), a mild temperature range in contrast to those used for ablative therapies (>50 °C)<sup>146</sup>. Compared to control samples at 37 °C, we observed



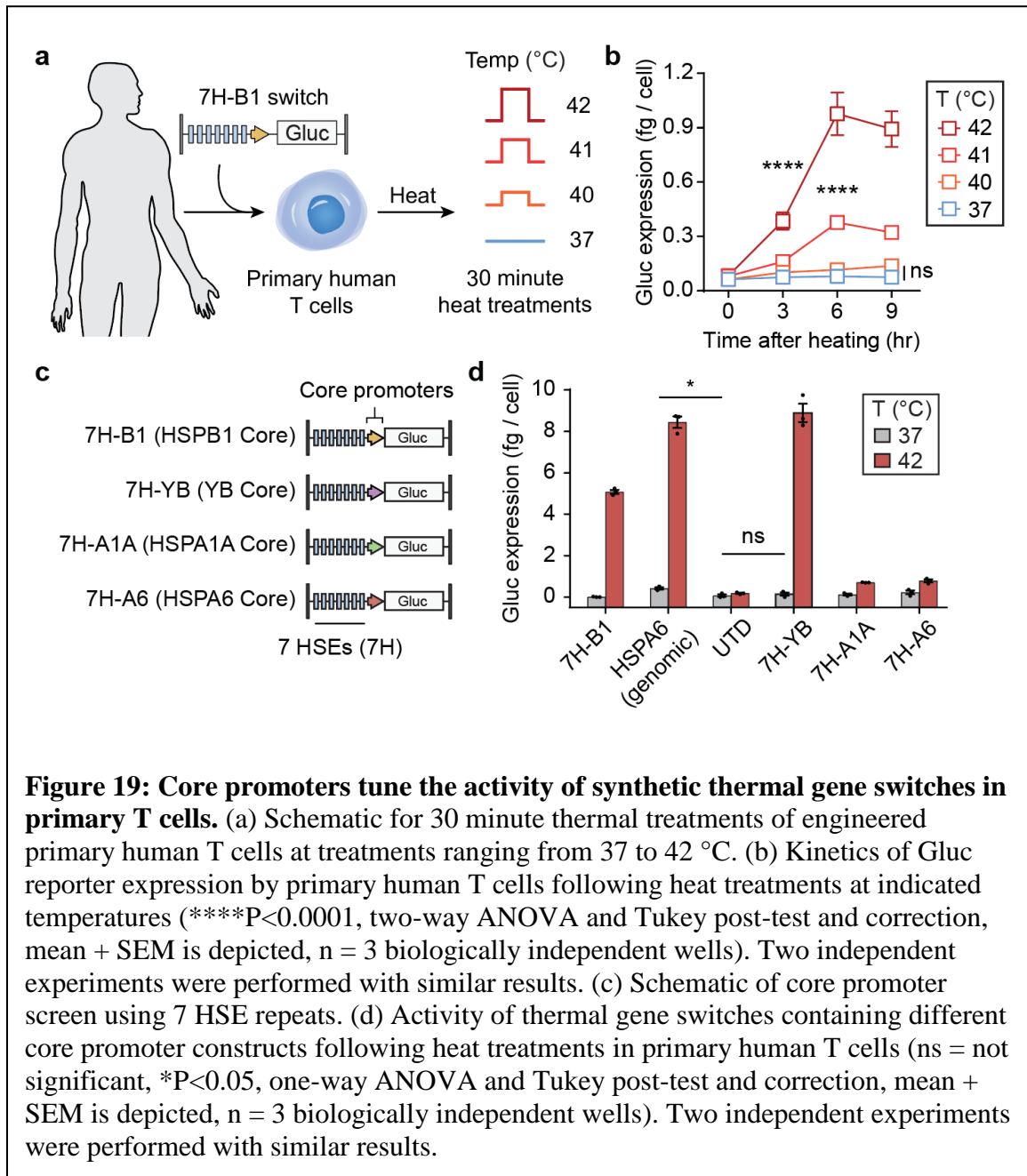
increased expression of the reporter *Gussia luciferase* (Gluc) as the temperature and number of HSEs increased (Figure 17a). Constructs containing 5–7 HSE repeats (5H-B1 to 7H-B1) resulted in significantly higher thermal responses compared to those with 2–4 HSEs (2H-B1 to 4H-B1) (Figure 17b). Collectively, these data confirmed that our synthetic thermal gene switches were heat-sensitive and that the magnitude of the response was dependent on HSE number.

We next tested thermal specificity using hypoxia and heavy metal toxicity as two representative non-thermal stresses<sup>212-214</sup>. As a benchmark, we compared with the endogenous HSPA6 promoter, which is a highly stress-inducible HSP promoter<sup>215</sup> previously used for thermal control of gene expression<sup>216-219</sup>. We tested the gene switches by incubating transduced Jurkat T cells with the hypoxia-mimetic agent  $\text{CoCl}_2$  – a stabilizer of the hypoxia response’s master regulator Hypoxia Inducible Factor-1 $\alpha$  (Hif-1 $\alpha$ )<sup>220</sup> – as

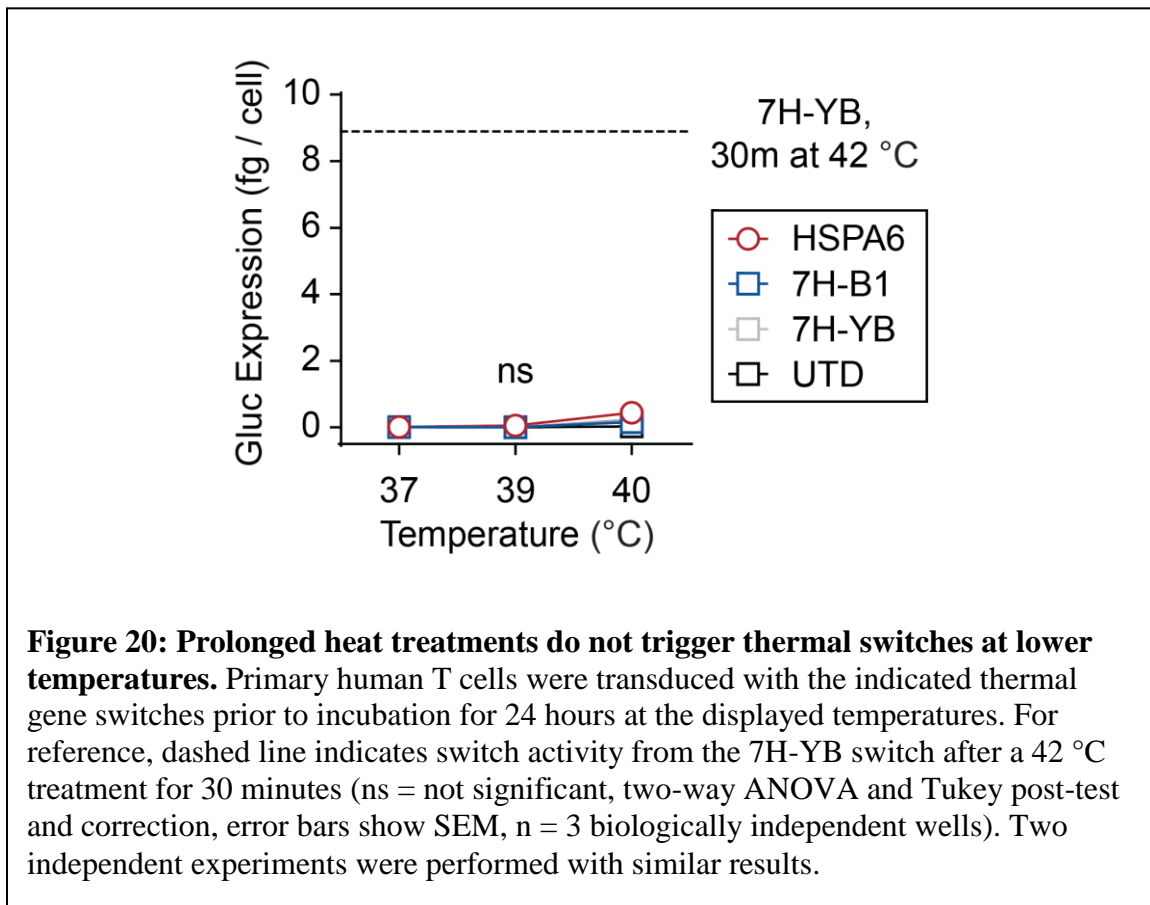


well as the heavy metal complex cadmium chloride ( $\text{CdCl}_2$ ). Whereas Jurkat T cells cloned with the HSPA6 promoter showed dose-dependent activation by hypoxia (Figure 18a) and cadmium toxicity (Figure 18b), T cells transduced with our synthetic gene switches (3H-B1 to 7H-B1) were not activated and remained statistically identical to untransduced (UTD) controls up to concentrations above the ranges commonly used to test cellular responses to hypoxia and cadmium<sup>220-223</sup> ( $1000 \mu\text{M CoCl}_2$  and  $500 \mu\text{M CdCl}_2$ ) (Figure 18a, b). These results confirmed that our synthetic gene switches have increased thermal-specificity compared to endogenous HSPs and are not cross-activated when exposed to non-thermal stresses.

To test whether these constructs work in primary human T cells, we transduced T cells with the 7H-B1 thermal switch (Figure 19a). Above a threshold temperature of 40 °C, we observed thermal switch activation that peaked between 3 to 6 hours after heating but was ~40% less responsive compared to the endogenous HSPA6 (Figure 19b-d). Because the Hspb1 core promoter was initially selected from a screen of murine T cells, we reasoned



that thermal responses in primary human T cells may be further tuned with different core promoters. Thus, we compared additional core promoters including ones cloned from the HSPA1A gene identified in the qPCR screen (Figure 16), the human HSPA6 gene, and a synthetic core promoter (YB) described previously<sup>224, 225</sup> (Figure 19c). Consistent with our previous observations, we observed negligible activation with heat treatments at 37–40 °C for 24 hours across all 4 constructs tested (Figure 20). By contrast, after 30 minutes at 42 °C, the 7H-YB construct produced the highest Gluc reporter levels while maintaining statistically identical basal activity at 37 °C compared to untransduced controls. This corresponded to a ~60-fold increase in thermal switch activity compared to ~20-fold increases by the endogenous HSPA6 (Figure 19d). On the basis of these data, we selected

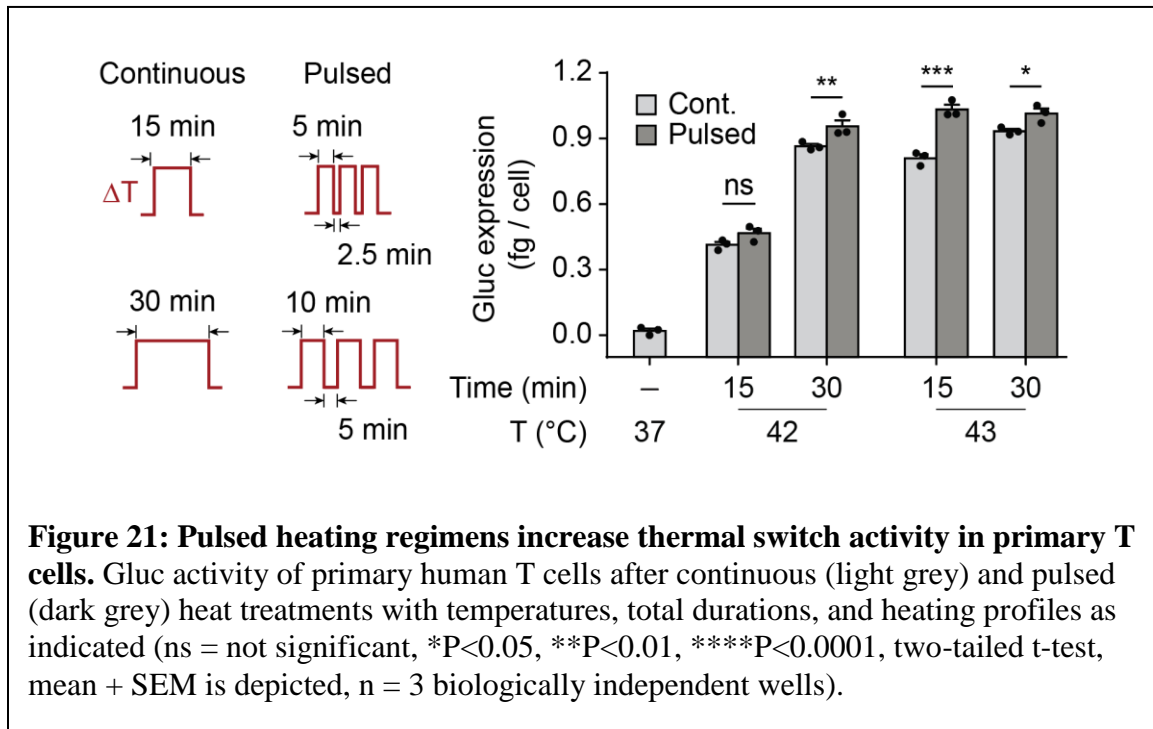


7H-YB for subsequent experiments due to its improved thermal specificity and high thermal response.

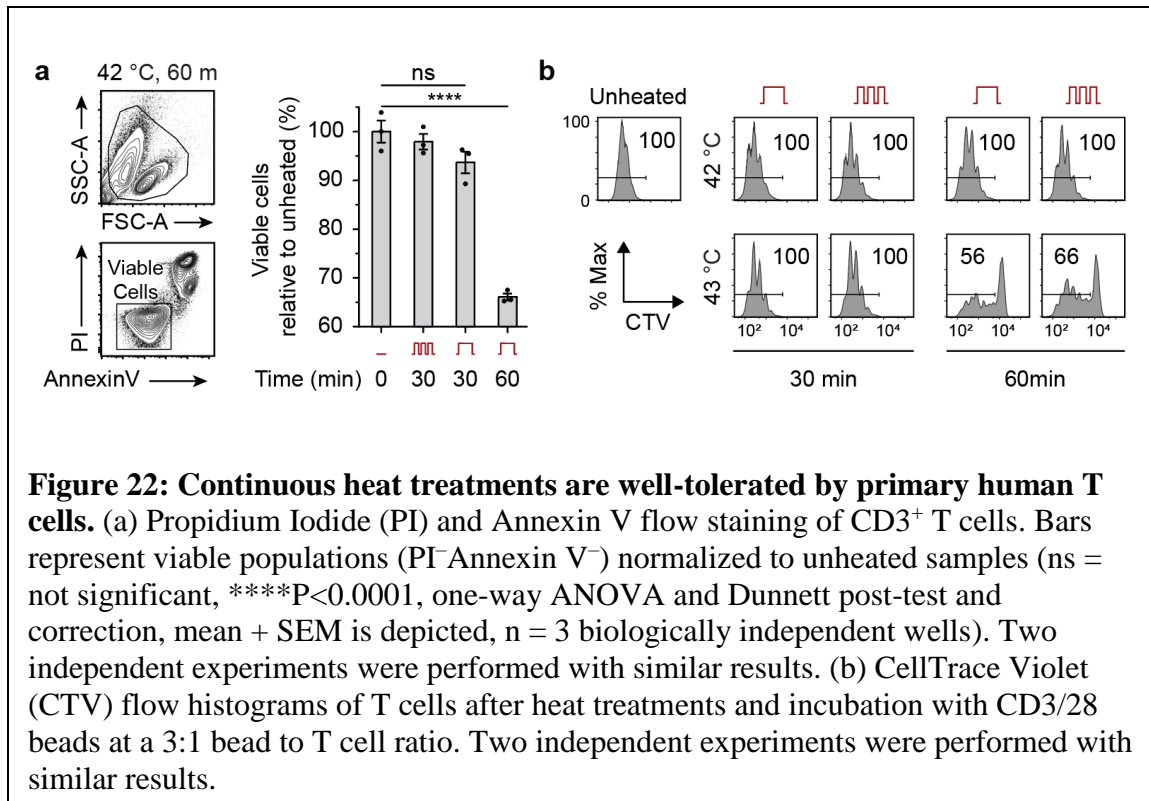
### *1.11.2 Primary T cells maintain key functions after thermal treatments*

Next, we sought to identify the range of thermal delivery profiles that would be well-tolerated by primary T cells without affecting key functions including proliferation, migration, and cytotoxicity. In thermal medicine, heating target sites to temperatures greater than 50 °C is used to locally ablate tissue by inducing tumor cell apoptosis and coagulative necrosis<sup>146</sup>. By contrast, mild hyperthermia therapy (40–42 °C) is used to enhance transport of small molecules such as in Hyperthermic Intraperitoneal Chemotherapy (HIPEC) where abdominal infusions of heated chemotherapy serve as adjuvant treatment following surgical debulking in advanced ovarian cancer patients<sup>147, 226, 227</sup>. At temperatures below 45 °C, transient exposure to mild hyperthermia is well-tolerated by cells and tissues due to induction of stress-response pathways including HSPs<sup>228</sup>. In addition to temperature range, we also considered T cell responses to continuous and fractionated heat treatments. Dose fractionation is a commonly used approach in radiotherapy to reduce damage to normal tissues<sup>229</sup> while maximizing the effect of radiation on cancer. Based on our previous observations that thermal pulse trains increased Jurkat T cell tolerance compared to continuous heat treatments with an identical treatment

area-under-the-curve (AUC)<sup>230</sup>, we sought to additionally probe the effect of thermal dose fractionation on primary T cells.



We first compared pulsed heat treatments at 67% duty cycles comprised of three discrete thermal pulses (5 or 10 min each) separated by intervening rest periods at 37 °C (2.5 or 5 min each) to their unfractionated counterparts (15 or 30 min continuous heating) (Figure 21). Across the conditions tested, we observed significant increases in Gluc reporter expression with pulsed heat treatments at 42 (30 min AUC) and 43 °C (15 and 30 min AUC) by up to ~30% compared to continuous delivery. To assess T cell viability, we quantified death (PI) and apoptotic (Annexin V) markers and observed no significant difference in viability between unheated, pulsed, and continuously heated samples for up to 30 minutes (Figure 22a). By contrast a ~34% reduction in T cell viability was observed in positive control samples that were continuously heat treated for 60 minutes. Similar



trends were observed in T cell proliferation assays by dye (CTV) dilution where the percent of proliferated T cells following incubation with CD3/28 beads was unaffected by both continuous and pulsed heating for 30 minutes at 42 or 43 °C while positive control samples that were heated for 60 minutes resulted in reduced T cell proliferation (Figure 22b).

To probe the effects of thermal treatments on T cell migration, we used transwell assays to assess T cell chemotaxis and observed that heat treatments (42 °C for 30 min) did not significantly affect T cell migration into lower wells containing the chemokine CXCL12 compared to unheated controls whereas T cells heated to 50 °C were affected (Figure 23a). To test longitudinal activation, we re-heated T cells over the course of 8 days and observed similar increases in GFP mean fluorescent intensity (MFI), as well as GFP activation and decay half-lives ( $t_{1/2}$  ~0.5 and 1 day, respectively), suggesting that the magnitude and kinetics of T cell responses are unaffected by multiple heat treatments

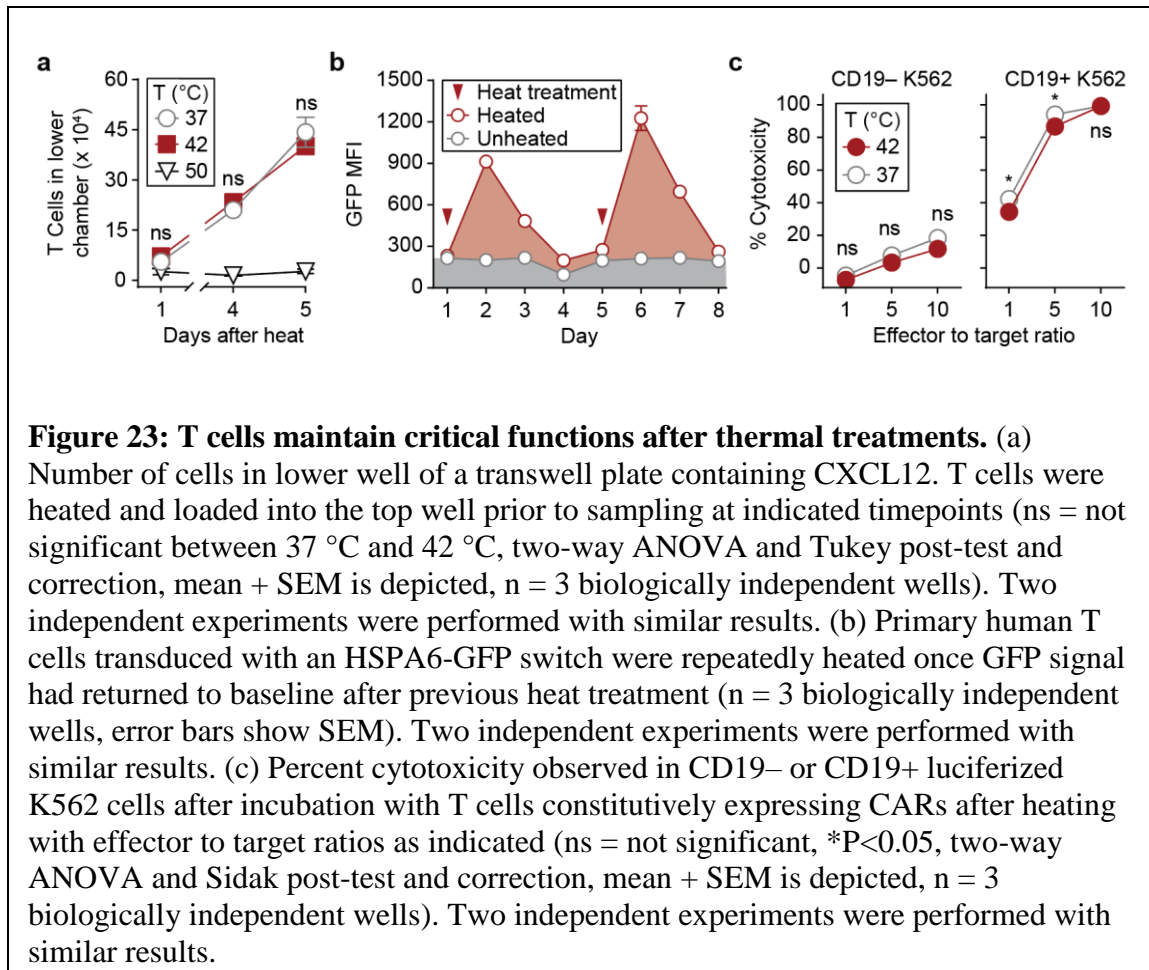
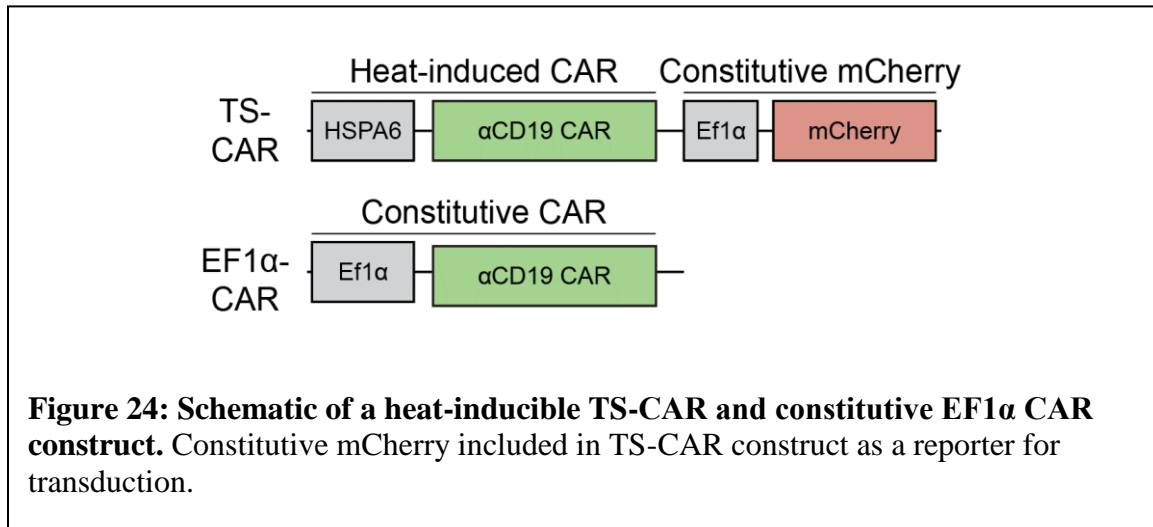
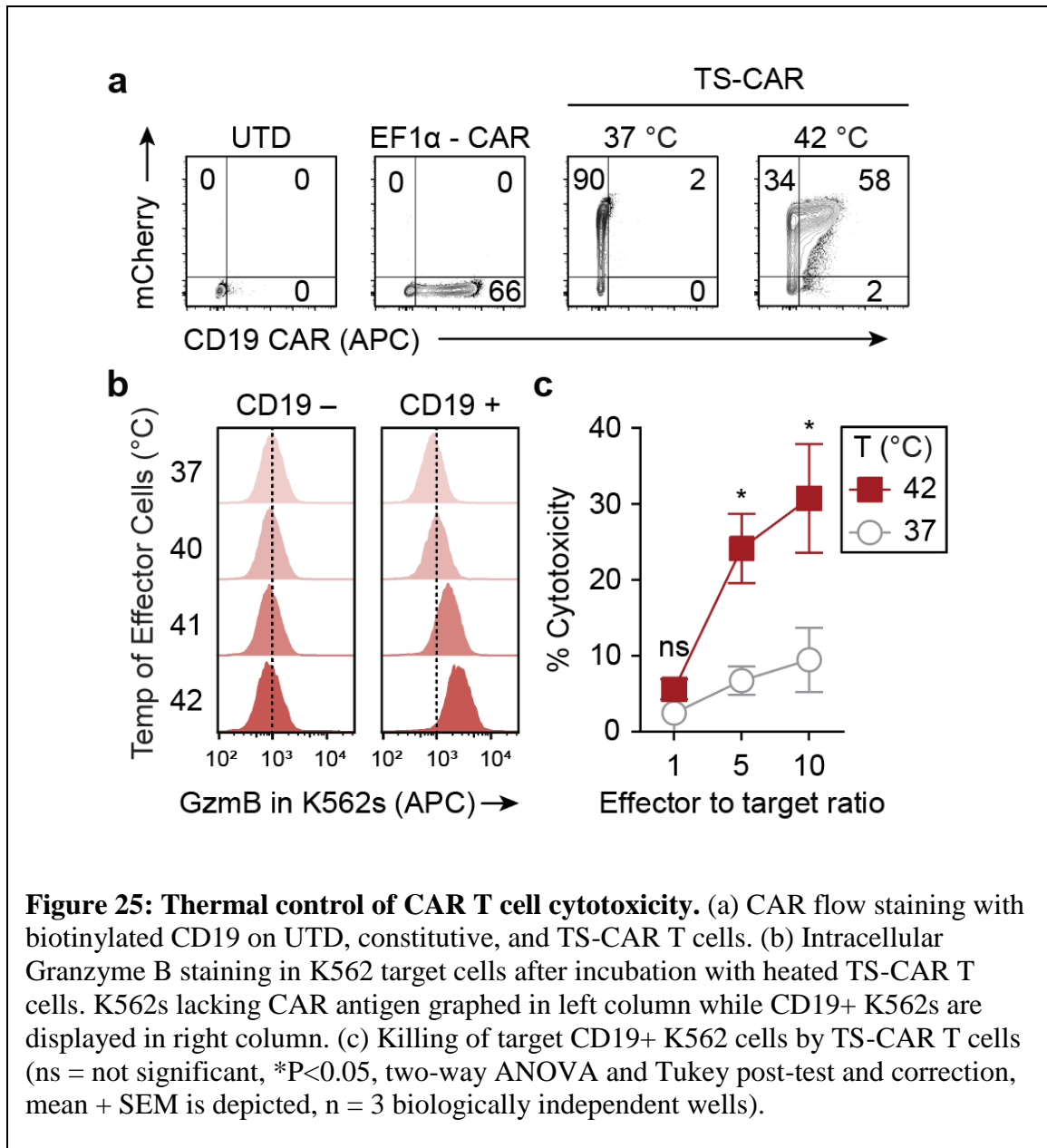


(Figure 23b). To quantify the effect of heat on T cell cytotoxicity, we incubated primary human T cells expressing an  $\alpha$ CD19 CAR under a constitutive EF1 $\alpha$  promoter with either CD19+ or CD19- K562s containing a luciferase reporter to allow quantification of cell death by loss of luminescence (Figure 23c). At all effector to target cell ratios tested (1:1, 5:1, 10:1), heated T cells maintained greater than 90% of the cytotoxicity observed in unheated samples while no significant difference in cytotoxicity was observed in samples containing CD19- K562 target cells (Figure 23c). Collectively, these data demonstrate that primary human T cells maintain the ability to proliferate, migrate, and kill target cells following short heat treatments delivered in continuous or pulsed wave forms for less than 30 minutes in duration.

### 1.11.3 Thermal control of CAR T cell functions



The factors that contribute to durable anti-tumor responses include the degree to which key steps in the immunity cycle can be effectively directed against tumors<sup>3</sup>. Here we sought to build thermal circuitry to allow control over key CAR T functions including proliferation, antigen recognition, and T cell killing. We first explored thermal control of CAR T cell killing where the expression of an  $\alpha$ CD19 CAR was placed under control of a thermal switch (TS-CAR) (Figure 24). Following heat treatment, TS-CAR T cells expressed  $\alpha$ CD19 CARs to levels comparable to control T cells transduced with a constitutive vector (EF1 $\alpha$ -CAR) (Figure 25a). To test heat-triggered control of cytotoxicity, we heated TS-CAR T cells across a range of activation temperatures (40, 41, and 42 °C) and incubated them with either CD19<sup>-</sup> or CD19<sup>+</sup> K562 target cells. We observed that intracellular Granzyme B levels – a cytotoxic effector molecule released by T cells – increased in CD19<sup>+</sup> target cells as a function of temperature in contrast to control cells that lacked the CAR antigen (Figure 25b). This was further supported by a TS-CAR T cell killing assay where we observed significant increases in CD19<sup>+</sup> K562 cell death as the effector to target cell ratio was increased following thermal treatments at 42 °C (Figure 25c).



We further sought to determine whether thermal control could enhance T cell activation and proliferation. To do this, we cloned a single-chain IL-15 superagonist (IL-15 SA) comprised of the cytokine tethered to the sushi domain of the IL-15R $\alpha$  subunit<sup>231</sup> under control of our thermal vector (TS-IL15). IL-15 SAs are potent stimulants of CD8 T cells and NK cells and a clinical candidate, ALT-803, is currently under investigation for a wide range of cancers<sup>78, 232</sup>. To verify heat-triggered secretion of IL-15 SA, we analyzed

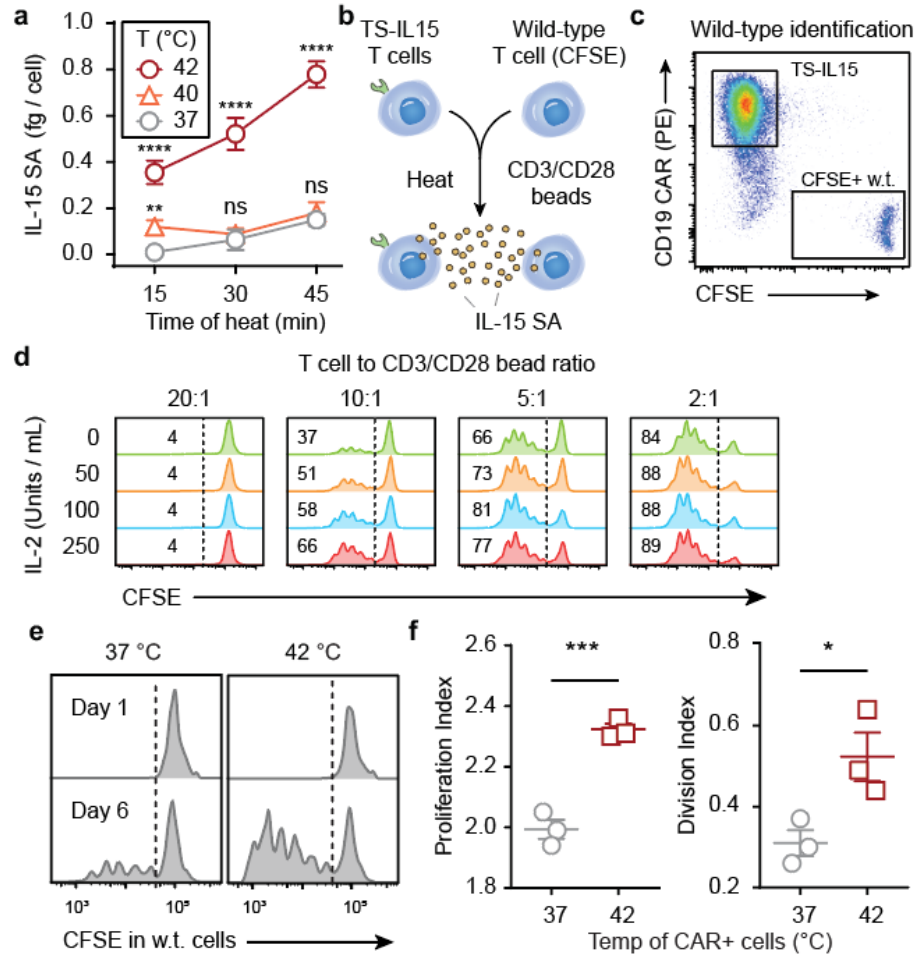
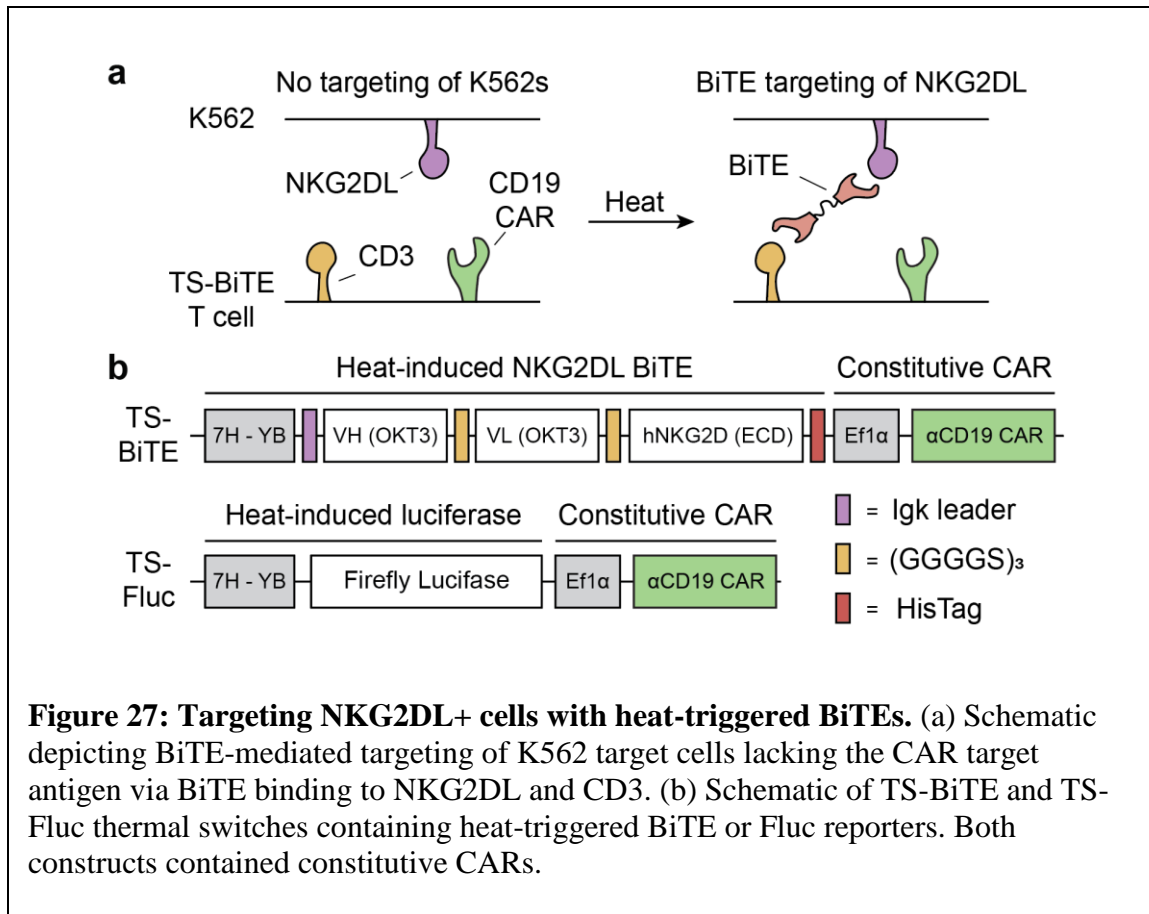
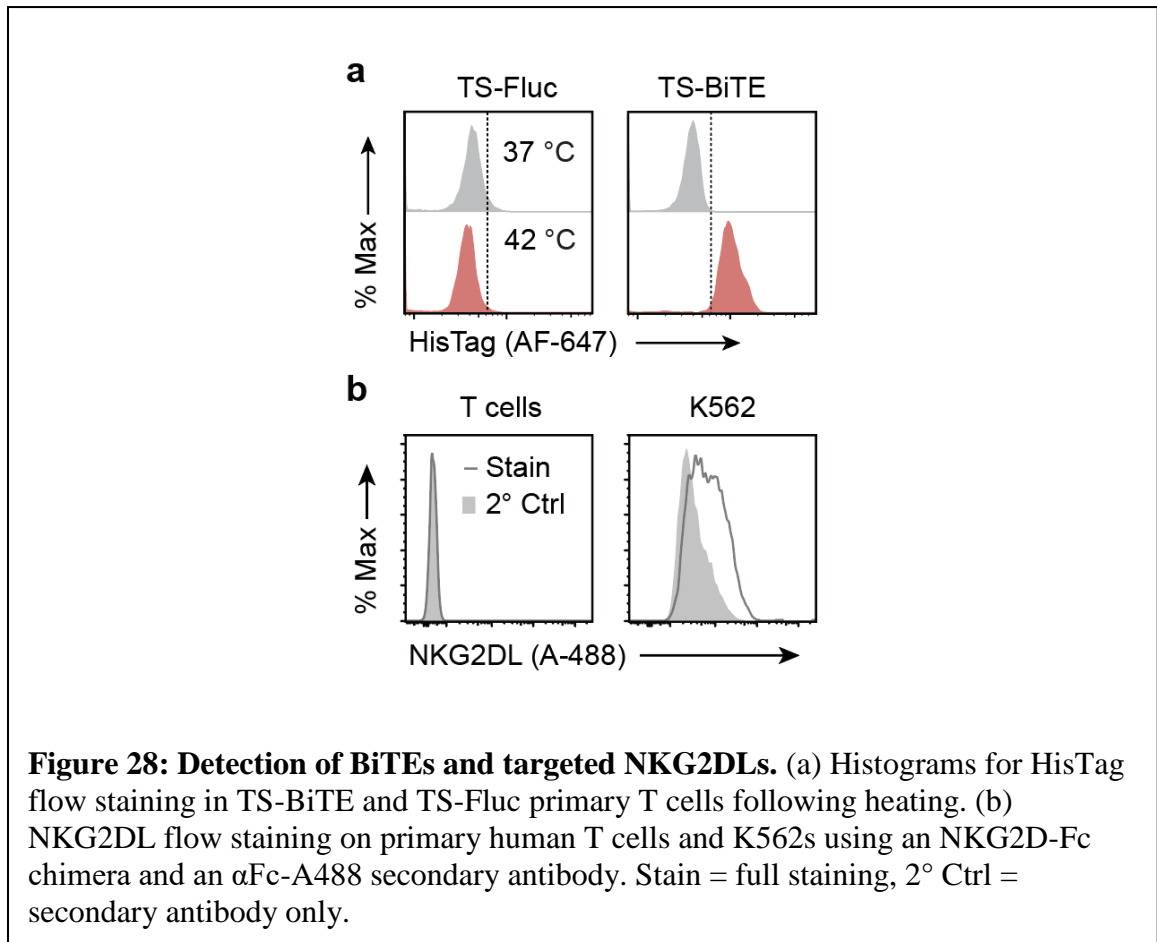


**Figure 26: Thermal control of T cell proliferation.** (a) IL-15 superagonist concentrations in supernatant of TS-IL15 T cells following heat treatments. Temperature and duration of treatments are as indicated (ns = not significant,  $**P < 0.01$ ,  $****P < 0.0001$ , two-way ANOVA and Tukey post-test and correction, mean + SEM is depicted,  $n = 3$  biologically independent wells, comparisons are to unheated control). Two independent experiments were performed with similar results. (b) Experimental design for co-culture assay of TS-IL15 cells and CFSE-labeled wild-type cells. CD3/28 beads were added at 1:10 bead to T cell ratio. (c) Gating strategy for mixed proliferation experiment. Transduced TS-15 cells were identified by CAR expression. Proliferation of CFSE+ wild-type cells was assessed by dye dilution and FlowJo proliferation tool. (d) T cells were labeled with CFSE and incubated with low levels of activating beads. For reference, routine expansion and culture of T cells uses 3 beads for every T cell. Increasing amounts of IL-2 were added to each bead ratio. All samples were assayed after 4 day incubations at indicated conditions. Two independent experiments were performed with similar results. (e) Representative flow histograms and (f) quantified proliferation and division indices as calculated by FlowJo proliferation tool of the CFSE-labeled wild-type T cell population ( $*P < 0.05$ , two-tailed t-test, mean + SEM is depicted,  $n = 3$  biologically independent wells).

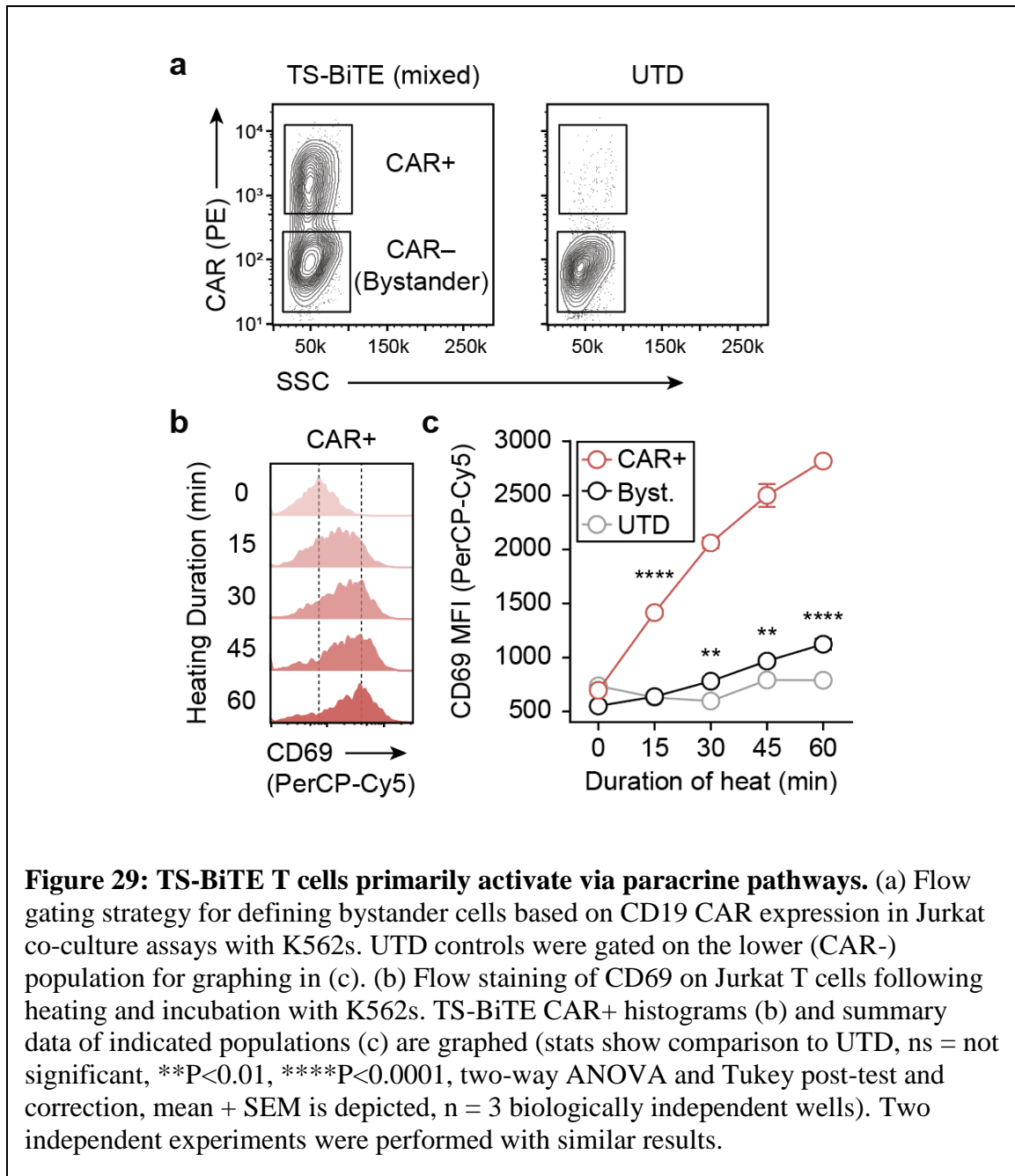


conditioned media by ELISA and found that IL-15 SA levels increased with the duration and temperature of thermal treatment (Figure 26a). To test whether heat-induced IL-15 SA was functionally active, we developed a T cell proliferation assay using CFSE-labeled wild-type T cells incubated with CD3/28 beads at a 10:1 ratio without supplemental cytokines. We found that this condition was insufficient to induce T cell proliferation compared to conditions when cytokines such as IL-2 was present in media (Figure 26b-d). Therefore, to test thermal control of IL-15 SA, we added heated or unheated TS-IL15 T cells to samples containing CFSE-labeled wild-type T cells with CD3/28 beads at a 10:1 T cell to bead ratio (Figure 26b-d). Compared to unheated controls, we found that CFSE-labeled T cells in heated samples expanded with significantly higher proliferation and

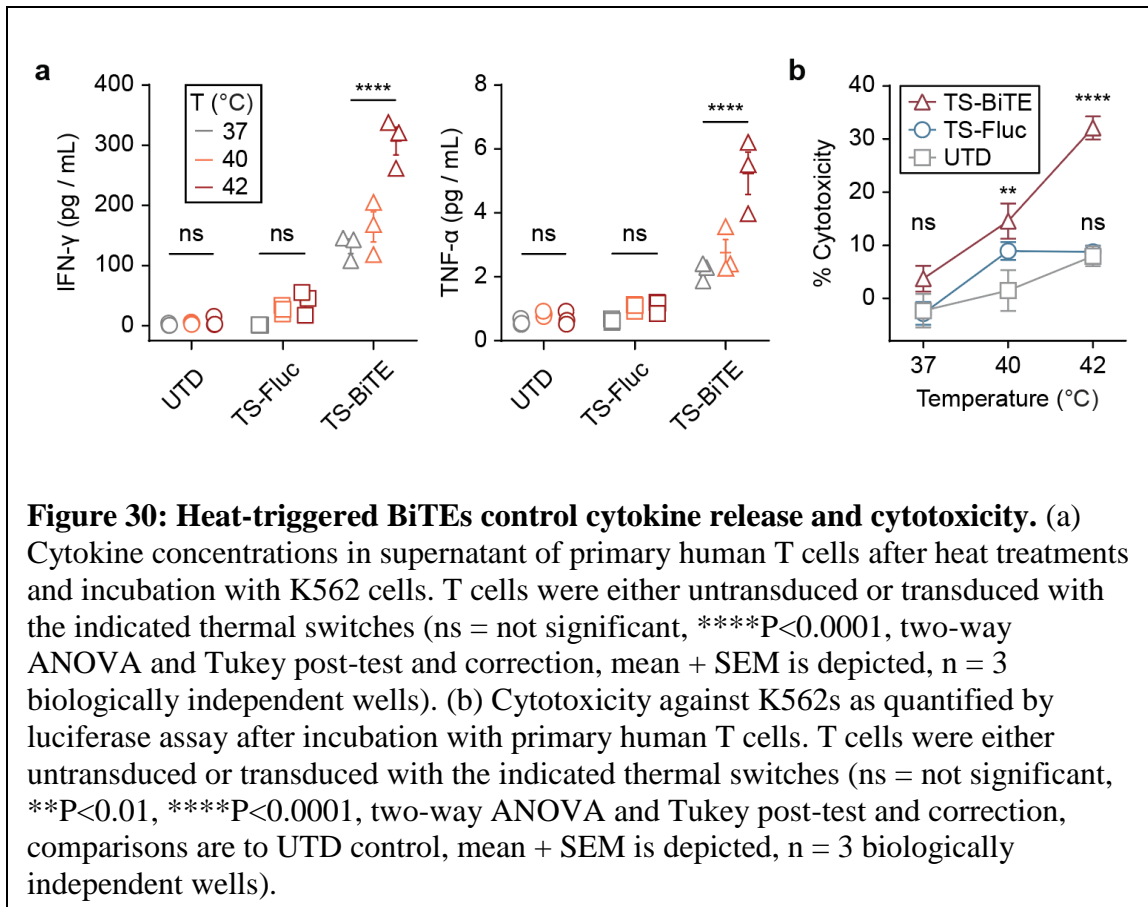
division indices (Figure 26e, f), demonstrating that TS-IL15 T cells are capable of producing physiologically active levels of IL-15 SA following a single thermal treatment.



Last, we explored thermal control to expand CAR T recognition of tumor-associated antigens to include NKG2D ligands (NKG2DLs), which are upregulated on a wide range of cancers as well as suppressor cells<sup>26, 233-235</sup>. Targeting NKG2DLs is limited by their expression in healthy cells such as intestinal epithelial cells and bone marrow stromal cells<sup>25</sup>. To enable thermal control of CAR T cells to target NKG2DL+ cells, we cloned a previously described NKG2DL-BiTE containing CD3-recognition domains from the OKT3 antibody linked to the extracellular domain of the human NKG2D receptor<sup>235</sup>. Our vector (TS-BiTE) included an I $\kappa$ g leader sequence for BiTE secretion, a HisTag



reporter, and a constitutive  $\alpha$ CD19 CAR (Figure 27a, b). After heat treatment, we observed that TS-BiTE T cells were stained positively on the cell surface by anti-HisTag antibodies compared to control cells transduced with a Fluc reporter vector (TS-Fluc) (Figure 28a). Based on this, we postulated that T cells would activate by local BiTE binding to CD3 expressed by the same T cell (i.e., autocrine activation) before additional BiTEs would



engage bystander T cells (i.e., paracrine activation). To test this, we heated a mixture of TS-BiTE transduced Jurkat T cells (i.e., CAR+) with untransduced cells (i.e., CAR-) as bystanders prior to co-incubation with NKG2DL+ CD19- K562 target cells (Figure 28b, Figure 29a). This experimental setup allowed us to isolate T cell activation based on BiTE engagement without confounding factors due to CD19 CAR binding. We found that expression of the early activation marker CD69 on TS-BiTE Jurkat T cells was significantly upregulated compared to bystander cells as heating durations were extended (red versus black) (Figure 29b, c). By contrast, CD69 was minimally upregulated on bystander cells compared to untransduced (UTD) Jurkat T cells that were incubated with K562 cells and heated in separate wells as controls (black versus gray). These data provided support that TS-BiTE T cells are primarily activated to target NKG2D ligands in an

autocrine path. Finally, to quantify cytotoxicity from heat-triggered expression of BiTEs, we co-incubated primary human TS-BiTE T cells with NKG2DL+ CD19- K562 cells. In contrast to untransduced or TS-Fluc controls, TS-BiTE T cells secreted increasing levels of T<sub>h</sub>1 cytokines IFN- $\gamma$  and TNF- $\alpha$  as temperatures were raised from 37 to 42 °C (Figure 30a). We also observed temperature-dependent increases in K562 cytotoxicity but not at 37 °C compared to UTD controls, demonstrating lack of BiTE-induced killing at basal temperatures (Figure 30b). Taken together, our data showed that thermal control can be extended to broad classes of immunomodulatory molecules to direct CAR T cell functions including proliferation, targeting, and cytotoxicity.

#### 1.11.4 Photothermal targeting of CAR T cells enhances anti-tumor therapy

We next sought to determine whether thermal control of CAR T cells would enhance efficacy of adoptive therapies. To locally heat tumors, we used plasmonic gold nanorods (AuNRs) as antennas to convert incident near infra-red (NIR) light (~650-900 nm) into heat<sup>171</sup>. PEG-coated AuNRs are well-studied nanomaterials with long circulation times that

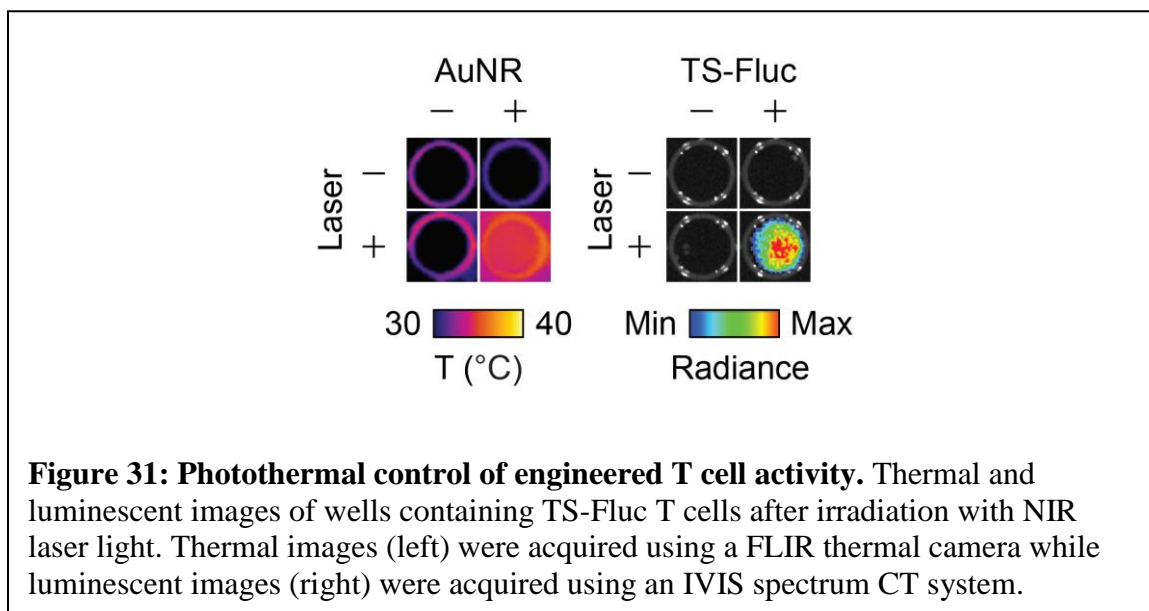
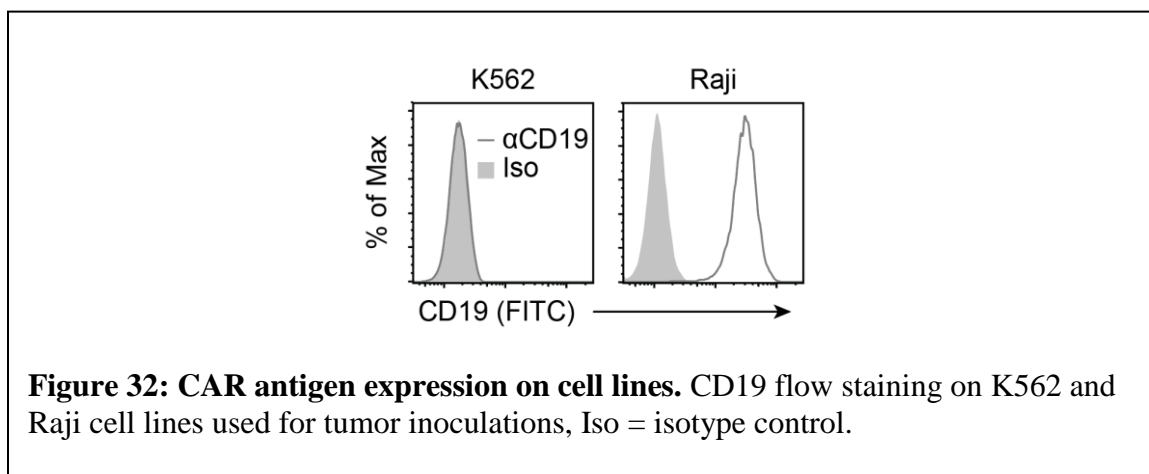


**Figure 31: Photothermal control of engineered T cell activity.** Thermal and luminescent images of wells containing TS-Fluc T cells after irradiation with NIR laser light. Thermal images (left) were acquired using a FLIR thermal camera while luminescent images (right) were acquired using an IVIS spectrum CT system.

passively accumulate in tumors following intravenous administration<sup>184, 236</sup>. To confirm photothermal heating and thermal switch activation, primary T cells transduced with TS-Fluc were co-incubated with AuNRs in 96-well plates and irradiated with 808 nm laser light. In wells that reached 40–45 °C as monitored by a thermal camera, we observed a marked increase in luminescent signals when TS-Fluc T cells were present but not in wells containing untransduced controls (Figure 31), confirming plasmonic photothermal control of engineered T cells.



To implement photothermal targeting in living mice, we inoculated NSG mice with bilateral flank tumors with one cohort receiving CD19– K562 cells and a separate cohort receiving CD19+ Raji cells to model CAR antigen positive and negative tumors (Figure 32 and Figure 33a). Following intravenous injection of AuNRs and adoptive transfer of T cells with constitutively expressed  $\alpha$ CD19 CAR and thermal Fluc (TS-Fluc vector), we irradiated tumors with NIR laser light under the guidance of a thermal camera (Figure 33b) to maintain target skin temperatures (Figure 33c). After 20-minute heat treatments, luminescence was contained within Raji tumors receiving NIR light with Fluc activity upregulated greater than 30-fold at these sites compared to unheated Raji tumors in the

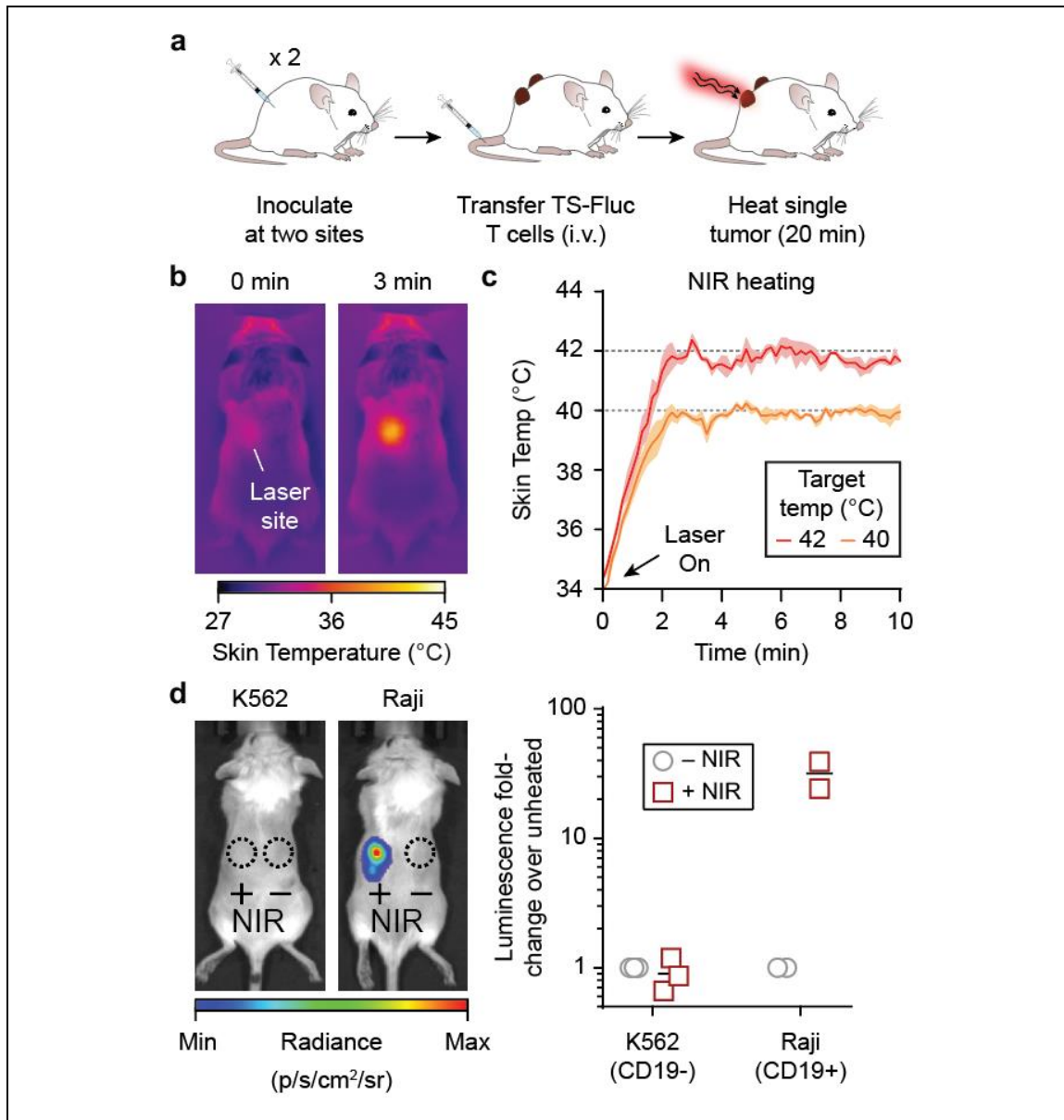
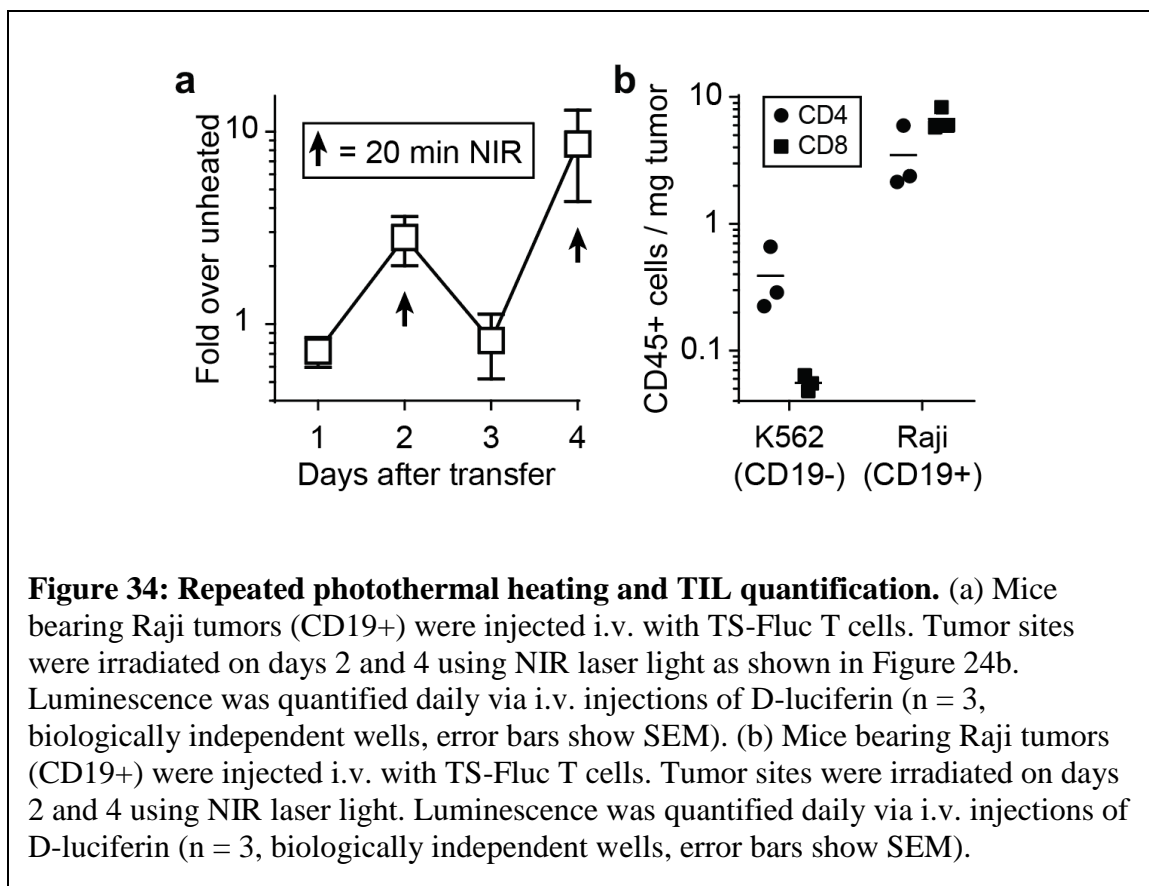


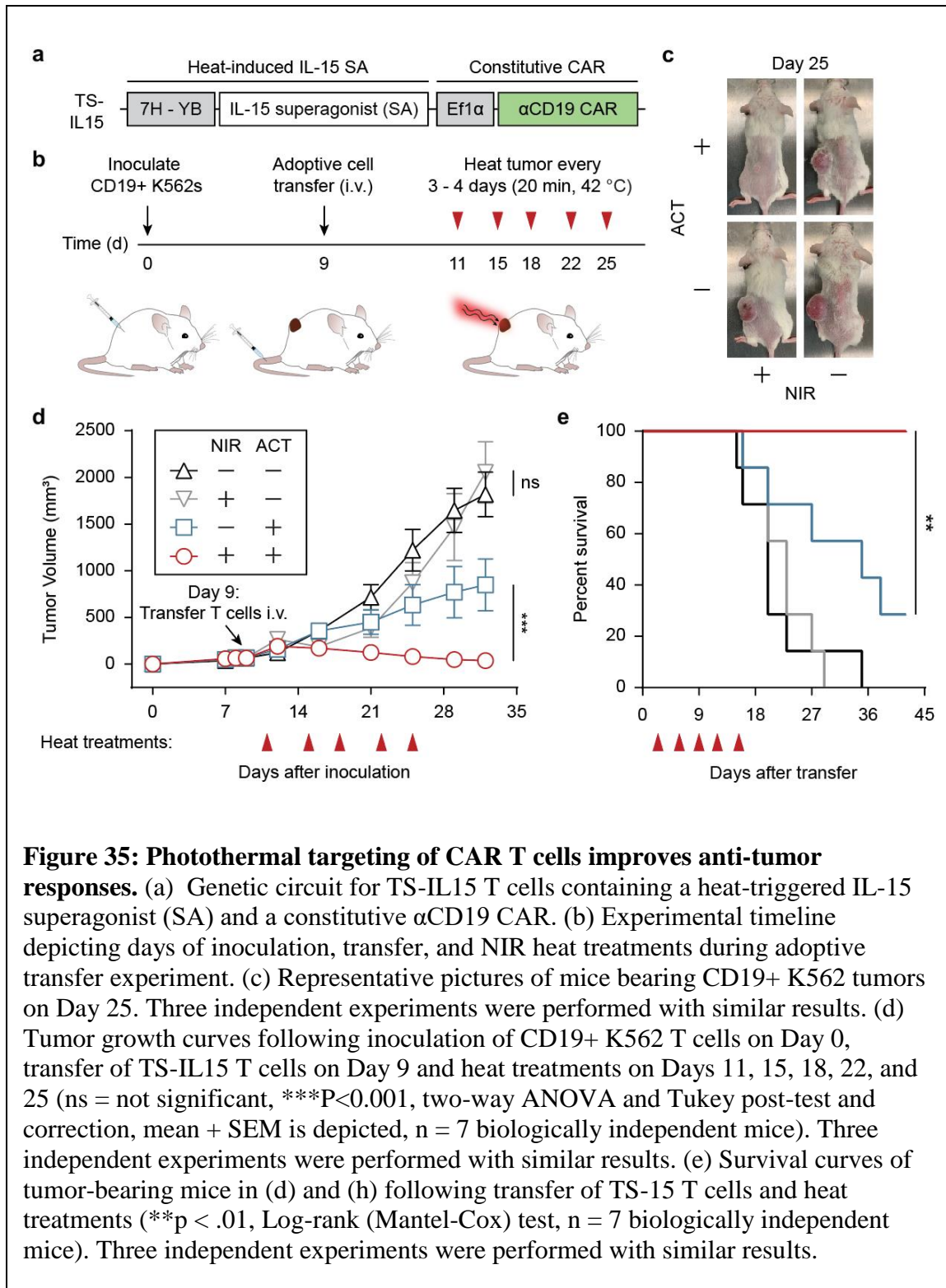
**Figure 33: Remote control of intratumoral T cell activity.** (a) Schematic for experimental timeline where both flanks of each mouse were inoculated with the same cell line. TS-Fluc T cells were transferred via intravenous tail-vein injections and only one side of the mouse was heated. (b) Serial thermal images of tumor-bearing mouse during laser irradiation to heat tumor site. Timepoints are as indicated. (c) Thermal kinetic traces (colored lines) show average skin temperature of a 3 x 3 pixel ROI centered on laser site. Shaded regions around traces show standard deviation of 3 heating runs on a representative mouse that did not receive engineered T cells. (d) Left: Luminescent images of heated mice bearing either K562 (CD19-) or Raji (CD19+) tumors. Signal indicates luciferase activity by transferred TS-Fluc T cells. Right: Luminescence of each tumor site relative to the luminescence from the unheated tumor in the same animal. ROI's were drawn as indicated in left panel (n = 2-3 biologically independent mice).

same animal (Figure 33d). Similar to *in vitro* experiments, CAR T cells could be repeatedly



activated in Raji tumors (Figure 34a) but by contrast, we did not observe increased activity within antigen-negative K562 tumors following NIR heating (Figure 33d). We attributed this lack of heat-induced activity to the greater than 20-fold lower density of intratumoral CAR T cells in resected K562 tumors that lack the CD19 CAR antigen (Figure 34b). Collectively these data demonstrate that the activity of intratumoral T cells engineered with thermal gene switches can be controlled by localized photothermal heating.

To augment CAR T cell therapies by thermal targeting, we adoptively transferred T cells transduced with TS-IL15 vector into NSG mice bearing CD19+ K562 tumors to allow thermal control of the single-chain IL-15 superagonist by cells constitutively expressing an  $\alpha$ CD19 CAR (Figure 35a). Photothermal heating of tumors was then carried out every 3-4 days (Days 11, 15, 18, 22, and 25) for a total of five treatments (Figure 35b). Compared to



control mice that did not receive CAR T cells or heat treatments (black), thermal treatment of tumor sites alone did not lead to reduction in tumor burden or improvement in survival

(gray) (Figure 35c-e). Transfer of TS-IL-15 CAR T cells alone significantly reduced tumor burden and improved survival (blue) yet greater than 70% (5/7) of animals reached euthanasia criteria within 38 days of ACT. By contrast, ACT of TS-IL15 CAR T cells combined with NIR treatments markedly reduced tumor burden and no animals reached euthanasia criteria within the time window of the study. Together, these data demonstrated that thermal targeting of tumors to control CAR T cell production of an IL-15 superagonist significantly improved tumor control and therapeutic outcomes.

## 1.12 Discussion

Here we developed a platform for remote thermal control of T cell activity. Remote control of T cells by small-molecules or light<sup>140, 237</sup> either require systemic administration or are limited by light penetration through tissue. By contrast, thermal targeting of tissues can be accomplished by several platforms<sup>146</sup> including focused ultrasound, which was recently demonstrated for control of T cell gene expression<sup>238</sup> or thermal control of bacteria engineered with temperature-sensitive repressors<sup>152</sup>. To provide T cells the capacity to respond to heat, we designed synthetic thermal gene switches comprised of arrays of heat shock elements upstream of a core promoter. This architecture eliminated sensitivity to non-thermal stresses such as hypoxia and its thermal response was tunable based on the number of HSEs or different core promoters. While we tested constructs containing up to 7 HSEs paired with 4 core promoters, future work could explore a larger library of building parts including temperature-sensitive transcription factors such as HSF1 to tune response to heat. Importantly, we observed negligible activation of our thermal gene switches at temperatures  $\leq 40$  °C even when T cells were incubated for over 24 hours. This provides support that the temperature threshold for activation is higher than the range of typical

fevers (~38-40 °C)<sup>239-241</sup> in patients with cytokine release syndrome (CRS), which would prevent T cell activation without a targeted thermal input. Despite this, we envision that the development of future thermal gene switches with lower temperature activation thresholds may be useful as a sense-and-respond circuit to autonomously detect fever temperatures and trigger expression of therapeutic agents such as tocilizumab to attenuate CRS.

With our current platform, we demonstrated thermal control of T cell activity using several classes of immunostimulatory genes including CARs, BiTEs, and cytokines. Engineered T cells that constitutively express similar classes of molecules have demonstrated strong anti-tumor efficacy but their therapeutic applications are limited by off-tumor effects and toxicities in healthy tissues<sup>197, 198</sup>. Thus, targeted expression of these genes within tumors could potentially contain potent T cell activity within the local TME and improve therapeutic outcomes. Given that the classes of molecules we studied included surface receptors, secreted cytokines, and bi-specific T cell engagers, we expect that a wide range of biologics are amenable for thermal control without potential loss of function due to protein misfolding or aggregation in T cells by heat stress. In the future, we anticipate that thermal targeting may have clinical use to treat cancer types that present as primary tumors with limited metastasis such as glioblastoma (GBM) or manage locally disseminated disease such as liver, lung, or brain oligometastases that are currently treated by surgical resection or ablation.

### **1.13 Methods**

*Plasmid construction.* Synthetic thermal switches were produced as gene blocks by IDT and cloned into the Lego-C backbone (Addgene plasmid #27348). The core promoters were truncated immediately upstream of their previously described TATA boxes at their 5'-termini and at their translational start site on their 3'-termini<sup>182, 242, 243</sup>. The genomic HSPA6 promoter was amplified from genomic DNA using PCR primers listed in a previous publication<sup>230</sup>. The NKG2DL BiTE sequence was described previously<sup>235</sup> and modified to include an Ig $\kappa$  leader sequence to facilitate secretion from T cells as well as a HisTag for construct detection. This combined sequence was synthesized (ATUM) and cloned downstream of synthetic thermal gene switches. The IL-15 superagonist sequence was described previously<sup>231</sup> and synthesized by ATUM without modification. The constitutive  $\alpha$ CD19 CAR was kindly provided by Dr. Krishnendu Roy (Georgia Institute of Technology). All unique materials can be made available by the corresponding author on reasonable request.

*Culture of primary human T cells and cell lines.* CD19+ K562 (acquired from Dr. Yvonne Chen) and wild-type K562s (acquired from Dr. Krishnendu Roy) were cultured in Isocove's Modified Dulbecco's Medium (ThermoFisher #12440053) supplemented with 10% FBS (Fisher #16140071) and 10 U/ml Penicillin-Streptomycin (Life Technologies #15140-122). Raji cells were obtained from Dr. Krishnendu Roy and cultured in RPMI-1640 media supplemented with 10% FBS. Primary Human CD3+ cells were obtained from an anonymous donor blood after apheresis (AllCells) and were cryopreserved in 90% FBS and 10% DMSO until subsequent use. After thawing, cells were cultured in human T cell media comprised of X-VIVO 10 (Lonza #04-380Q), 5% human AB serum (Valley Biomedical #HP1022), 10 mM N-acetyl L-Cysteine (Sigma #A9165), and 55  $\mu$ M 2-

mercaptoethanol (Sigma #M3148-100ML) supplemented with 50 units/ mL human IL-2 (Sigma #11147528001).

*Lentiviral production and primary cell transduction.* VSV-G pseudotyped lentivirus was produced via transfection of HEK 293T cells (ATCC) using psPAX2 (Addgene #12260) and pMD2.G (Addgene #12259); viral supernatant was concentrated using PEG-it virus precipitation solution (System Biosciences LV825A-1) according to manufacturer instructions. For viral transductions, primary human T cells were thawed, incubated for 24 hours, and activated with Human T-Activator Dynabeads (Life Technologies #11131D) at a 3:1 bead:cell ratio for 24 hours. To transduce the activated T cells, concentrated lentivirus was added to non-TC treated 6-well plates which were coated with retronectin (Takara #T100B) according to manufacturer's instructions and spun at 1200 x g for 90 min at room temperature. Following centrifugation, viral solution was aspirated and 2 mL of human T cells (250,000 cells / mL) in human T cell media containing 100 units / mL hIL-2 were added and spun at 1200 x g for 60 min at 37 °C and moved to an incubator. Cells were incubated on a virus-coated plate for 24 hours prior to expansion and Dynabeads were removed 7 days after T cell activation. For cells flow-sorted prior to adoptive cell transfer, Dynabeads were added immediately after sorting at 3:1 ratios for 48 hours.

*Staining and flow cytometry.* To detect CAR expression, biotinylated CD19 (10 µg / mL; Acro Biosystems #CD9-H8259) and Streptavidin-APC (ThermoFisher #S868) were used according to manufacturer instructions. NKG2DL expression was assessed by staining with NKG2D-Fc chimera (10 µg / mL; Fisher 1299NK050) followed by an αFc secondary stain (Invitrogen #A-10631). NIR Live/Dead (ThermoFisher #L34976), CFSE (LifeTech #C34554) and CellTrace Violet (CTV; LifeTech #C34557) were used according to

manufacturer instructions. Human Fc block (BD #564220) was used prior to staining with any antibodies. For intracellular staining for Granzyme B, intracellular fixation and permeabilization buffers (eBioscience #88-8823-88) were used according to manufacturer instructions with Brefeldin A being added ~4 hours prior to staining. Antibodies for Granzyme B (GB12; ThermoFisher), CD69 (FN50; BD), CD4 (RPA-T4; BioLegend); CD8 (RPA-T8; BioLegend), CD3 (UCHT1; BD), CD45 (HI30; BD), CD19 (HIB19; BioLegend), and HisTags (4E3D10H2/E3; ThermoFisher) were all used at 1:100 dilutions.

*In vitro luciferase and thermotolerance assays.* Primary human T cells were heated in a thermal cycler and transferred to culture plates for incubation at 37 °C. Unless otherwise noted, cellular supernatant was sampled for luciferase activity 24 hours after conclusion of thermal treatment. Non-thermal treatments were conducted by incubating engineered cells at indicated concentrations of CoCl<sub>2</sub> (Sigma #232696-5G) or CdCl<sub>2</sub> (Sigma #202908). When indicated, luminescence was compared to a ladder of recombinant Gaussia Luciferase (NanoLight #321-500) quantified using a Gaussia Luciferase Glow Assay Kit (ThermoFisher #16161) according to manufacturer's instructions. For viability and proliferation studies, primary human T cells were heated in the thermal cycler prior to assaying with an apoptosis detection kit (BD # 556547) or CellTrace Violet (Fisher # C34571). Viability was assessed 24 hours after heating. For migration studies, wild-type cells were added to the top insert of a transwell plate (Sigma #CLS3421) while CXCL12 (50 ng / mL, Peprotech #300-28A) was added to the lower chamber. Cells in lower chamber were counted by hemocytometer at indicated times.

*Cytotoxicity and T cell activation assays.* For cytometric analysis, TS-CAR T cells were heated in a thermal cycler and co-incubated with K562 target cells at a 10:1 effector cell to

target cell ratio for 24 hrs prior to staining as described above. For luciferase-based assays, K562s were luciferized with either Firefly luciferase (CD19+) or Renilla luciferase (CD19-) and incubated with effector cells after heating. Unless otherwise noted, a 10:1 effector to target ratio was used. After incubation, either D-luciferin (Fisher #LUCK-2G; 150 µg / mL read concentration) or Rluc substrate (VWR # PAP1232; 17 µM read concentration). Maximum cytotoxicity was defined as luminescent signal from wells containing only media while no cytotoxicity was defined by wells containing only target cells. Supernatant was collected after incubation and assayed for cytokines using the human Th1/Th2/Th17 CBA kit (BD # 560484). IL-15 superagonist was quantified using the human IL-15/IL-15R alpha complex DuoSet ELISA (R&D Systems DY6924). For BiTE experiments with primary human T cells, two heat treatments (42 °C, 30 minutes) separated by 6 hours were applied to T cells prior to incubation with target cells.

*IL-15 superagonist Dynabead experiment:* Wild-type primary human T cells were labeled with CFSE and incubated with either heated or unheated TS-IL15 cells. Beads were added at a 10:1 T cell to bead ratio that was determined not to induce strong proliferation in untransduced T cells without cytokine support. CFSE labeling allowed discrimination from TS-IL15 cells (Figure 26c, d) and proliferation and division indices were calculated in FlowJo using the Proliferation tool.

*Animals:* Eight- to sixteen-week old female NSG mice were used for all in vivo experiments. Mice were bred and housed in the Georgia Tech Physiological Research Laboratory (GT PRL) prior to start of experiments. All animal protocols were approved by Georgia Tech IACUC (protocols no. A100190 and 100191). All authors have complied with relevant ethical regulations while conducting this study.

*Photothermal heating and in vivo bioluminescence imaging:* AuNRs were purchased from Nanopartz (# A12-10-808-CTAB-500) and pegylated (Laysam Bio # #MPEG-SH-5000-5g) to replace the CTAB coating. These AuNRs were intravenously injected into tumor-bearing mice (10 mg / kg) ~48 hrs before adoptive transfer of T cells. Mice were anesthetized with isoflurane gas, and target sites were irradiated using an 808 nm laser (Coherent) under guidance of a thermal camera (FLIR model 450sc). Fluc activity was measured using an IVIS Spectrum CT (Perkin Elmer) ~5 minutes after intravenous injections of D-luciferin (Fisher #LUCK-2G).

*Adoptive cell transfer (ACT) experiments:* NSG mice were inoculated subcutaneously with  $5 \times 10^6$  Raji or K562 cell lines after the site was shaved and sterilized using an isopropyl wipe (GT PRL). ~48 hrs prior to adoptive transfer of human T cells, pegylated AuNRs were injected intravenously via tail vein. Once tumors had reached ~100-150 mm<sup>3</sup>,  $1.5 \times 10^6$  CAR+ primary human T cells were injected via tail vein in 200  $\mu$ L of sterile saline. Cells were transduced and sorted based on CD19 CAR expression prior to transfer as described above. After >24 hrs, photothermal heat treatments were administered and monitored as described above. Tumors were measured using digital calipers and volume calculated based on the equation length x width x depth x 0.52. Mice were euthanized when tumor volume exceeded 1500 mm<sup>3</sup>.

*Software and Statistical Analysis.* All results are presented as mean, and error bars depict SEM. Statistical analysis was performed using GraphPad Prism statistical software. For all graphs, \* p <0.05, \*\* p <0.01, \*\*\* p<0.001, \*\*\*\* p<0.0001, ns = not significant. Flow cytometry data were analyzed using FlowJo X (FlowJo, LLC). *In vitro* luminescent data were collected with Gen5 2.07 (Biotek). *In vivo* luminescence data were collected and

analyzed with Living Image 4.4.5 (PerkinElmer). Flow-cytometry data were collected with BD FACSDIVA v8 (BD Biosciences). Thermal imaging data were acquired and analyzed using Research IR Max (FLIR). Figures were designed in Adobe Illustrator.

## CONCLUSIONS

### 1.14 Summary of advancements

The emerging field of cellular therapies is rapidly developing new control mechanisms that allow engineered T cells to respond to various stimuli including the presence of target antigens or small-molecule agents<sup>197</sup>. Engineered sensitivity to these biochemical cues has enhanced the specificity of anti-tumor responses and improved control of *in vivo* immune activity motivating hundreds of clinical trials which are translating these advances into the clinic. As the field continues to mature, new strategies are expanding the clinical toolkit to complement its existing strengths. In this context, the capacity to target engineered T cell activity to tumors based on their spatial location would reduce off-tumor effects that limit the safety and efficacy of current T cell therapies.

As a remote trigger that can be localized to tumors, heat represents a physical cue that can be generated using platforms such as LITT, FUS, and RFA<sup>146</sup>. While these platforms are intended to ablate tumors, transient exposure to hyperthermia is well-tolerated by disease and normal tissues alike due to the cellular heat shock response. The platform described here re-engineers T cell heat shock responses to enhance the activity of therapeutic T cells through the heat-induced expression of immunostimulatory genes including Chimeric Antigen Receptors (CARs), cytokine superagonists, and Bispecific T cell Engagers (BiTEs). These results illustrate that a wide range of biological drugs and cellular processes are amenable for thermal control including T cell effector functions such as proliferation, recognition of target cells, and cytotoxicity. Thus, localized thermal treatments, in conjunction with adoptive transfer of T cells engineered with synthetic

thermal gene switches, could trigger emergent immune cell activity in an otherwise immunosuppressive TME while attenuating concerns of off-tumor toxicity.

Because prolonged exposure to hyperthermia can result in low cell viability, we explored non-continuous heating regimens inspired by the concept of dose fractionation in radiation oncology to improve thermal tolerance of heated cells. In Jurkat T cells, we observed that pulsed heat treatments, in comparison to continuous treatments with identical AUCs, increased the viability and switch activity of engineered cells following thermal treatments. Although continuous heat treatments were well-tolerated by primary human T cells under the conditions tested here, pulsed treatments could be explored in the future to further enhance switch activity and thermal tolerance of primary human T cells. Ultimately, optimal heating regimens, either continuous or pulsed, should allow sustained, longitudinal control over engineered T cell activity at a tumor site.

We also constructed synthetic thermal gene switches characterized by improved thermal specificity and high on-off ratios compared to endogenous heat shock promoters. Because endogenous heat shock promoters respond to diverse non-thermal inputs such as hypoxia or heavy metals<sup>155, 156</sup>, we screened panels of synthetic thermal gene switches containing combinations of Heat Shock Elements (HSEs) and core promoters. In doing so, we identified a synthetic architecture with superior activation characteristics compared to endogenous heat shock promoters which eliminated sensitivity to non-thermal stresses. These synthetic thermal gene switches are therefore leading candidates for future applications using thermal control platforms. In the future, we envision that such platforms could improve the clinical treatment of tumors primarily treated with surgical resection or

ablation of focal lesions such as primary GBM tumors as well as regionally disseminated oligometastases in the brain, liver, or lungs.

### **1.15 Future directions of the technology**

Given that this work presents a platform technology, there are numerous applications that could be explored in the future. A few potential applications include:

#### *1.15.1 Fever-induced switch activity*

Because fever often presents with clinical CRS<sup>240, 241</sup>, synthetic thermal gene switches triggered by fever-range temperatures (up to ~40 °C) would respond to endogenous hyperthermic cues at the onset of a pathological state. Because these cues are not localized to a particular site, synthetic thermal gene switch design could be adapted to this new trigger to enhance treatment outcomes. For example, the fever-range temperatures could trigger the synthesis of anti-inflammatory biologics such as the IL-6 blocking antibody tocilizumab which is currently administered to treat CRS. This strategy would generate an autonomous thermal control mechanism that could help improve the safety profile of existing CAR T cell therapies. Although we did not observe strong activation of our synthetic thermal gene switches below 40 °C even when the heat treatment was maintained for 24 hours (Figure 20), alternative switch architectures could tune this activation threshold to fever ranges. For example, different core promoters or response elements could be incorporated to allow differential regulation of switch transcriptional activity. Additionally, engineering the heat-sensitive domains of the HSF1 transcription factor could also modulate its activation characteristics under hyperthermic conditions<sup>190, 244</sup>. By

screening construct libraries for heat-induced activity in Jurkat T cells, candidate synthetic thermal gene switches could be identified prior to validation in primary T cells.

#### *1.15.2 Heat-triggered chemotaxis to a targeted site*

The synthetic thermal gene switches described here incorporated immunostimulatory genes designed to enhance the proliferation and cytotoxicity of T cells already within a heated tumor. However, augmenting chemotaxis *to* a heated tumor could also improve anti-tumor immune responses by recruiting effector populations or APCs to the site. This effect could be induced by incorporating chemokines such as CXCL12 or MIP3 $\alpha$  into synthetic thermal gene switches to attract additional T cells or DCs to the heated tumor after infusion of engineered T cells. Because the concentration gradient of the heat-triggered chemokines would be highest at the tumor, this process could preferentially increase tumor infiltration of desired cell populations that propagate anti-tumor responses. If the heat-attracted cells were DCs for example, this process could enhance the presentation of antigens found within the heated tumor and potentially accelerate epitope spreading for TAAs.

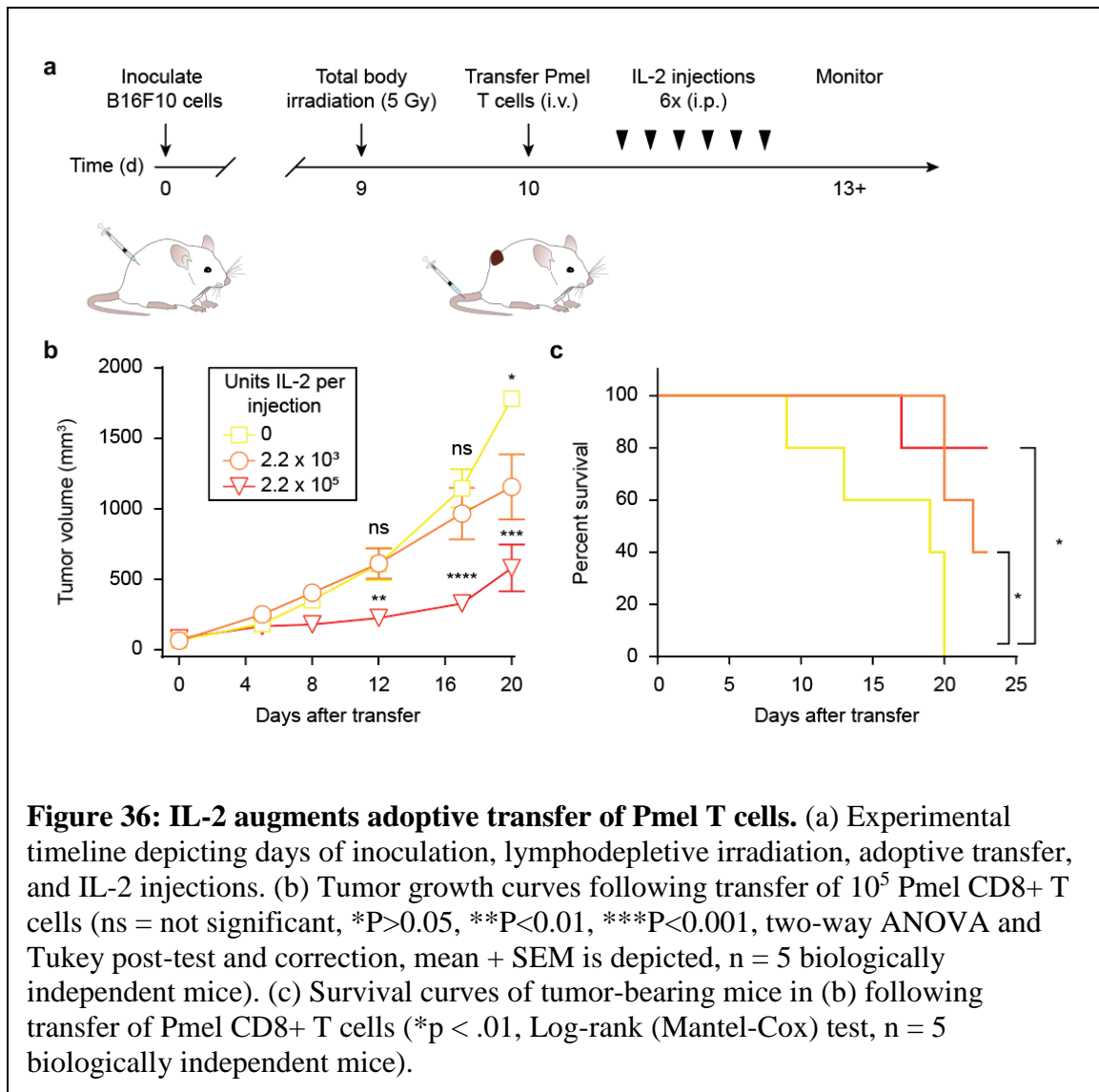
#### *1.15.3 Expanding T cell specificity in vivo*

One challenge facing cellular therapies is the heterogeneous expression of TAAs by cancer cells and outgrowth of malignant cells lacking the target antigens<sup>197</sup>. Furthermore, non-malignant cells in the tumor microenvironment such as tumor-associated macrophages (TAMs) and myeloid derived suppressor cells (MDSCs) contribute to disease progression yet do not express markers that readily differentiate them from healthy cells. Thus, locally broadening the pool of target antigens recognized by engineered T cells in the TME could improve treatment outcomes without promoting cytotoxicity of normal tissues expressing

these same target antigens. To expand the range of cells that could be targeted by engineered T cells in the TME while still maintaining tolerance of the same antigens in healthy tissues, heat-triggered expression of BiTEs or CARs could be contained within a heated tumor. We have already performed preliminary experiments towards this end by demonstrating that *in vitro* differentiated MDSCs can be targeted using NKG2DL BiTEs based on their expression of the cognate ligands (Appendix A.4). Subsequent experiments could incorporate these cells into *in vivo* models to recapitulate immunosuppressive niches found within patient tumors.

## APPENDIX A. SUPPORTING INFORMATION

### A.1 Bolus injections of IL-2 augment adoptive transfer in immunocompetent mice



To establish a model for adoptive transfer of T cells that recognize tumor-associated antigens, we performed exploratory studies in a syngeneic model using B16-F10 melanoma in C56BL/6J mice. ACT in such models incorporate lymphodepletion regimens to clear

space in the lymphatic compartment and reduce the numbers of cells that compete for homeostatic cytokines which support the transferred cells<sup>245</sup>. Thus, we irradiated all tumor-bearing mice with 5 Gy of total body irradiation prior to infusion of transgenic Pmel CD8+ T cells which recognize a fragment of the gp100 molecule in the context of H2-D<sup>b</sup> MHC-I molecules<sup>246, 247</sup>. To identify the minimum amount IL-2 required to sustain these transferred cells after infusion, we conducted dose-escalation experiments in which we systemically injected different doses of IL-2 following intravenous ACT (Figure 36a). Following this protocol, mice receiving six injections of  $2.2 \times 10^3$  and  $2.2 \times 10^5$  IU of recombinant human IL-2 (PeproTech # 200-02) exhibited significantly reduced tumor burden and prolonged survival compared to mice receiving control injections of sterile saline (Figure 36). Future studies seeking to characterize synthetic thermal gene switch activity within an immunocompetent model may follow similar protocols modified to incorporate *ex vivo* transduction of the transferred cells. In this manner, the activity of lymphocyte populations observed in patient tumors (e.g. T<sub>regs</sub> which are missing in NSG mice) could be more fully elucidated in the context of ACT experiments.

## A.2 Endogenous switch activity in primary murine T cells

In Chapter 3, we describe a qPCR screen in primary murine T cells which identified several genes that were transcriptionally upregulated following heat treatment (Figure 16). In addition to using the core promoters of these genes to construct synthetic thermal gene switches (Figure 19c, d), we also tested the genomic promoters to evaluate their potential as thermal gene switches in primary murine T cells. After harvesting primary murine T cells and transducing them with constructs containing HSPA1A, HSPA1B, HSPA6, and HSPB1 promoters, we heated the cells and assayed switch activity by expression of a GFP reporter linked to the promoters. Although samples containing the HSPA1A and HSPA1B switches exhibited increases in switch activity following heating, we also observed populations characterized by higher basal activity at 37 °C compared to the HSPA6 or HSPB1 samples (Figure 37). To better characterize this heterogeneous switch activity, we sorted cells transduced with an HSPA1B switch into four different populations based on their switch activity and transduction level as quantified by mCherry expression (Figure 38a, b). Surprisingly, cells which only weakly expressed the mCherry transduction marker (Population 3) displayed the highest fold-increases in Gluc activity following heating compared to unheated cells (>25-fold increases at 42 °C). These increases were larger than those observed in cells with higher mCherry expression but similar thermal switch activity at sorting (Population 1). Additionally, cells which did not express the transduction marker, yet displayed slightly elevated switch activity (Population 4) exhibited the strongest reporter activity following heating. Notably, none of the populations exhibited >3.5-fold increases at 40 °C (Figure 38c). These data underscore the need to better understand the

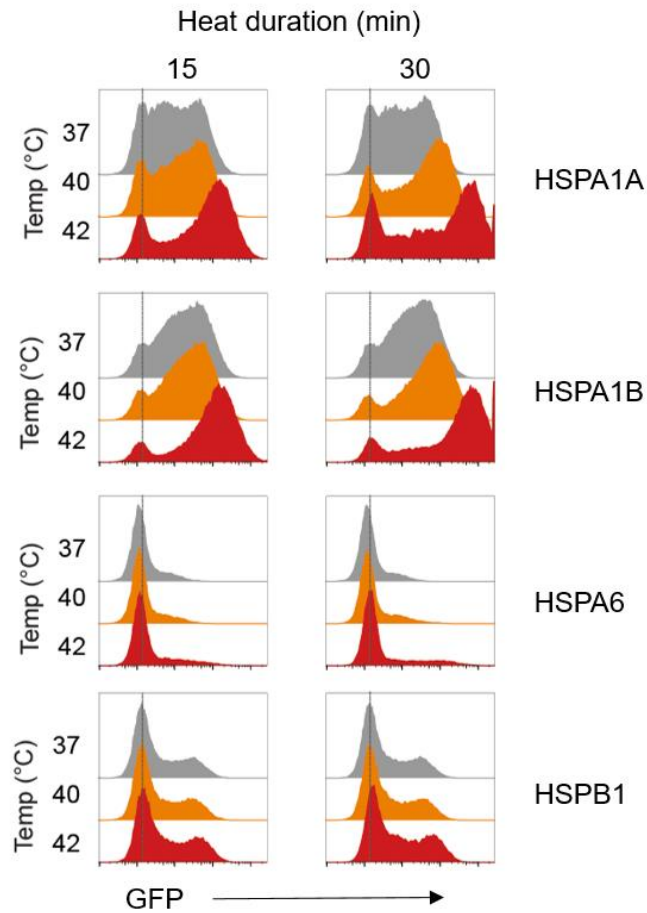
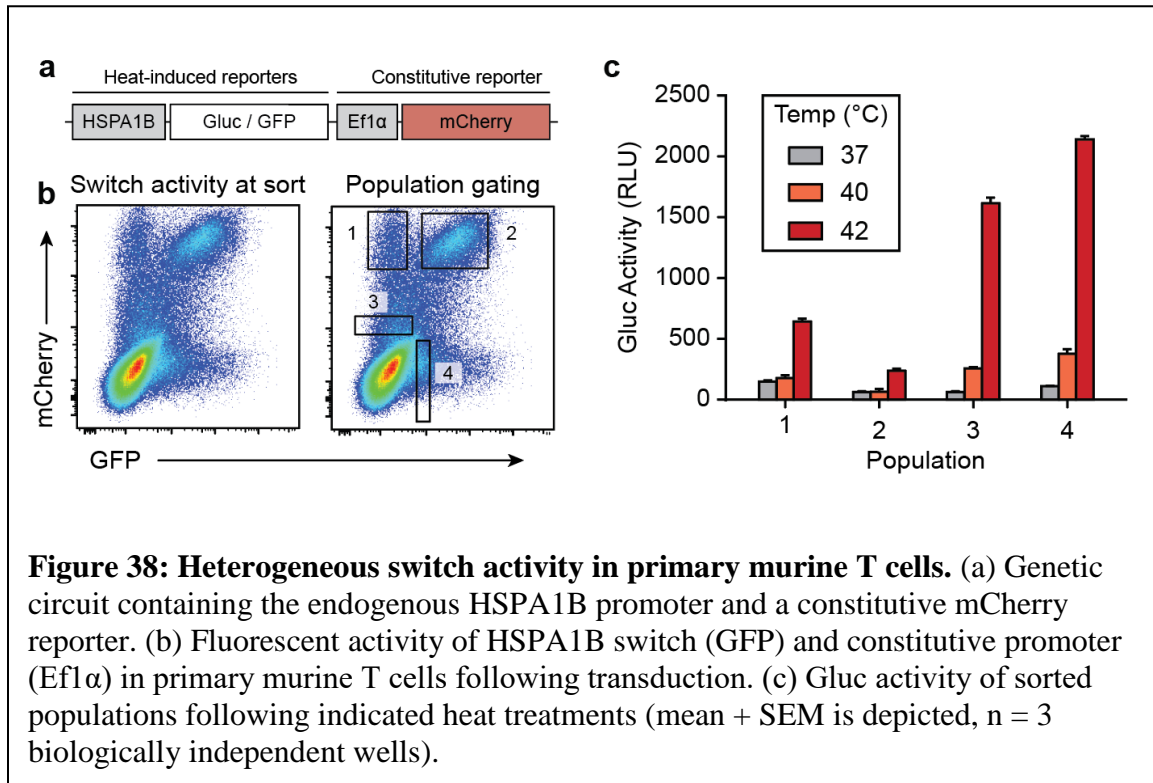
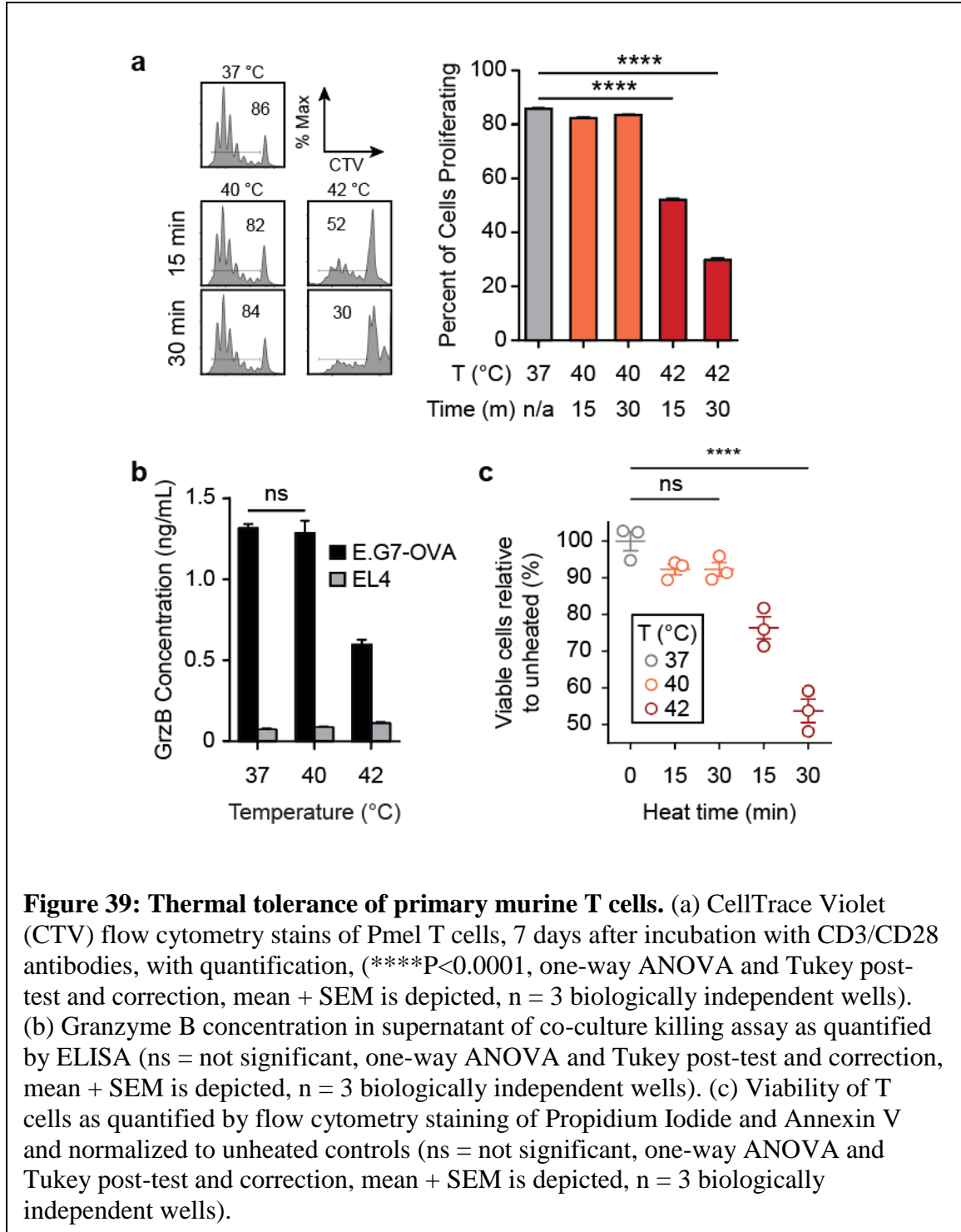


**Figure 37: Thermal switch activity in primary murine T cells.** GFP expression in primary murine T cells following transduction with endogenous thermal switches and heat treatment.

effects of viral transductions on bulk populations of primary T cells as these heterogeneous behaviors would likely influence *in vivo* activity. Factors such as number of integrations, integration sites, and changes in the epigenetic landscape of these sites may all play important roles in determining thermal switch responses and represent potential areas for future investigation.



### A.3 Thermal tolerance of primary murine T cells

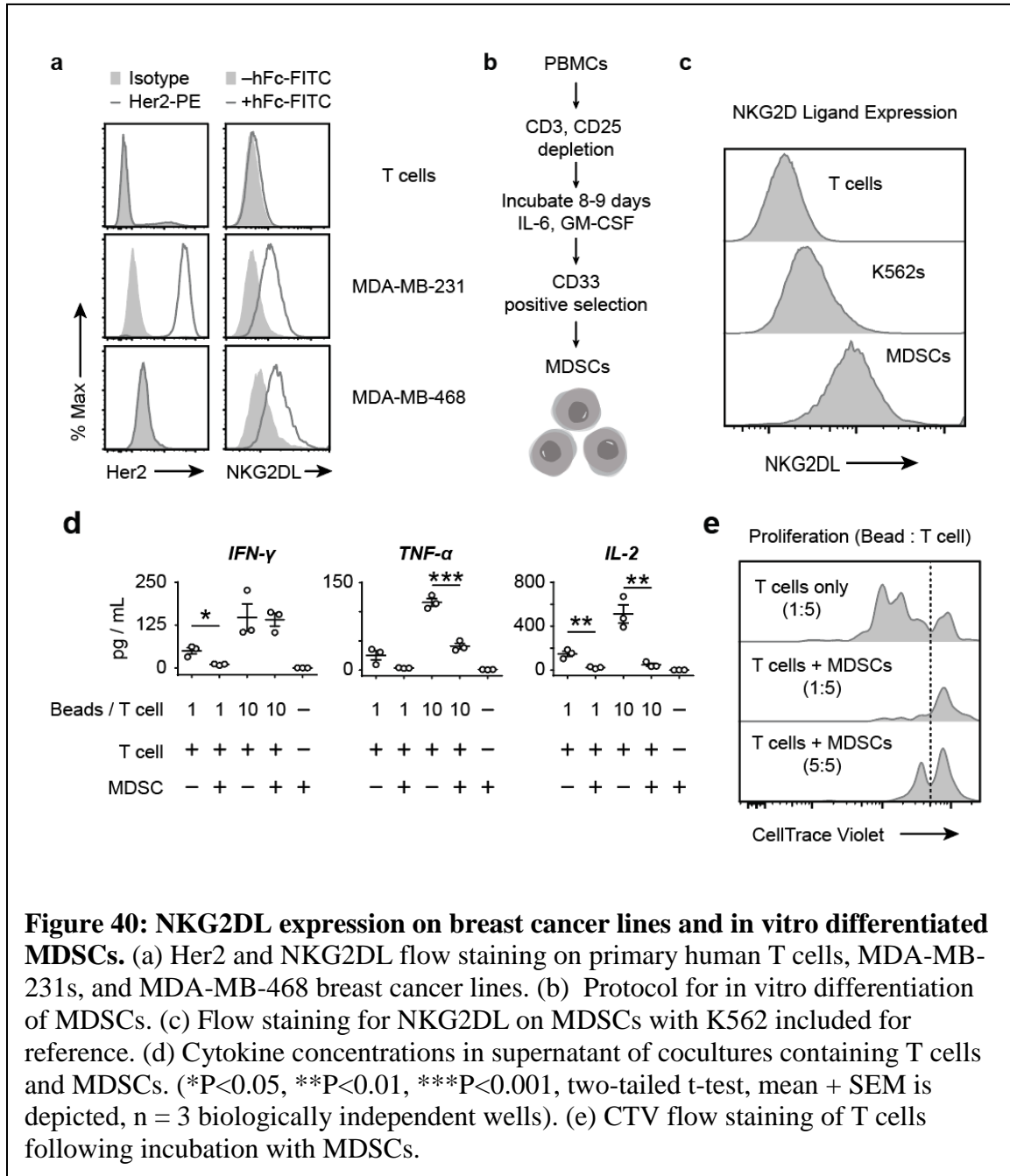


To assess the thermal tolerance of primary murine T cells, lymphocytes were harvested from Pmel mice (Jackson Labs #005023) prior to negative selection of T cells using a T

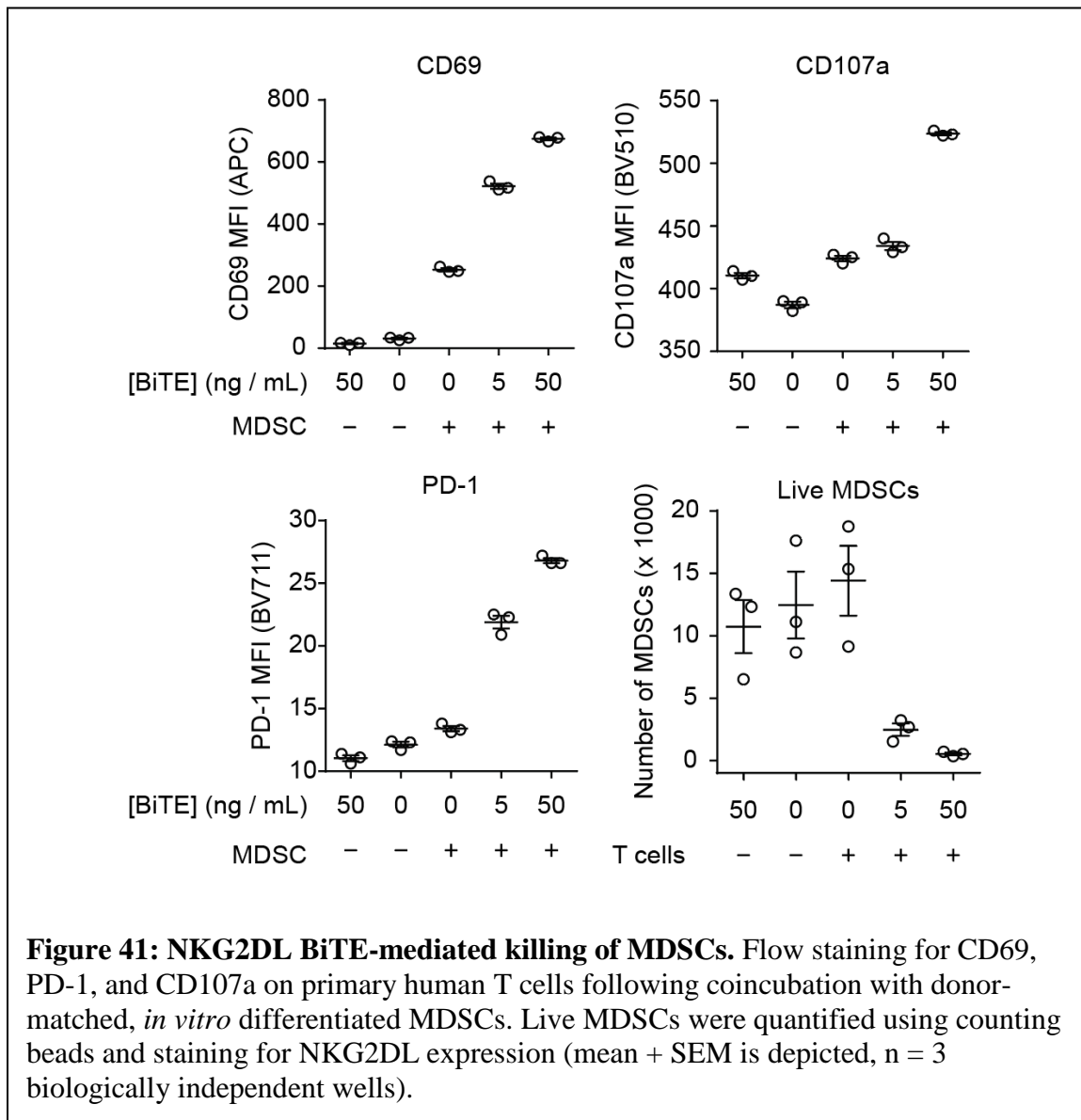
cell isolation kit (Miltenyi # 130-104-075). The T cells were heated and either plated with CD3 and CD28 platebound antibodies to quantify proliferation (Figure 39a), incubated with antigen-specific target cells to assess cytotoxicity (Figure 39b), or stained for apoptotic markers (Figure 39c). With these assays, we observed ~50% reductions in the fraction of proliferated cells under activating conditions, the concentration of Granzyme B (a cytotoxic effector molecule released by T cells) in the supernatant of co-cultures containing target cells, as well as viability of T cells after incubations at 42 °C for 30 minutes (Figure 39). These data suggest that primary murine T cells have lower tolerances for hyperthermia compared to those observed in primary human T cells (Figure 22 and Figure 23). Combined with the observations that murine T cells required >40 °C heat treatments for strong thermal switch activation (Figure 38c), these data led us to conduct the bulk of our studies using primary human T cells. Although we did not test pulsed heating regimens with murine cells, it remains possible that such profiles could also improve thermal tolerance as observed in Jurkat T cells (Figure 9f).

#### A.4 Broader targeting using TS-BiTE T cells

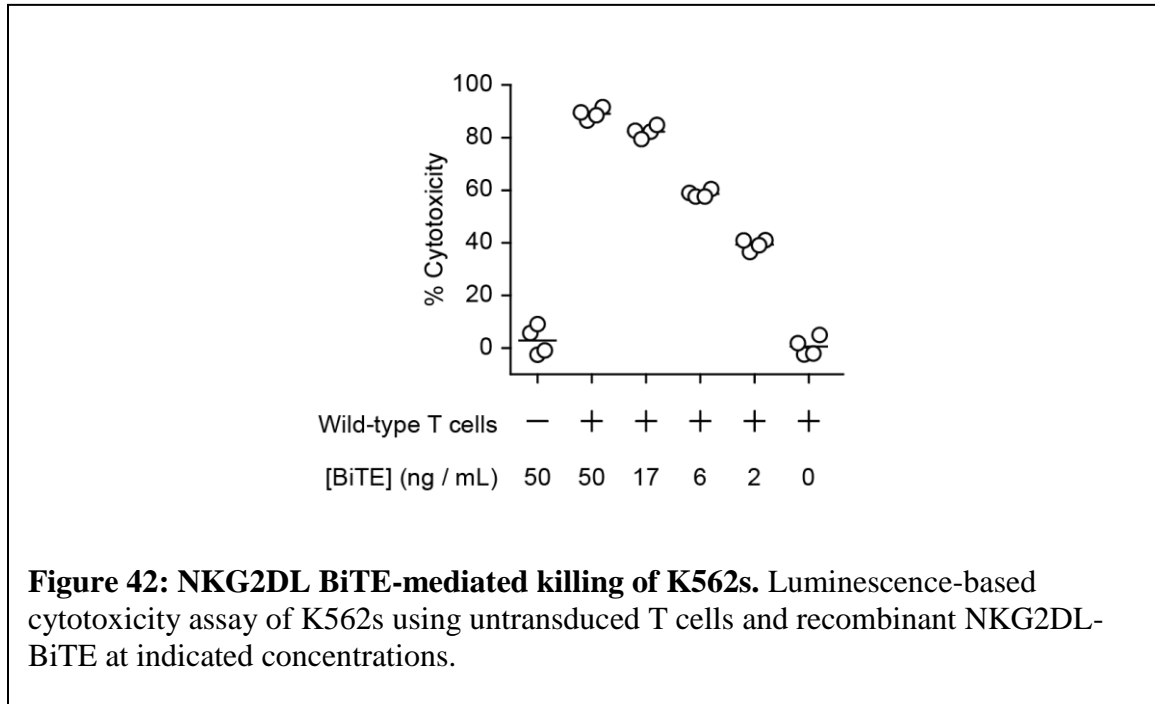
In addition to K562s, NKG2D ligands are expressed by a wide range of cells found in the TME<sup>25, 233</sup>. Indeed, the primary reason for incorporating the NKG2DL BiTE into the synthetic thermal gene switches was its potential to expand T cell specificity to include



multiple cell types. For example, two breast cancer lines, MDA-MB-231 and MDA-MB-468, both stain positive for NKG2DLs making them potential candidates for heat-triggered targeting by T cells containing TS-BiTE switches (Figure 40a). Canonically, NKG2DLs are also strongly expressed by myeloid derived suppressor cells (MDSCs) and several strategies have attempted to target these cells via this axis<sup>26</sup>. To explore this possibility we first differentiated MDSC target cells according to previously published guidelines<sup>26</sup> and confirmed their expression of NKG2DLs (Figure 40b, c). Next, we confirmed the



suppressive phenotype of these cells by co-incubating them with T cells and CD3/CD28 beads to provide signals 1 and 2. We observed that addition of MDSCs to the culture reduced the secretion of immunostimulatory cytokines such as IFN- $\gamma$ , TNF- $\alpha$ , and IL-2 (Figure 40d). Under similar activating conditions with CD3/CD28 beads, addition of MDSCs inhibited T cell proliferation and this inhibition was unable to be recovered even

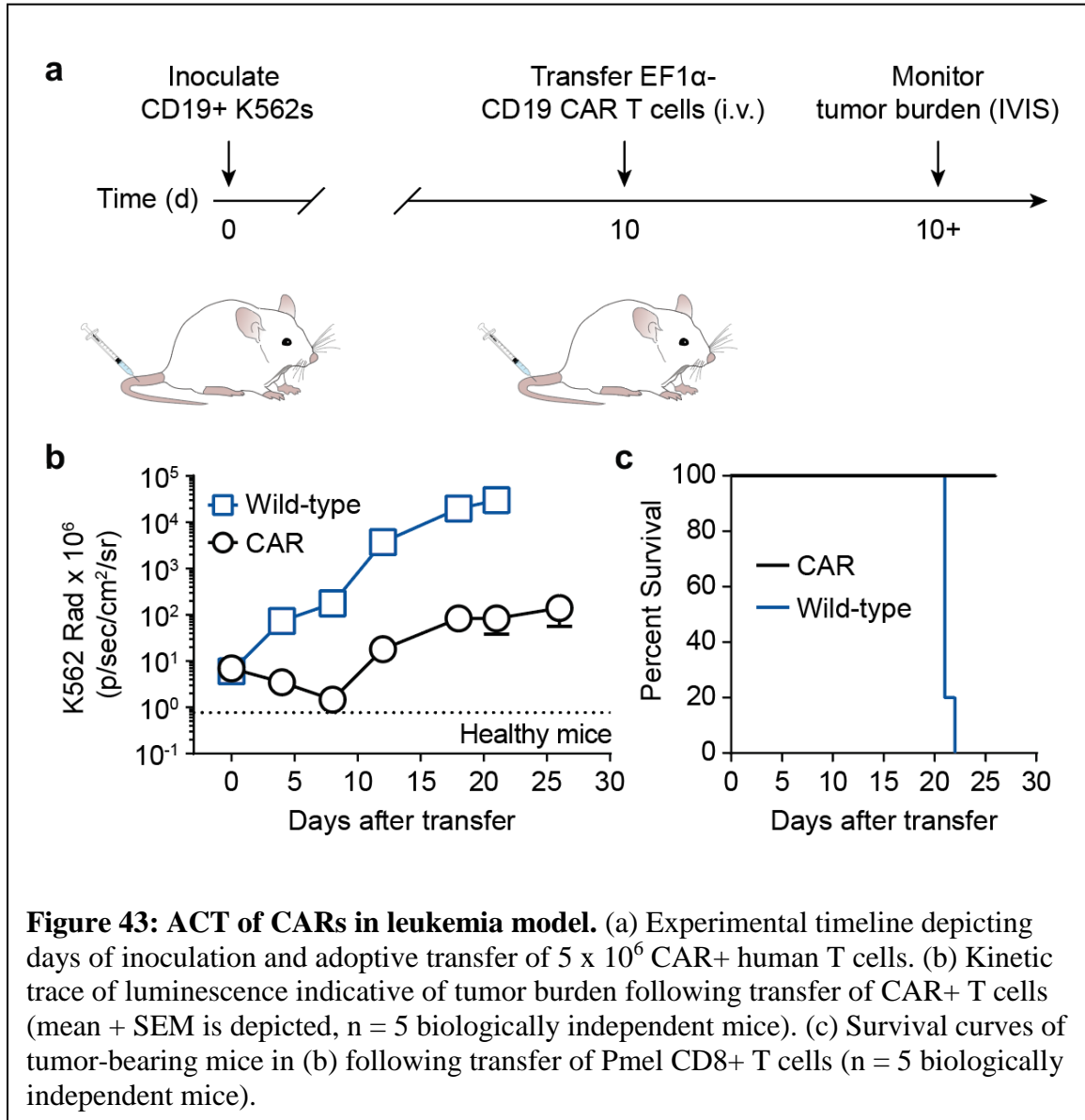


at higher bead to T cell ratios (Figure 40e). These data confirmed the suppressive phenotype of the *in vitro* differentiated MDSC which raised the question as to whether redirected T cells could kill these suppressive cells.

To test whether NKG2DL BiTEs could trigger MDSC killing by otherwise unreactive T cells, we incubated primary human T cells with the *in vitro* differentiated MDSCs in the presence of recombinant BiTE expressed by CHO cells. To reduce the potential for alloreactivity, the same donor was used for both the T cells and MDSCs. After 24 hours of coinubation with NKG2D BiTEs and MDSCs, T cells exhibited dose-

dependent upregulation of activation markers (CD69 and PD-1) as well as the degranulation marker CD107a suggesting cytotoxic responses towards MDSCs. This cytotoxicity was confirmed at concentrations as low as 5 ng/mL by quantifying the number of live MDSCs using counting beads (Figure 41). This same BiTE concentration was also capable of inducing ~50% cytotoxicity in K562s suggesting that the suppressive phenotype of the MDSCs did not compromise BiTE-mediated killing. Future studies could incorporate these MDSCs into implanted tumor models to recapitulate immunosuppressive niches observed in patient samples and inhibit the activity of tumor-reactive T cells. Heat-triggered expression of BiTEs could then trigger cytotoxicity against the MDSCs and ultimately improve anti-tumor responses.

### A.5 Adoptive transfer of constitutive CAR T cells in a leukemia model



To establish a xenograft model of cancer in which primary human T cells are infused into tumor-bearing mice, we injected luciferized CD19+ K562 cells into NSG mice. These mice lack T cells, B cells, and NK cells allowing for engraftment of human cells and *in vivo* modeling of CAR T cell activity<sup>248, 249</sup> (Figure 43a). As early as three days after infusion of T cells which constitutively expressed an  $\alpha$ CD19 CAR, luminescence (indicative of tumor burden) was reduced compared to controls receiving wild-type T cells. These levels

approached the luminescence observed in healthy mice (dotted line) before beginning to increase 8 days post-transfer (Figure 43b). This reduction in tumor burden also corresponded to prolonged survival in mice receiving transduced cells (Figure 43). These data confirmed that adoptively transferred human T cells could mediate anti-tumor responses in a xenograft model of leukemia. Additionally, the increases in tumor burden after Day 8 in the CAR group could indicate exhaustion or lack of sustained proliferation by the transferred cells; phenotypic studies of these cells would elucidate these possibilities. Furthermore, incorporating synthetic thermal gene switches into the transferred cells has the potential to improve the durability of this therapeutic response by allowing transient expression of a CAR to prevent continuous CAR signaling or the inclusion of heat-triggered cytokines (e.g. the IL-15 SA) to support the formation of memory populations.

## A.6 Synthetic thermal gene switch sequences

**Table 2: Synthetic thermal gene switch sequences.**

3 HSE	<u>TGAAAGTTCTAGAACGACGAGAACGTTCTAGAAGGTCTAGAACGT</u> <u>TCTAGAAC</u>
4 HSE	<u>AGAAGCTTCTAGAATGTGCTGAAAGTTCTAGAACGACGAGAACGT</u> <u>TCTAGAAGGTCTAGAACGTTCTAGAAC</u>
5 HSE	<u>AGAACGTTCTAGAACCTGGAGAAGCTTCTAGAATGTGCTGAAAGT</u> <u>TCTAGAACGACGAGAACGTTCTAGAAGGTCTAGAACGTTCTAGAA</u> C
6 HSE	<u>AGAACGTTTCATGAACGCTGAGAACGTTCTAGAACCTGGAGAAGCT</u> <u>TCTAGAATGTGCTGAAAGTTCTAGAACGACGAGAACGTTCTAGAA</u> <u>GGTCTAGAACGTTCTAGAAC</u>
7 HSE	<u>AGAAGCTTCATGAACGTGCAGAACGTTTCATGAACGCTGAGAACGT</u> <u>TCTAGAACCTGGAGAAGCTTCTAGAATGTGCTGAAAGTTCTAGAA</u> <u>CGACGAGAACGTTCTAGAAGGTCTAGAACGTTCTAGAAC</u>

Note: Heat Shock Elements (HSEs) are underlined

## A.7 Core promoter sequences

**Table 3: Core promoter sequences.**

YB	TCTAGAGGGTATATAATGGGGGCCACTAGTCTACTACCAGAAAG CTTGGTACCGAGCTCGGATCCAGCCACC
HSPB1	TTGCCATTAATAGAGACCTGAAGCACCGCCTGCTAAAAATACCC GGCTGGGCACACATAAAAGCACGCTGGGGCTCCAGTCCGGCACT TCTCGGATCCTCAGCCCAGTGCTTCTAGATCCTCAGCCTTGACCA GCCAAGAACATGAC
HSPA1A	TTAAAGGCGCAGGGCGGCGAGCAGGTCACCAGACGCTGACAGC TACTCAGAACCAAATCTGGTTCCATCCAGAGACAAGCGAAGACA AGAGAAGCAGAGCGAGCGGCGGTTCCCGATCCTCGGCCAGGA CCAGCCTTCCCCAGAGCATCCCTGCCGCGGAGCGCAACCTTCCC AGGAGCATCCCTGCCGCGGAGCGCAACTTCCCCGGAGCATCCA CGCCGCGGAGCACAGCCTTCCAGAAGCAGAGCGCGGCGCCCTC GAG
HSPA6	TAAAAGCCCGTGGAAGCGGAGCTGAGCAGATCCGAGCCGGGC TGGCTGCAGAGAAACCGCAGGGAGAGCCTCACTGCTGAGCGCC CCTCGACGGCGGAGCGGCAGCAGCCTCCGTGGCCTCCAGCATCC GACAAGAAGCTTCAGCCACCGGTCTCGAG

## A.8 Immunostimulatory gene sequences

**Table 4: Immunostimulatory gene sequences.**

<p>IL-15 superagonist</p>	<p>ATGGCACACGCAGAGCCAGAGGTTGCCGGACTCTCGGACT GCCCCGACTGCTGCTCCTCCTGCTTCTTCGGCCGCCTGCCACT AGAGGGGACTACAAGGACGACGATGACAAGATCGAAGGGA GGATTACGTGTCCTCCCCGATGTCCGTGGAACACGCGGACA TCTGGGTCAAGTCTATTCTTGTACTCCCGCGAGCGGTACA TTTGCAACTCCGGCTTTAAGCGCAAAGCTGGCACCAGCTCCC TCACTGAATGCGTGCTGAACAAGGCCACTAATGTGGCCCATT GGACCACCCCTCGCTGAAGTGCATCCGGGACCCTGCCTTGG TCCACCAACGCCCTGCACCTCCATCCGGAGGATCAGGCGGA GGAGGTTCCGGGTGGTGGTTCCGGTGGAGGAGGGAGCCTCCA GAACTGGGTGAACGTGATCAGCGACCTTAAGAAAATCGAGG ATCTGATTCAGTCAATGCACATCGACGCGACCCTCTACACCG AAAGCGACGTCCACCCGAGCTGCAAGGTCACCGCCATGAAG TGCTTCCTGCTGGAACCTCAAGTCATTTGCTGGAGAGCGGC GATGCTTCAATCCACGACACTGTGGAAAACCTGATCATTCTG GCAAACAACCTCCTCTTTCGAATGGGAACGTGACCGAGTCC GGCTGCAAGGAGTGCGAGGAGCTGGAGGAAAAGAACATCA AAGAGTTCCTGCAGTCCTTCGTCCACATCGTGCAGATGTTCA TCAACACCTCGTAA</p>
<p>NKG2DL BiTE</p>	<p>ATGGAGACTGACACCCTGCTTCTCTGGGTGCTCTTGCTTTGG GTGCCTGGAAGCACCGGCGACCAAGTCCAACAGTC AGGCGCCGAACTGGCTCGGCCTGGAGCTTCTGTGAAGATGTC GTGCAAAGCATCCGGCTACACCTTTACTCGCTACACCATGCA CTGGGTCAAGCAAAGGCCCGGACAGGGACTGGAGTGGATTG GGTACATCAACCCTTCGCGGGGGTACACTAACTACAACCAG AAGTTTAAGGACAAGGCCACGCTGACCACCGACAAGTCCTC GTCCACTGCATACATGCAGCTCTCCTCCCTGACCTCCGAGGA CTCCGCCGTGTACTIONACTGCGCCCGCTACTACGACGACCACTA CTGCCTGGACTACTGGGGCCAGGGTACTACCCTCACCGTGTC GTCAGGAGGCGGAGGAAGCGGTGGCGGTGGAAGTGGAGGA GGAGGAAGCCAGATCGTGCTGACTCAGTCCCCGGCGATCAT GTCCGCGTCACCTGGCGAAAAGGTCACCATGACTTGTAGCGC CTCAAGCAGCGTGTCTACATGAACTGGTATCAGCAGAAGTC CGGCACATCCCCAAGCGGTGGATCTATGACACTTCCAAGCT GGCCTCAGGAGTGCTGCACATTTCCGCGGGTCTGGTTCGGG</p>

	<p>CACCTCCTACTCCCTGACTATCTCGGGGATGGAAGCTGAGGA  TGCGGCCACCTACTACTGCCAACAAATGGTCCAGCAACCCCTT  CACCTTCGGGAGCGGCACTAAGCTGGAAATCAATGGGGGTG  GAGGATCGGGTGGAGGCGGATCAGGAGGGGGAGGGTCGTTC  TTGAATAGCCTGTTCAACCAAGAAGTGCAGATCCCCCTGACC  GAATCGTATTGTGGCCCGTGCCCAAAGAAGTGGATTTGCTAC  AAGAACAAGTGTACTACCAGTTCTTCGATGAGTCCAAGAATTGG  TACGAGTCACAGGCCTCCTGCATGAGCCAGAACGCCTCCCTC  CTGAAAGTGTACTCGAAGGAGGACCAGGATCTGCTGAAGCT  GGTCAAGTCCTACCATTGGATGGGCCTGGTGCACATCCCGAC  CAACGGGTCCTGGCAGTGGGAGGATGGGTCGATCCTGAGCC  CTAATCTCCTCACCATCATCGAGATGCAGAAGGGAGACTGC  GCCCTGTACGCGAGCTCATTCAAGGGCTACATAGAGAAGTGT  TCAACTCCCAACACCTACATCTGCATGCAGCGGACCGTGCAC  CACCACCATCACCCTAA</p>
<p>αCD19 CAR</p>	<p>ATGGCCTTACCAGTGACCGCCTTGCTCCTGCCGCTGGCCTTG  CTGCTCCACGCCGCCAGGCCGGACATCCAGATGACACAGAC  TACATCCTCCCTGTCTGCCTCTCTGGGAGACAGAGTCACCAT  CAGTTGCAGGGCAAGTCAGGACATTAGTAAATATTTAAATTG  GTATCAGCAGAAACCAGATGGAAGTGTAAACTCCTGATCTA  CCATACATCAAGATTACACTCAGGAGTCCCATCAAGGTTGAG  TGGCAGTGGGTCTGGAACAGATTATTCTCTCACCATTAGCAA  CCTGGAGCAAGAAGATATTGCCACTTACTTTTGCCAACAGGG  TAATACGCTTCCGTACACGTTCCGGAGGGGGGACCAAGCTGG  AGATCACAGGTGGCGGTGGCTCGGGCGGTGGTGGGTCGGGT  GGCGGCGGATCTGAGGTGAAACTGCAGGAGTCAGGACCTGG  CCTGGTGGCGCCCTCACAGAGCCTGTCCGTCACATGCACTGT  CTCAGGGGTCTCATTACCCGACTATGGTGTAAGCTGGATTG  CCAGCCTCCACGAAAGGGTCTGGAGTGGCTGGGAGTAATAT  GGGGTAGTGAAACCACATACTATAATTCAGCTCTCAAATCCA  GACTGACCATCATCAAGGACAAGTCCAAGAGCCAAGTTTTCT  TAAAAATGAACAGTCTGCAAAGTGTGACACAGCCATTTACT  ACTGTGCCAAACATTATTACTACGGTGGTAGCTATGCTATGG  ACTACTGGGGCCAAGGAACCTCAGTCACCGTCTCCTCAACCA  CGACGCCAGCGCCGCGACCACCAACACCGGCGCCACCATC  GCGTCGCAGCCCCTGTCCCTGCGCCCAGAGGCGTGCCGGCC  AGCGGCGGGGGGCGCAGTGCACACGAGGGGGCTGGACTTCG  CCTGTGATATCTACATCTGGGCGCCCTTGGCCGGGACTTGTG  GGGTCCTTCTCCTGTCACTGGTTATCACCTTTACTGCAAACG</p>

	GGGCAGAAAGAAACTCCTGTATATATTCAAACAACCATTTAT GAGACCAGTACAACTACTCAAGAGGAAGATGGCTGTAGCT GCCGATTTCCAGAAGAAGAAGGAGGATGTGAACTGAGA GTGAAGTTCAGCAGGAGCGCAGACGCCCCCGCGTACAAGCA GGGCCAGAACCAGCTCTATAACGAGCTCAATCTAGGACGAA GAGAGGAGTACGATGTTTTGGACAAGAGACGTGGCCGGGAC CCTGAGATGGGGGGAAAGCCGAGAAGGAAGAACCCTCAGG AAGGCCTGTACAATGAACTGCAGAAAGATAAGATGGCGGAG GCCTACAGTGAGATTGGGATGAAAGGCGAGCGCCGGAGGGG CAAGGGGCACGATGGCCTTTACCAGGGTCTCAGTACAGCCA CCAAGGACACCTACGACGCCCTTCACATGCAGGCCCTGCCCC CTCGCTGA
--	--

**Domains of the immunostimulatory genes:**

*IL-15 superagonist:*

- 1 – 90: IL-15 signal peptide
- 91 – 114: FLAG tag
- 115 – 126: Factor Xa site
- 127 – 357: Sushi domain of IL-15 R $\alpha$
- 358 – 414: Linker
- 415 – 762: Mature IL-15

*NKG2DL BiTE:*

- 1 – 63: Igk leader sequence
- 64 – 420: VH-OKT3
- 421 – 465: Linker
- 466 – 783: VL-OKT3
- 784 – 828: Linker
- 829 – 1245: Extracellular domain of NKG2D
- 1246 – 1263: HisTag

*αCD 19 CAR:*

- 1 – 63: Leader sequence
- 64 – 789: αCD19 scFv domain
- 790 – 924: Hinge region
- 925 – 996: Transmembrane domain
- 997 – 1122: 4-1BB intracellular domain
- 1123 – 1461: CD3ζ domain

## REFERENCES

1. Mukherjee, S. The emperor of all maladies : a biography of cancer, Edn. 1st Scribner trade paperback. (Scribner, New York; 2011).
2. Mellman, I., Coukos, G. & Dranoff, G. Cancer immunotherapy comes of age. *Nature* **480**, 480-489 (2011).
3. Chen, D.S. & Mellman, I. Oncology meets immunology: the cancer-immunity cycle. *Immunity* **39**, 1-10 (2013).
4. Baumeister, S.H., Freeman, G.J., Dranoff, G. & Sharpe, A.H. Coinhibitory Pathways in Immunotherapy for Cancer. *Annu Rev Immunol* **34**, 539-573 (2016).
5. Goebeler, M.E. & Bargou, R.C. T cell-engaging therapies - BiTEs and beyond. *Nat Rev Clin Oncol* (2020).
6. Steel, J.C., Waldmann, T.A. & Morris, J.C. Interleukin-15 biology and its therapeutic implications in cancer. *Trends Pharmacol Sci* **33**, 35-41 (2012).
7. Weber, J.S., Kahler, K.C. & Hauschild, A. Management of immune-related adverse events and kinetics of response with ipilimumab. *J Clin Oncol* **30**, 2691-2697 (2012).
8. Conlon, K.C. et al. Redistribution, hyperproliferation, activation of natural killer cells and CD8 T cells, and cytokine production during first-in-human clinical trial of recombinant human interleukin-15 in patients with cancer. *J Clin Oncol* **33**, 74-82 (2015).
9. Waldmann, T.A. et al. Safety (toxicity), pharmacokinetics, immunogenicity, and impact on elements of the normal immune system of recombinant human IL-15 in rhesus macaques. *Blood* **117**, 4787-4795 (2011).
10. Fischbach, M.A., Bluestone, J.A. & Lim, W.A. Cell-based therapeutics: the next pillar of medicine. *Sci Transl Med* **5**, 179ps177 (2013).
11. Rosenberg, S.A. et al. Use of tumor-infiltrating lymphocytes and interleukin-2 in the immunotherapy of patients with metastatic melanoma. A preliminary report. *N Engl J Med* **319**, 1676-1680 (1988).
12. Rosenberg, S.A. et al. Treatment of patients with metastatic melanoma with autologous tumor-infiltrating lymphocytes and interleukin 2. *J Natl Cancer Inst* **86**, 1159-1166 (1994).
13. Dunbar, C.E. et al. Gene therapy comes of age. *Science* **359** (2018).

14. Robbins, P.F. et al. Tumor regression in patients with metastatic synovial cell sarcoma and melanoma using genetically engineered lymphocytes reactive with NY-ESO-1. *J Clin Oncol* **29**, 917-924 (2011).
15. Morgan, R.A. et al. Cancer regression in patients after transfer of genetically engineered lymphocytes. *Science* **314**, 126-129 (2006).
16. Morris, E.C. & Stauss, H.J. Optimizing T-cell receptor gene therapy for hematologic malignancies. *Blood* **127**, 3305-3311 (2016).
17. Zhao, Y. et al. High-affinity TCRs generated by phage display provide CD4+ T cells with the ability to recognize and kill tumor cell lines. *J Immunol* **179**, 5845-5854 (2007).
18. Rapoport, A.P. et al. NY-ESO-1-specific TCR-engineered T cells mediate sustained antigen-specific antitumor effects in myeloma. *Nat Med* **21**, 914-921 (2015).
19. Li, Y. et al. Directed evolution of human T-cell receptors with picomolar affinities by phage display. *Nat Biotechnol* **23**, 349-354 (2005).
20. Chapuis, A.G. et al. T cell receptor gene therapy targeting WT1 prevents acute myeloid leukemia relapse post-transplant. *Nat Med* **25**, 1064-1072 (2019).
21. Chapuis, A.G. et al. Transferred WT1-reactive CD8+ T cells can mediate antileukemic activity and persist in post-transplant patients. *Sci Transl Med* **5**, 174ra127 (2013).
22. Restifo, N.P., Dudley, M.E. & Rosenberg, S.A. Adoptive immunotherapy for cancer: harnessing the T cell response. *Nat Rev Immunol* **12**, 269-281 (2012).
23. Garrido, F., Aptsiauri, N., Doorduijn, E.M., Garcia Lora, A.M. & van Hall, T. The urgent need to recover MHC class I in cancers for effective immunotherapy. *Curr Opin Immunol* **39**, 44-51 (2016).
24. Crowther, M.D. et al. Genome-wide CRISPR-Cas9 screening reveals ubiquitous T cell cancer targeting via the monomorphic MHC class I-related protein MR1. *Nat Immunol* **21**, 178-185 (2020).
25. Eagle, R.A., Jafferji, I. & Barrow, A.D. Beyond Stressed Self: Evidence for NKG2D Ligand Expression on Healthy Cells. *Curr Immunol Rev* **5**, 22-34 (2009).
26. Parihar, R. et al. NK Cells Expressing a Chimeric Activating Receptor Eliminate MDSCs and Rescue Impaired CAR-T Cell Activity against Solid Tumors. *Cancer Immunol Res* **7**, 363-375 (2019).

27. VanSeggelen, H. et al. T Cells Engineered With Chimeric Antigen Receptors Targeting NKG2D Ligands Display Lethal Toxicity in Mice. *Mol Ther* **23**, 1600-1610 (2015).
28. Taylor, M.J., Husain, K., Gartner, Z.J., Mayor, S. & Vale, R.D. A DNA-Based T Cell Receptor Reveals a Role for Receptor Clustering in Ligand Discrimination. *Cell* **169**, 108-119 e120 (2017).
29. Wang, D. et al. Chlorotoxin-directed CAR T cells for specific and effective targeting of glioblastoma. *Sci Transl Med* **12** (2020).
30. June, C.H., O'Connor, R.S., Kawalekar, O.U., Ghassemi, S. & Milone, M.C. CAR T cell immunotherapy for human cancer. *Science* **359**, 1361-1365 (2018).
31. Majzner, R.G. & Mackall, C.L. Clinical lessons learned from the first leg of the CAR T cell journey. *Nat Med* **25**, 1341-1355 (2019).
32. Schuster, S.J. et al. Tisagenlecleucel in Adult Relapsed or Refractory Diffuse Large B-Cell Lymphoma. *N Engl J Med* **380**, 45-56 (2019).
33. Schuster, S.J. et al. Chimeric Antigen Receptor T Cells in Refractory B-Cell Lymphomas. *N Engl J Med* **377**, 2545-2554 (2017).
34. Maude, S.L. et al. Tisagenlecleucel in Children and Young Adults with B-Cell Lymphoblastic Leukemia. *N Engl J Med* **378**, 439-448 (2018).
35. Johnson, L.A. et al. Gene therapy with human and mouse T-cell receptors mediates cancer regression and targets normal tissues expressing cognate antigen. *Blood* **114**, 535-546 (2009).
36. Parkhurst, M.R. et al. T cells targeting carcinoembryonic antigen can mediate regression of metastatic colorectal cancer but induce severe transient colitis. *Mol Ther* **19**, 620-626 (2011).
37. Morgan, R.A. et al. Case report of a serious adverse event following the administration of T cells transduced with a chimeric antigen receptor recognizing ERBB2. *Mol Ther* **18**, 843-851 (2010).
38. Ali, S.A. et al. T cells expressing an anti-B-cell maturation antigen chimeric antigen receptor cause remissions of multiple myeloma. *Blood* **128**, 1688-1700 (2016).
39. Cameron, B.J. et al. Identification of a Titin-derived HLA-A1-presented peptide as a cross-reactive target for engineered MAGE A3-directed T cells. *Sci Transl Med* **5**, 197ra103 (2013).
40. Morgan, R.A. et al. Cancer regression and neurological toxicity following anti-MAGE-A3 TCR gene therapy. *J Immunother* **36**, 133-151 (2013).

41. Liu, X. et al. Affinity-Tuned ErbB2 or EGFR Chimeric Antigen Receptor T Cells Exhibit an Increased Therapeutic Index against Tumors in Mice. *Cancer Res* **75**, 3596-3607 (2015).
42. Chmielewski, M., Hombach, A., Heuser, C., Adams, G.P. & Abken, H. T cell activation by antibody-like immunoreceptors: increase in affinity of the single-chain fragment domain above threshold does not increase T cell activation against antigen-positive target cells but decreases selectivity. *J Immunol* **173**, 7647-7653 (2004).
43. Gan, H.K., Kaye, A.H. & Luwor, R.B. The EGFRvIII variant in glioblastoma multiforme. *J Clin Neurosci* **16**, 748-754 (2009).
44. O'Rourke, D.M. et al. A single dose of peripherally infused EGFRvIII-directed CAR T cells mediates antigen loss and induces adaptive resistance in patients with recurrent glioblastoma. *Sci Transl Med* **9** (2017).
45. Fischer, J. et al. CD19 Isoforms Enabling Resistance to CART-19 Immunotherapy Are Expressed in B-ALL Patients at Initial Diagnosis. *J Immunother* **40**, 187-195 (2017).
46. Sotillo, E. et al. Convergence of Acquired Mutations and Alternative Splicing of CD19 Enables Resistance to CART-19 Immunotherapy. *Cancer Discov* **5**, 1282-1295 (2015).
47. Gardner, R. et al. Acquisition of a CD19-negative myeloid phenotype allows immune escape of MLL-rearranged B-ALL from CD19 CAR-T-cell therapy. *Blood* **127**, 2406-2410 (2016).
48. Zah, E., Lin, M.Y., Silva-Benedict, A., Jensen, M.C. & Chen, Y.Y. T Cells Expressing CD19/CD20 Bispecific Chimeric Antigen Receptors Prevent Antigen Escape by Malignant B Cells. *Cancer Immunol Res* **4**, 498-508 (2016).
49. Martyniszyn, A., Krahl, A.C., Andre, M.C., Hombach, A.A. & Abken, H. CD20-CD19 Bispecific CAR T Cells for the Treatment of B-Cell Malignancies. *Hum Gene Ther* **28**, 1147-1157 (2017).
50. Motz, G.T. & Coukos, G. Deciphering and reversing tumor immune suppression. *Immunity* **39**, 61-73 (2013).
51. Pivarcsi, A. et al. Tumor immune escape by the loss of homeostatic chemokine expression. *Proc Natl Acad Sci U S A* **104**, 19055-19060 (2007).
52. Molon, B. et al. Chemokine nitration prevents intratumoral infiltration of antigen-specific T cells. *J Exp Med* **208**, 1949-1962 (2011).
53. Bouzin, C., Brouet, A., De Vriese, J., Dewever, J. & Feron, O. Effects of vascular endothelial growth factor on the lymphocyte-endothelium interactions:

- identification of caveolin-1 and nitric oxide as control points of endothelial cell energy. *J Immunol* **178**, 1505-1511 (2007).
54. Buckanovich, R.J. et al. Endothelin B receptor mediates the endothelial barrier to T cell homing to tumors and disables immune therapy. *Nat Med* **14**, 28-36 (2008).
  55. Brown, C.E. et al. Regression of Glioblastoma after Chimeric Antigen Receptor T-Cell Therapy. *N Engl J Med* **375**, 2561-2569 (2016).
  56. Murad, J.P. et al. Effective Targeting of TAG72(+) Peritoneal Ovarian Tumors via Regional Delivery of CAR-Engineered T Cells. *Front Immunol* **9**, 2268 (2018).
  57. Priceman, S.J. et al. Regional Delivery of Chimeric Antigen Receptor-Engineered T Cells Effectively Targets HER2(+) Breast Cancer Metastasis to the Brain. *Clin Cancer Res* **24**, 95-105 (2018).
  58. Proost, P. et al. Proteolytic processing of CXCL11 by CD13/aminopeptidase N impairs CXCR3 and CXCR7 binding and signaling and reduces lymphocyte and endothelial cell migration. *Blood* **110**, 37-44 (2007).
  59. Russell, S.J. & Barber, G.N. Oncolytic Viruses as Antigen-Agnostic Cancer Vaccines. *Cancer Cell* **33**, 599-605 (2018).
  60. Flavell, R.A., Sanjabi, S., Wrzesinski, S.H. & Licona-Limon, P. The polarization of immune cells in the tumour environment by TGFbeta. *Nat Rev Immunol* **10**, 554-567 (2010).
  61. Rabinovich, G.A., Gabrilovich, D. & Sotomayor, E.M. Immunosuppressive strategies that are mediated by tumor cells. *Annu Rev Immunol* **25**, 267-296 (2007).
  62. Munn, D.H. & Mellor, A.L. IDO and tolerance to tumors. *Trends Mol Med* **10**, 15-18 (2004).
  63. Weissleder, R. & Pittet, M.J. The expanding landscape of inflammatory cells affecting cancer therapy. *Nat Biomed Eng* **4**, 489-498 (2020).
  64. Sata, M. & Walsh, K. TNFalpha regulation of Fas ligand expression on the vascular endothelium modulates leukocyte extravasation. *Nat Med* **4**, 415-420 (1998).
  65. Whiteside, T.L. Tumor-induced death of immune cells: its mechanisms and consequences. *Semin Cancer Biol* **12**, 43-50 (2002).
  66. Hamanishi, J. et al. Programmed cell death 1 ligand 1 and tumor-infiltrating CD8+ T lymphocytes are prognostic factors of human ovarian cancer. *Proc Natl Acad Sci U S A* **104**, 3360-3365 (2007).

67. Ren, X. et al. Involvement of cellular death in TRAIL/DR5-dependent suppression induced by CD4(+)CD25(+) regulatory T cells. *Cell Death Differ* **14**, 2076-2084 (2007).
68. Wang, L.C. et al. Targeting fibroblast activation protein in tumor stroma with chimeric antigen receptor T cells can inhibit tumor growth and augment host immunity without severe toxicity. *Cancer Immunol Res* **2**, 154-166 (2014).
69. Tran, E. et al. Immune targeting of fibroblast activation protein triggers recognition of multipotent bone marrow stromal cells and cachexia. *J Exp Med* **210**, 1125-1135 (2013).
70. Long, A.H. et al. Reduction of MDSCs with All-trans Retinoic Acid Improves CAR Therapy Efficacy for Sarcomas. *Cancer Immunol Res* **4**, 869-880 (2016).
71. Munn, D.H. & Mellor, A.L. The tumor-draining lymph node as an immune-privileged site. *Immunol Rev* **213**, 146-158 (2006).
72. Weiden, J., Tel, J. & Figdor, C.G. Synthetic immune niches for cancer immunotherapy. *Nat Rev Immunol* **18**, 212-219 (2018).
73. Ribas, A. & Wolchok, J.D. Cancer immunotherapy using checkpoint blockade. *Science* **359**, 1350-1355 (2018).
74. Waldmann, T.A. The biology of interleukin-2 and interleukin-15: implications for cancer therapy and vaccine design. *Nat Rev Immunol* **6**, 595-601 (2006).
75. Rosenberg, S.A. Interleukin-2 and the development of immunotherapy for the treatment of patients with cancer. *Cancer J Sci Am* **6 Suppl 1**, S2-7 (2000).
76. Rosenberg, S.A. et al. Treatment of 283 consecutive patients with metastatic melanoma or renal cell cancer using high-dose bolus interleukin 2. *JAMA* **271**, 907-913 (1994).
77. Klebanoff, C.A. et al. IL-15 enhances the in vivo antitumor activity of tumor-reactive CD8+ T cells. *Proc Natl Acad Sci U S A* **101**, 1969-1974 (2004).
78. Robinson, T.O. & Schluns, K.S. The potential and promise of IL-15 in immunoncogenic therapies. *Immunol Lett* **190**, 159-168 (2017).
79. Alexandrov, L.B. et al. Signatures of mutational processes in human cancer. *Nature* **500**, 415-421 (2013).
80. Priestley, P. et al. Pan-cancer whole-genome analyses of metastatic solid tumours. *Nature* **575**, 210-216 (2019).
81. Baeuerle, P.A., Kufer, P. & Bargou, R. BiTE: Teaching antibodies to engage T-cells for cancer therapy. *Curr Opin Mol Ther* **11**, 22-30 (2009).

82. McLane, L.M., Abdel-Hakeem, M.S. & Wherry, E.J. CD8 T Cell Exhaustion During Chronic Viral Infection and Cancer. *Annu Rev Immunol* **37**, 457-495 (2019).
83. Fuller, M.J. & Zajac, A.J. Ablation of CD8 and CD4 T cell responses by high viral loads. *J Immunol* **170**, 477-486 (2003).
84. Wherry, E.J., Blattman, J.N., Murali-Krishna, K., van der Most, R. & Ahmed, R. Viral persistence alters CD8 T-cell immunodominance and tissue distribution and results in distinct stages of functional impairment. *J Virol* **77**, 4911-4927 (2003).
85. Fuller, M.J., Khanolkar, A., Tebo, A.E. & Zajac, A.J. Maintenance, loss, and resurgence of T cell responses during acute, protracted, and chronic viral infections. *J Immunol* **172**, 4204-4214 (2004).
86. Zarour, H.M. Reversing T-cell Dysfunction and Exhaustion in Cancer. *Clin Cancer Res* **22**, 1856-1864 (2016).
87. Pauken, K.E. et al. Epigenetic stability of exhausted T cells limits durability of reinvigoration by PD-1 blockade. *Science* **354**, 1160-1165 (2016).
88. Sen, D.R. et al. The epigenetic landscape of T cell exhaustion. *Science* **354**, 1165-1169 (2016).
89. Busch, D.H., Frassle, S.P., Sommermeyer, D., Buchholz, V.R. & Riddell, S.R. Role of memory T cell subsets for adoptive immunotherapy. *Semin Immunol* **28**, 28-34 (2016).
90. Wang, X. et al. Phase 1 studies of central memory-derived CD19 CAR T-cell therapy following autologous HSCT in patients with B-cell NHL. *Blood* **127**, 2980-2990 (2016).
91. Wang, X. et al. Phenotypic and functional attributes of lentivirus-modified CD19-specific human CD8<sup>+</sup> central memory T cells manufactured at clinical scale. *J Immunother* **35**, 689-701 (2012).
92. Sabatino, M. et al. Generation of clinical-grade CD19-specific CAR-modified CD8<sup>+</sup> memory stem cells for the treatment of human B-cell malignancies. *Blood* **128**, 519-528 (2016).
93. Xu, Y. et al. Closely related T-memory stem cells correlate with in vivo expansion of CAR-CD19-T cells and are preserved by IL-7 and IL-15. *Blood* **123**, 3750-3759 (2014).
94. Weber, E.W. et al. Pharmacologic control of CAR-T cell function using dasatinib. *Blood Adv* **3**, 711-717 (2019).
95. Mestermann, K. et al. The tyrosine kinase inhibitor dasatinib acts as a pharmacologic on/off switch for CAR T cells. *Sci Transl Med* **11** (2019).

96. Rosenberg, S.A., Yang, J.C. & Restifo, N.P. Cancer immunotherapy: moving beyond current vaccines. *Nat Med* **10**, 909-915 (2004).
97. Klebanoff, C.A., Acquavella, N., Yu, Z. & Restifo, N.P. Therapeutic cancer vaccines: are we there yet? *Immunol Rev* **239**, 27-44 (2011).
98. Gu, L. & Mooney, D.J. Biomaterials and emerging anticancer therapeutics: engineering the microenvironment. *Nat Rev Cancer* **16**, 56-66 (2016).
99. Wang, H. & Mooney, D.J. Biomaterial-assisted targeted modulation of immune cells in cancer treatment. *Nat Mater* **17**, 761-772 (2018).
100. Ali, O.A., Emerich, D., Dranoff, G. & Mooney, D.J. In situ regulation of DC subsets and T cells mediates tumor regression in mice. *Sci Transl Med* **1**, 8ra19 (2009).
101. Kim, J. et al. Injectable, spontaneously assembling, inorganic scaffolds modulate immune cells in vivo and increase vaccine efficacy. *Nat Biotechnol* **33**, 64-72 (2015).
102. Singh, A., Suri, S. & Roy, K. In-situ crosslinking hydrogels for combinatorial delivery of chemokines and siRNA-DNA carrying microparticles to dendritic cells. *Biomaterials* **30**, 5187-5200 (2009).
103. Hori, Y., Stern, P.J., Hynes, R.O. & Irvine, D.J. Engulfing tumors with synthetic extracellular matrices for cancer immunotherapy. *Biomaterials* **30**, 6757-6767 (2009).
104. Hori, Y., Winans, A.M., Huang, C.C., Horrigan, E.M. & Irvine, D.J. Injectable dendritic cell-carrying alginate gels for immunization and immunotherapy. *Biomaterials* **29**, 3671-3682 (2008).
105. Hori, Y., Winans, A.M. & Irvine, D.J. Modular injectable matrices based on alginate solution/microsphere mixtures that gel in situ and co-deliver immunomodulatory factors. *Acta Biomater* **5**, 969-982 (2009).
106. Smith, T.T. et al. Biopolymers codelivering engineered T cells and STING agonists can eliminate heterogeneous tumors. *J Clin Invest* **127**, 2176-2191 (2017).
107. Stephan, S.B. et al. Biopolymer implants enhance the efficacy of adoptive T-cell therapy. *Nat Biotechnol* **33**, 97-101 (2015).
108. Stephan, M.T., Moon, J.J., Um, S.H., Bershteyn, A. & Irvine, D.J. Therapeutic cell engineering with surface-conjugated synthetic nanoparticles. *Nat Med* **16**, 1035-1041 (2010).
109. Tang, L. et al. Enhancing T cell therapy through TCR-signaling-responsive nanoparticle drug delivery. *Nat Biotechnol* **36**, 707-716 (2018).

110. Pickar-Oliver, A. & Gersbach, C.A. The next generation of CRISPR-Cas technologies and applications. *Nat Rev Mol Cell Biol* **20**, 490-507 (2019).
111. Liu, X. et al. CRISPR-Cas9-mediated multiplex gene editing in CAR-T cells. *Cell Res* **27**, 154-157 (2017).
112. Ren, J. et al. Multiplex Genome Editing to Generate Universal CAR T Cells Resistant to PD1 Inhibition. *Clin Cancer Res* **23**, 2255-2266 (2017).
113. Ren, J. et al. A versatile system for rapid multiplex genome-edited CAR T cell generation. *Oncotarget* **8**, 17002-17011 (2017).
114. Stadtmauer, E.A. et al. CRISPR-engineered T cells in patients with refractory cancer. *Science* **367** (2020).
115. Bendle, G.M. et al. Lethal graft-versus-host disease in mouse models of T cell receptor gene therapy. *Nat Med* **16**, 565-570, 561p following 570 (2010).
116. Provasi, E. et al. Editing T cell specificity towards leukemia by zinc finger nucleases and lentiviral gene transfer. *Nat Med* **18**, 807-815 (2012).
117. Schober, K. et al. Orthotopic replacement of T-cell receptor alpha- and beta-chains with preservation of near-physiological T-cell function. *Nat Biomed Eng* **3**, 974-984 (2019).
118. Fraietta, J.A. et al. Disruption of TET2 promotes the therapeutic efficacy of CD19-targeted T cells. *Nature* **558**, 307-312 (2018).
119. Zhou, P. et al. In vivo discovery of immunotherapy targets in the tumour microenvironment. *Nature* **506**, 52-57 (2014).
120. Araki, K. et al. mTOR regulates memory CD8 T-cell differentiation. *Nature* **460**, 108-112 (2009).
121. Pegram, H.J. et al. Tumor-targeted T cells modified to secrete IL-12 eradicate systemic tumors without need for prior conditioning. *Blood* **119**, 4133-4141 (2012).
122. Rafiq, S. et al. Targeted delivery of a PD-1-blocking scFv by CAR-T cells enhances anti-tumor efficacy in vivo. *Nat Biotechnol* **36**, 847-856 (2018).
123. Choi, B.D. et al. CAR-T cells secreting BiTEs circumvent antigen escape without detectable toxicity. *Nature Biotechnology* **37**, 1049-+ (2019).
124. Zhang, L. et al. Tumor-infiltrating lymphocytes genetically engineered with an inducible gene encoding interleukin-12 for the immunotherapy of metastatic melanoma. *Clin Cancer Res* **21**, 2278-2288 (2015).

125. Zimmermann, K. et al. Design and Characterization of an "All-in-One" Lentiviral Vector System Combining Constitutive Anti-GD2 CAR Expression and Inducible Cytokines. *Cancers (Basel)* **12** (2020).
126. Kunert, A. et al. Intra-tumoral production of IL18, but not IL12, by TCR-engineered T cells is non-toxic and counteracts immune evasion of solid tumors. *Oncoimmunology* **7**, e1378842 (2017).
127. Chang, Z.L. et al. Rewiring T-cell responses to soluble factors with chimeric antigen receptors. *Nat Chem Biol* **14**, 317-324 (2018).
128. Roybal, K.T. et al. Precision Tumor Recognition by T Cells With Combinatorial Antigen-Sensing Circuits. *Cell* **164**, 770-779 (2016).
129. Kloss, C.C., Condomines, M., Cartellieri, M., Bachmann, M. & Sadelain, M. Combinatorial antigen recognition with balanced signaling promotes selective tumor eradication by engineered T cells. *Nat Biotechnol* **31**, 71-75 (2013).
130. Srivastava, S. et al. Logic-Gated ROR1 Chimeric Antigen Receptor Expression Rescues T Cell-Mediated Toxicity to Normal Tissues and Enables Selective Tumor Targeting. *Cancer Cell* **35**, 489-503 e488 (2019).
131. Fedorov, V.D., Themeli, M. & Sadelain, M. PD-1- and CTLA-4-based inhibitory chimeric antigen receptors (iCARs) divert off-target immunotherapy responses. *Sci Transl Med* **5**, 215ra172 (2013).
132. Gamboa, L., Zamat, A.H. & Kwong, G.A. Synthetic immunity by remote control. *Theranostics* **10**, 3652-3667 (2020).
133. Bonifant, C.L., Jackson, H.J., Brentjens, R.J. & Curran, K.J. Toxicity and management in CAR T-cell therapy. *Mol Ther Oncolytics* **3**, 16011 (2016).
134. Brudno, J.N. & Kochenderfer, J.N. Recent advances in CAR T-cell toxicity: Mechanisms, manifestations and management. *Blood Rev* **34**, 45-55 (2019).
135. Gargett, T. & Brown, M.P. The inducible caspase-9 suicide gene system as a "safety switch" to limit on-target, off-tumor toxicities of chimeric antigen receptor T cells. *Front Pharmacol* **5**, 235 (2014).
136. Zhou, X. et al. Long-term outcome after haploidentical stem cell transplant and infusion of T cells expressing the inducible caspase 9 safety transgene. *Blood* **123**, 3895-3905 (2014).
137. Hoyos, V. et al. Engineering CD19-specific T lymphocytes with interleukin-15 and a suicide gene to enhance their anti-lymphoma/leukemia effects and safety. *Leukemia* **24**, 1160-1170 (2010).

138. Budde, L.E. et al. Combining a CD20 chimeric antigen receptor and an inducible caspase 9 suicide switch to improve the efficacy and safety of T cell adoptive immunotherapy for lymphoma. *PLoS One* **8**, e82742 (2013).
139. Wu, C.Y., Roybal, K.T., Puchner, E.M., Onuffer, J. & Lim, W.A. Remote control of therapeutic T cells through a small molecule-gated chimeric receptor. *Science* **350**, aab4077 (2015).
140. Fenno, L., Yizhar, O. & Deisseroth, K. The development and application of optogenetics. *Annu Rev Neurosci* **34**, 389-412 (2011).
141. Xu, Y. et al. Optogenetic control of chemokine receptor signal and T-cell migration. *Proc Natl Acad Sci U S A* **111**, 6371-6376 (2014).
142. Allen, M.E. et al. An AND-Gated Drug and Photoactivatable Cre-loxP System for Spatiotemporal Control in Cell-Based Therapeutics. *Acs Synth Biol* **8**, 2359-2371 (2019).
143. He, L. et al. Near-infrared photoactivatable control of Ca(2+) signaling and optogenetic immunomodulation. *Elife* **4** (2015).
144. Zhao, B. et al. An Optogenetic Controllable T Cell System for Hepatocellular Carcinoma Immunotherapy. *Theranostics* **9**, 1837-1850 (2019).
145. Tan, P., He, L., Han, G. & Zhou, Y. Optogenetic Immunomodulation: Shedding Light on Antitumor Immunity. *Trends Biotechnol* **35**, 215-226 (2017).
146. Chu, K.F. & Dupuy, D.E. Thermal ablation of tumours: biological mechanisms and advances in therapy. *Nat Rev Cancer* **14**, 199-208 (2014).
147. van Driel, W.J. et al. Hyperthermic Intraperitoneal Chemotherapy in Ovarian Cancer. *N Engl J Med* **378**, 230-240 (2018).
148. Partanen, A. et al. Mild hyperthermia with magnetic resonance-guided high-intensity focused ultrasound for applications in drug delivery. *Int J Hyperthermia* **28**, 320-336 (2012).
149. Mitchell, D. et al. A heterogeneous tissue model for treatment planning for magnetic resonance-guided laser interstitial thermal therapy. *Int J Hyperthermia* **34**, 943-952 (2018).
150. Medvid, R. et al. Current Applications of MRI-Guided Laser Interstitial Thermal Therapy in the Treatment of Brain Neoplasms and Epilepsy: A Radiologic and Neurosurgical Overview. *AJNR Am J Neuroradiol* **36**, 1998-2006 (2015).
151. Lubner, M.G., Brace, C.L., Hinshaw, J.L. & Lee, F.T., Jr. Microwave tumor ablation: mechanism of action, clinical results, and devices. *J Vasc Interv Radiol* **21**, S192-203 (2010).

152. Piraner, D.I., Abedi, M.H., Moser, B.A., Lee-Gosselin, A. & Shapiro, M.G. Tunable thermal bioswitches for in vivo control of microbial therapeutics. *Nat Chem Biol* **13**, 75-80 (2017).
153. Gardner, T.S., Cantor, C.R. & Collins, J.J. Construction of a genetic toggle switch in *Escherichia coli*. *Nature* **403**, 339-342 (2000).
154. Kortmann, J. & Narberhaus, F. Bacterial RNA thermometers: molecular zippers and switches. *Nat Rev Microbiol* **10**, 255-265 (2012).
155. Lindquist, S. The Heat-Shock Response. *Annu Rev Biochem* **55**, 1151-1191 (1986).
156. Richter, K., Haslbeck, M. & Buchner, J. The heat shock response: life on the verge of death. *Mol Cell* **40**, 253-266 (2010).
157. Andersson, H.A., Kim, Y.S., O'Neill, B.E., Shi, Z.Z. & Serda, R.E. HSP70 promoter-driven activation of gene expression for immunotherapy using gold nanorods and near infrared light. *Vaccines (Basel)* **2**, 216-227 (2014).
158. Deckers, R. et al. Image-guided, noninvasive, spatiotemporal control of gene expression. *Proc Natl Acad Sci U S A* **106**, 1175-1180 (2009).
159. Huang, Q. et al. Heat-induced gene expression as a novel targeted cancer gene therapy strategy. *Cancer Res* **60**, 3435-3439 (2000).
160. Siddiqui, F. et al. A phase I trial of hyperthermia-induced interleukin-12 gene therapy in spontaneously arising feline soft tissue sarcomas. *Mol Cancer Ther* **6**, 380-389 (2007).
161. Auslander, S. & Fussenegger, M. From gene switches to mammalian designer cells: present and future prospects. *Trends Biotechnol* **31**, 155-168 (2013).
162. Lienert, F., Lohmueller, J.J., Garg, A. & Silver, P.A. Synthetic biology in mammalian cells: next generation research tools and therapeutics. *Nat Rev Mol Cell Bio* **15**, 95-107 (2014).
163. Fenno, L., Yizhar, O. & Deisseroth, K. The Development and Application of Optogenetics. *Annu Rev Neurosci* **34**, 389-412 (2011).
164. Swartz, M.A., Hirosue, S. & Hubbell, J.A. Engineering approaches to immunotherapy. *Sci Transl Med* **4**, 148rv149 (2012).
165. Park, J.S. et al. Synthetic control of mammalian-cell motility by engineering chemotaxis to an orthogonal bioinert chemical signal. *Proc Natl Acad Sci U S A* **111**, 5896-5901 (2014).
166. Huang, B. et al. Active targeting of chemotherapy to disseminated tumors using nanoparticle-carrying T cells. *Sci Transl Med* **7**, 291ra294 (2015).

167. Jackson, H.J., Rafiq, S. & Brentjens, R.J. Driving CAR T-cells forward. *Nat Rev Clin Oncol* **13**, 370-383 (2016).
168. Murphy, A.G. & Zheng, L. Small molecule drugs with immunomodulatory effects in cancer. *Hum Vaccin Immunother* **11**, 2463-2468 (2015).
169. Kaehler, K.C. et al. Update on immunologic therapy with anti-CTLA-4 antibodies in melanoma: identification of clinical and biological response patterns, immune-related adverse events, and their management. *Semin Oncol* **37**, 485-498 (2010).
170. Fagnoni, F.F., Zerbini, A., Pelosi, G. & Missale, G. Combination of radiofrequency ablation and immunotherapy. *Front Biosci* **13**, 369-381 (2008).
171. Jain, P.K., Lee, K.S., El-Sayed, I.H. & El-Sayed, M.A. Calculated absorption and scattering properties of gold nanoparticles of different size, shape, and composition: applications in biological imaging and biomedicine. *J Phys Chem B* **110**, 7238-7248 (2006).
172. Haar, G.T. & Coussios, C. High intensity focused ultrasound: physical principles and devices. *Int J Hyperthermia* **23**, 89-104 (2007).
173. Sabel, M.S. Cryo-immunology: a review of the literature and proposed mechanisms for stimulatory versus suppressive immune responses. *Cryobiology* **58**, 1-11 (2009).
174. Wust, P. et al. Hyperthermia in combined treatment of cancer. *Lancet Oncol* **3**, 487-497 (2002).
175. Lindquist, S. The heat-shock response. *Annu Rev Biochem* **55**, 1151-1191 (1986).
176. Feder, M.E. & Hofmann, G.E. Heat-shock proteins, molecular chaperones, and the stress response: evolutionary and ecological physiology. *Annu Rev Physiol* **61**, 243-282 (1999).
177. Miyako, E. et al. Photothermic regulation of gene expression triggered by laser-induced carbon nanohorns. *Proc Natl Acad Sci U S A* **109**, 7523-7528 (2012).
178. Deguchi, T. et al. Infrared laser-mediated local gene induction in medaka, zebrafish and *Arabidopsis thaliana*. *Dev Growth Differ* **51**, 769-775 (2009).
179. Ramos, D.M., Kamal, F., Wimmer, E.A., Cartwright, A.N. & Monteiro, A. Temporal and spatial control of transgene expression using laser induction of the hsp70 promoter. *BMC Dev Biol* **6**, 55 (2006).
180. Jaque, D. et al. Nanoparticles for photothermal therapies. *Nanoscale* **6**, 9494-9530 (2014).

181. Akerfelt, M., Morimoto, R.I. & Sistonen, L. Heat shock factors: integrators of cell stress, development and lifespan. *Nat Rev Mol Cell Biol* **11**, 545-555 (2010).
182. Ramirez, V.P., Stamatis, M., Shmukler, A. & Aneskievich, B.J. Basal and stress-inducible expression of HSPA6 in human keratinocytes is regulated by negative and positive promoter regions. *Cell Stress Chaperones* **20**, 95-107 (2015).
183. Hamajima, F., Hasegawa, T., Nakashima, I. & Isobe, K. Genomic cloning and promoter analysis of the GAHSP40 gene. *J Cell Biochem* **84**, 401-407 (2002).
184. von Maltzahn, G. et al. Nanoparticles that communicate in vivo to amplify tumour targeting. *Nat Mater* **10**, 545-552 (2011).
185. von Maltzahn, G. et al. Computationally guided photothermal tumor therapy using long-circulating gold nanorod antennas. *Cancer Res* **69**, 3892-3900 (2009).
186. Kim, P.S. & Ahmed, R. Features of responding T cells in cancer and chronic infection. *Curr Opin Immunol* **22**, 223-230 (2010).
187. Kregel, K.C. Heat shock proteins: modifying factors in physiological stress responses and acquired thermotolerance. *J Appl Physiol (1985)* **92**, 2177-2186 (2002).
188. Rabindran, S.K., Haroun, R.I., Clos, J., Wisniewski, J. & Wu, C. Regulation of heat shock factor trimer formation: role of a conserved leucine zipper. *Science* **259**, 230-234 (1993).
189. Clos, J. et al. Molecular cloning and expression of a hexameric Drosophila heat shock factor subject to negative regulation. *Cell* **63**, 1085-1097 (1990).
190. Hentze, N., Le Breton, L., Wiesner, J., Kempf, G. & Mayer, M.P. Molecular mechanism of thermosensory function of human heat shock transcription factor Hsf1. *Elife* **5** (2016).
191. Hensen, S.M., Heldens, L., van Genesen, S.T., Pruijn, G.J. & Lubsen, N.H. A delayed antioxidant response in heat-stressed cells expressing a non-DNA binding HSF1 mutant. *Cell Stress Chaperones* **18**, 455-473 (2013).
192. Heldens, L. et al. Co-chaperones are limiting in a depleted chaperone network. *Cell Mol Life Sci* **67**, 4035-4048 (2010).
193. Neef, D.W., Jaeger, A.M. & Thiele, D.J. Genetic selection for constitutively trimerized human HSF1 mutants identifies a role for coiled-coil motifs in DNA binding. *G3 (Bethesda)* **3**, 1315-1324 (2013).
194. Khlebtsov, N. & Dykman, L. Biodistribution and toxicity of engineered gold nanoparticles: a review of in vitro and in vivo studies. *Chem Soc Rev* **40**, 1647-1671 (2011).

195. Stephan, S.B. et al. Biopolymer implants enhance the efficacy of adoptive T-cell therapy. *Nature Biotechnology* **33**, 97-U277 (2015).
196. Jensen, M.C. & Riddell, S.R. Designing chimeric antigen receptors to effectively and safely target tumors. *Curr Opin Immunol* **33**, 9-15 (2015).
197. Lim, W.A. & June, C.H. The Principles of Engineering Immune Cells to Treat Cancer. *Cell* **168**, 724-740 (2017).
198. Weber, E.W., Maus, M.V. & Mackall, C.L. The Emerging Landscape of Immune Cell Therapies. *Cell* **181**, 46-62 (2020).
199. John, L.B. et al. Anti-PD-1 antibody therapy potently enhances the eradication of established tumors by gene-modified T cells. *Clin Cancer Res* **19**, 5636-5646 (2013).
200. John, L.B., Kershaw, M.H. & Darcy, P.K. Blockade of PD-1 immunosuppression boosts CAR T-cell therapy. *Oncoimmunology* **2**, e26286 (2013).
201. Slaney, C.Y., Wang, P., Darcy, P.K. & Kershaw, M.H. CARs versus BiTEs: A Comparison between T Cell-Redirection Strategies for Cancer Treatment. *Cancer Discov* **8**, 924-934 (2018).
202. Amin, J., Ananthan, J. & Voellmy, R. Key features of heat shock regulatory elements. *Mol Cell Biol* **8**, 3761-3769 (1988).
203. Sakurai, H. & Enoki, Y. Novel aspects of heat shock factors: DNA recognition, chromatin modulation and gene expression. *FEBS J* **277**, 4140-4149 (2010).
204. Jaeger, A.M., Makley, L.N., Gestwicki, J.E. & Thiele, D.J. Genomic heat shock element sequences drive cooperative human heat shock factor 1 DNA binding and selectivity. *J Biol Chem* **289**, 30459-30469 (2014).
205. Whitlock, N.A., Agarwal, N., Ma, J.X. & Crosson, C.E. Hsp27 upregulation by HIF-1 signaling offers protection against retinal ischemia in rats. *Invest Ophthalmol Vis Sci* **46**, 1092-1098 (2005).
206. Wu, B.J., Kingston, R.E. & Morimoto, R.I. Human HSP70 promoter contains at least two distinct regulatory domains. *Proc Natl Acad Sci U S A* **83**, 629-633 (1986).
207. Kalmar, B. & Greensmith, L. Induction of heat shock proteins for protection against oxidative stress. *Adv Drug Deliv Rev* **61**, 310-318 (2009).
208. Vilaboa, N.E. et al. cAMP increasing agents prevent the stimulation of heat-shock protein 70 (HSP70) gene expression by cadmium chloride in human myeloid cell lines. *J Cell Sci* **108** ( Pt 8), 2877-2883 (1995).

209. Xu, Q., Schett, G., Li, C., Hu, Y. & Wick, G. Mechanical stress-induced heat shock protein 70 expression in vascular smooth muscle cells is regulated by Rac and Ras small G proteins but not mitogen-activated protein kinases. *Circ Res* **86**, 1122-1128 (2000).
210. Kadonaga, J.T. Perspectives on the RNA polymerase II core promoter. *Wiley Interdiscip Rev Dev Biol* **1**, 40-51 (2012).
211. Flanagan, S.W., Ryan, A.J., Gisolfi, C.V. & Moseley, P.L. Tissue-specific HSP70 response in animals undergoing heat stress. *Am J Physiol* **268**, R28-32 (1995).
212. Klaassen, C.D., Liu, J. & Diwan, B.A. Metallothionein protection of cadmium toxicity. *Toxicol Appl Pharm* **238**, 215-220 (2009).
213. Safran, M. et al. Mouse model for noninvasive imaging of HIF prolyl hydroxylase activity: Assessment of an oral agent that stimulates erythropoietin production. *P Natl Acad Sci USA* **103**, 105-110 (2006).
214. Lokmic, Z., Musyoka, J., Hewitson, T.D. & Darby, I.A. Hypoxia and hypoxia signaling in tissue repair and fibrosis. *Int Rev Cell Mol Biol* **296**, 139-185 (2012).
215. Daugaard, M., Rohde, M. & Jaattela, M. The heat shock protein 70 family: Highly homologous proteins with overlapping and distinct functions. *FEBS Lett* **581**, 3702-3710 (2007).
216. Yamaguchi, M., Ito, A., Ono, A., Kawabe, Y. & Kamihira, M. Heat-inducible gene expression system by applying alternating magnetic field to magnetic nanoparticles. *Acs Synth Biol* **3**, 273-279 (2014).
217. Yin, P.T. et al. Stem cell-based gene therapy activated using magnetic hyperthermia to enhance the treatment of cancer. *Biomaterials* **81**, 46-57 (2016).
218. Nakatsuji, H. et al. Surface chemistry for cytosolic gene delivery and photothermal transgene expression by gold nanorods. *Sci Rep* **7**, 4694 (2017).
219. Gamboa, L. et al. Heat-Triggered Remote Control of CRISPR-dCas9 for Tunable Transcriptional Modulation. *ACS Chem Biol* **15**, 533-542 (2020).
220. Munoz-Sanchez, J. & Chanez-Cardenas, M.E. The use of cobalt chloride as a chemical hypoxia model. *J Appl Toxicol* **39**, 556-570 (2019).
221. Fotakis, G., Cemeli, E., Anderson, D. & Timbrell, J.A. Cadmium chloride-induced DNA and lysosomal damage in a hepatoma cell line. *Toxicol In Vitro* **19**, 481-489 (2005).
222. Mitchell, R.J. & Gu, M.B. Construction and characterization of novel dual stress-responsive bacterial biosensors. *Biosens Bioelectron* **19**, 977-985 (2004).

223. Phuagkhaopong, S. et al. Cadmium-induced IL-6 and IL-8 expression and release from astrocytes are mediated by MAPK and NF-kappaB pathways. *Neurotoxicology* **60**, 82-91 (2017).
224. Ede, C., Chen, X., Lin, M.Y. & Chen, Y.Y. Quantitative Analyses of Core Promoters Enable Precise Engineering of Regulated Gene Expression in Mammalian Cells. *Acs Synth Biol* **5**, 395-404 (2016).
225. Hansen, J. et al. Transplantation of prokaryotic two-component signaling pathways into mammalian cells. *Proc Natl Acad Sci U S A* **111**, 15705-15710 (2014).
226. Elias, D. et al. Optimization of hyperthermic intraperitoneal chemotherapy with oxaliplatin plus irinotecan at 43 degrees C after complete cytoreductive surgery: mortality and morbidity in 106 consecutive patients. *Ann Surg Oncol* **14**, 1818-1824 (2007).
227. Yang, X.J. et al. Cytoreductive surgery and hyperthermic intraperitoneal chemotherapy improves survival of patients with peritoneal carcinomatosis from gastric cancer: final results of a phase III randomized clinical trial. *Ann Surg Oncol* **18**, 1575-1581 (2011).
228. Nikfarjam, M., Muralidharan, V. & Christophi, C. Mechanisms of focal heat destruction of liver tumors. *J Surg Res* **127**, 208-223 (2005).
229. Hellevik, T. & Martinez-Zubiaurre, I. Radiotherapy and the tumor stroma: the importance of dose and fractionation. *Front Oncol* **4**, 1 (2014).
230. Miller, I.C., Castro, M.G., Maenza, J., Weis, J.P. & Kwong, G.A. Remote Control of Mammalian Cells with Heat-Triggered Gene Switches and Photothermal Pulse Trains. *Acs Synth Biol* **7**, 1167-1173 (2018).
231. Mortier, E. et al. Soluble interleukin-15 receptor alpha (IL-15R alpha)-sushi as a selective and potent agonist of IL-15 action through IL-15R beta/gamma. Hyperagonist IL-15 x IL-15R alpha fusion proteins. *J Biol Chem* **281**, 1612-1619 (2006).
232. Rhode, P.R. et al. Comparison of the Superagonist Complex, ALT-803, to IL15 as Cancer Immunotherapeutics in Animal Models. *Cancer Immunol Res* **4**, 49-60 (2016).
233. Steinbacher, J. et al. An Fc-optimized NKG2D-immunoglobulin G fusion protein for induction of natural killer cell reactivity against leukemia. *Int J Cancer* **136**, 1073-1084 (2015).
234. Xia, Y. et al. Treatment with a fusion protein of the extracellular domains of NKG2D to IL-15 retards colon cancer growth in mice. *J Immunother* **37**, 257-266 (2014).

235. Godbersen, C. et al. NKG2D Ligand-Targeted Bispecific T-Cell Engagers Lead to Robust Antitumor Activity against Diverse Human Tumors. *Mol Cancer Ther* **16**, 1335-1346 (2017).
236. von Maltzahn, G. et al. Computationally Guided Photothermal Tumor Therapy Using Long-Circulating Gold Nanorod Antennas. *Cancer Research* **69**, 3892-3900 (2009).
237. Lienert, F., Lohmueller, J.J., Garg, A. & Silver, P.A. Synthetic biology in mammalian cells: next generation research tools and therapeutics. *Nat Rev Mol Cell Biol* **15**, 95-107 (2014).
238. Pan, Y. et al. Mechanogenetics for the remote and noninvasive control of cancer immunotherapy. *Proc Natl Acad Sci U S A* **115**, 992-997 (2018).
239. Evans, S.S., Repasky, E.A. & Fisher, D.T. Fever and the thermal regulation of immunity: the immune system feels the heat. *Nat Rev Immunol* **15**, 335-349 (2015).
240. Giavridis, T. et al. CAR T cell-induced cytokine release syndrome is mediated by macrophages and abated by IL-1 blockade. *Nat Med* **24**, 731-738 (2018).
241. Norelli, M. et al. Monocyte-derived IL-1 and IL-6 are differentially required for cytokine-release syndrome and neurotoxicity due to CAR T cells. *Nat Med* **24**, 739-748 (2018).
242. Bevilacqua, A., Fiorenza, M.T. & Mangia, F. A developmentally regulated GAGA box-binding factor and Sp1 are required for transcription of the hsp70.1 gene at the onset of mouse zygotic genome activation. *Development* **127**, 1541-1551 (2000).
243. Gaestel, M., Gotthardt, R. & Muller, T. Structure and organisation of a murine gene encoding small heat-shock protein Hsp25. *Gene* **128**, 279-283 (1993).
244. Kroeger, P.E. & Morimoto, R.I. Selection of new HSF1 and HSF2 DNA-binding sites reveals difference in trimer cooperativity. *Mol Cell Biol* **14**, 7592-7603 (1994).
245. Ruella, M. & Kalos, M. Adoptive immunotherapy for cancer. *Immunol Rev* **257**, 14-38 (2014).
246. Ji, Y. et al. Identification of the genomic insertion site of Pmel-1 TCR alpha and beta transgenes by next-generation sequencing. *PLoS One* **9**, e96650 (2014).
247. Overwijk, W.W. et al. Tumor regression and autoimmunity after reversal of a functionally tolerant state of self-reactive CD8+ T cells. *J Exp Med* **198**, 569-580 (2003).
248. Shultz, L.D. et al. Human lymphoid and myeloid cell development in NOD/LtSz-scid IL2R gamma null mice engrafted with mobilized human hemopoietic stem cells. *J Immunol* **174**, 6477-6489 (2005).

249. Ishikawa, F. et al. Development of functional human blood and immune systems in NOD/SCID/IL2 receptor {gamma} chain(null) mice. *Blood* **106**, 1565-1573 (2005).


**Oncology Meets Immunology: The Cancer-Immunity Cycle**

Author: Daniel S. Chen, Ira Mellman  
 Publication: Immunity  
 Publisher: Elsevier  
 Date: 25 July 2013

Copyright © 2013 Elsevier Inc. All rights reserved.

**Order Completed**

Thank you for your order.

This Agreement between Ian Miller ("You") and Elsevier ("Elsevier") consists of your license details and the terms and conditions provided by Elsevier and Copyright Clearance Center.

Your confirmation email will contain your order number for future reference.

License Number: 4326780168037  
 License date: May 12, 2020

[Printable Details](#)

**Licensed Content**

Licensed Content Publisher: Elsevier  
 Licensed Content Publication: Immunity  
 Licensed Content Title: Oncology Meets Immunology: The Cancer-Immunity Cycle  
 Licensed Content Author: Daniel S. Chen, Ira Mellman  
 Licensed Content Date: Jul 25, 2013  
 Licensed Content Volume: 39  
 Licensed Content Issue: 1  
 Licensed Content Pages: 10  
 Journal Type: S&T

**Order Details**

Type of Use: reuse in a thesis/dissertation  
 Portion: figures/tables/illustrations  
 Number of figures/tables/illustrations: 1  
 Format: electronic  
 Are you the author of this Elsevier article?: No  
 Will you be translating?: No

**About Your Work**

Title: Remote control of CAR T cell Therapies by thermal targeting  
 Institution name: Georgia Institute of Technology  
 Expected presentation date: Aug 2020

**Additional Data**

Portions: Figure 1

**Requestor Location**

Requestor Location: Ian Miller  
 345 Farsi Dr  
 Room 3140  
 ATLANTA, GA 30332  
 United States  
 Attn: Ian Miller

**Tax Details**

Publisher Tax ID: 98-0297604

**Price**

Total: 0.00 USD

Permission for: Chen, D.S. & Mellman, I. Oncology meets immunology: the cancer-immunity cycle. *Immunity* **39**, 1-10 (2013).



**Adoptive cell transfer as personalized immunotherapy for human cancer**

Author: Steven A. Rosenberg, Nicholas P. Restifo  
 Publication: Science  
 Publisher: The American Association for the Advancement of Science  
 Date: Apr 3, 2015

Copyright © 2015, Copyright © 2015, American Association for the Advancement of Science

**Order Completed**

Thank you for your order.

This Agreement between Ian Miller ("You") and The American Association for the Advancement of Science ("The American Association for the Advancement of Science") consists of your license details and the terms and conditions provided by The American Association for the Advancement of Science and Copyright Clearance Center.

Your confirmation email will contain your order number for future reference.

License Number: 4841531450948 [Printable Details](#)

License date: Jun 03, 2020

**Licensed Content**

Licensed Content Publisher: The American Association for the Advancement of Science  
 Licensed Content Publication: Science  
 Licensed Content Title: Adoptive cell transfer as personalized immunotherapy for human cancer  
 Licensed Content Author: Steven A. Rosenberg, Nicholas P. Restifo  
 Licensed Content Date: Apr 3, 2015  
 Licensed Content Volume: 345  
 Licensed Content Issue: 6230

**Order Details**

Type of Use: Thesis / Dissertation  
 Requestor type: Scientist/individual at a research institution  
 Format: Electronic  
 Portion: Text Excerpt  
 Number of pages requested: 1

**About Your Work**

Title: Remote control of CAR T cell Therapies by thermal targeting  
 Institution name: Georgia Institute of Technology  
 Expected presentation date: Aug 2020

**Additional Data**

Portions: Figure 4

**Requestor Location**

Requestor Location: Ian Miller  
 345 First Dr  
 Room 3140  
 ATLANTA, GA 30332  
 United States  
 Attn: Ian Miller

**Tax Details**

## Remote Control of Mammalian Cells with Heat-Triggered Gene Switches and Photothermal Pulse Trains

Author: Ian C. Miller, Marielena Gamboa Castro, Joe Maenza, et al



Publication: ACS Synthetic Biology

Publisher: American Chemical Society

Date: Apr 1, 2018

Copyright © 2018, American Chemical Society

## PERMISSION/LICENSE IS GRANTED FOR YOUR ORDER AT NO CHARGE

This type of permission/license, instead of the standard Terms &amp; Conditions, is sent to you because no fee is being charged for your order. Please note the following:

- Permission is granted for your request in both print and electronic formats, and translations.
- If figures and/or tables were requested, they may be adapted or used in part.
- Please print this page for your records and send a copy of it to your publisher/graduate school.
- Appropriate credit for the requested material should be given as follows: "Reprinted (adapted) with permission from (COMPLETE REFERENCE CITATION). Copyright (YEAR) American Chemical Society." Insert appropriate information in place of the capitalized words.
- One-time permission is granted only for the use specified in your request. No additional uses are granted (such as derivative works or other editions). For any other uses, please submit a new request.

[BACK](#)[CLOSE WINDOW](#)

Permission for: Miller, I.C., Castro, M.G., Maenza, J., Weis, J.P. & Kwong, G.A. Remote Control of Mammalian Cells with Heat-Triggered Gene Switches and Photothermal Pulse Trains. *Acs Synth Biol* **7**, 1167-1173 (2018).



CAR T cell immunotherapy for human cancer

Author: Carl H. June,Roddy S. O'Connor,Omkar U. Kawalekar,Saba Ghassemi,Michael C. Milone  
Publication: Science  
Publisher: The American Association for the Advancement of Science  
Date: Mar 23, 2018

Copyright © 2018. Copyright © 2018 The Authors. Some rights reserved. Exclusive licensee American Association for the Advancement of Science. No claim to original U.S. Government Works. http://www.sciencemag.org/about/science-licenses/journal-article-reuse This is an article distributed under the terms of the Science Journals Default License.

Order Completed

Thank you for your order.

This Agreement between Ian Miller ("You") and The American Association for the Advancement of Science ("The American Association for the Advancement of Science") consists of your license details and the terms and conditions provided by The American Association for the Advancement of Science and Copyright Clearance Center.

Your confirmation email will contain your order number for future reference.

License Number 483439255714  
License date May 22, 2020

[Printable Details](#)

Licensed Content

Licensed Content Publisher The American Association for the Advancement of Science  
Licensed Content Publication Science  
Licensed Content Title CAR T cell immunotherapy for human cancer  
Licensed Content Author Carl H. June,Roddy S. O'Connor,Omkar U. Kawalekar,Saba Ghassemi,Michael C. Milone  
Licensed Content Date Mar 23, 2018  
Licensed Content Volume 359  
Licensed Content Issue 6382

Order Details

Type of Use Thesis / Dissertation  
Requestor type Scientist/individual at a research institution  
Format Electronic  
Portion Text Excerpt  
Number of pages requested 1

About Your Work

Title Remote control of CAR T cell Therapies by thermal targeting  
Institution name Georgia Institute of Technology  
Expected presentation date Aug 2020

Additional Data

Portions Figure 1.

Requestor Location

Requestor Location Ian Miller  
345 Ferst Dr  
Room 3140  
ATLANTA, GA 30332  
United States  
Attn: Ian Miller

Tax Details

Price

Total 0.00 USD

Permission for June, C.H., O'Connor, R.S., Kawalekar, O.U., Ghassemi, S. & Milone, M.C. CAR T cell immunotherapy for human cancer. *Science* **359**, 1361-1365 (2018).

# Curriculum Vitae

## Education

---

**Georgia Institute of Technology and Emory University**      *Fall 2014 – Summer 2020*  
Atlanta, GA  
*PhD in Biomedical Engineering (expected Summer 2020)*  
*Technology Innovation: Generating Economic Results (TI:GER) certificate, Scheller College of Business*

**Furman University**, Greenville, SC      *Fall 2010 – Spring 2014*  
*B.S. in Chemistry, Magna Cum Laude*  
*Alden Pre-Engineering scholarship (Full tuition for 6 semesters, 1 in class of 700)*

## Research Accomplishments

---

### Biomedical Engineering PhD – Georgia Institute of Technology

*PhD Thesis: Remote Thermal Control of Adoptive T Cell Therapies*

- Developed synthetic gene switches that exhibit sharp increases in transcriptional activity following mild hyperthermia (40–42 °C) yet eliminate cross-activation by non-thermal cues observed with natural heat shock promoters (e.g. by hypoxia or heavy metal toxins)
- Integrated thermal gene switches into CAR-encoding plasmids to control expression of immunostimulatory genes such as cytokine superagonists and Bispecific T Cell Engagers (BiTEs) by engineered T cells
- Assessed activity of heat-triggered genes with activation, proliferation, cytotoxicity, and cytokine secretion assays
- Demonstrated that targeted heat treatments enable local control of intratumoral T cell activity leading to eradication of tumors in preclinical models
- Investigated pulsed thermal treatments or dose fractionation to improve cellular viability and gene switch activity compared to continual heating regimens
- Efforts have resulted in two journal publications with another manuscript currently under review
- Worked with patent attorneys and Georgia Tech Technology Licensing Office to file patent protecting method for remote control of engineered cell activity using thermal cues (PCT/US18/53962)
- Established cross-disciplinary collaborations with laboratories specializing in drug delivery and cell therapy manufacturing resulting in a high-impact journal publication

**Knowledge Areas:** Design of synthetic gene circuits, genetic editing of primary human T cells, mammalian cell culture, adoptive transfer of engineered T cells in murine models, and cancer immunotherapy

**Skills:** Cloning of synthetic gene switches; lentiviral production and transduction of primary human T cells; flow cytometry (11-color); qRT-PCR; ELISA; *in vivo* imaging (IVIS); murine necropsy (tumor, spleen, lymph node harvest); i.p., s.c., and i.v., injections; assays for cellular viability migration, cytotoxicity and proliferation

**Software:** Adobe Illustrator, FlowJo, FACSDiva, GraphPad, Microsoft Office

## **Awards and Honors**

---

- Biomedical Engineering Travel Award 2016, 2019
- College of Engineering Travel Award 2016, 2019
- Student Government Association Travel Award 2016, 2019
- Petit Scholars Mentor, Petit Institute for Bioengineering and Bioscience 2015, 2019
- TI:GER Fellow, Scheller College of Business 2017 – 2018
- Honorable mention – National Science Foundation Graduate Research Fellowship Program 2016
- Graduated *magna cum laude*, Furman University 2014
- Keeler Chemistry Scholarship, Departmental Scholarship 2014
- Alden Pre-Engineering Scholar, Institutional Scholarship 2010 - 2013

## **Leadership Experience**

---

**Team Leader, Technological Innovation: Generating Economic Results (TI:GER) Program** 2017 – 2018

*Joint program between Georgia Tech's College of Business and Emory University's School of Law*

- Assembled and managed team of two Emory JD and three Georgia Tech MBA students to examine process of commercializing PhD project on thermal control of CAR T cells
- Conducted interviews with oncologists, FDA representatives, patent attorneys, entrepreneurs, and employees of biotechnology companies to understand interests of stake holders in the translational process
- Deliverables: prior art search, freedom to operate analysis, industry analysis, business plan

**Mentor, Petit Research Scholars and Laboratory for Synthetic Immunity** 2015 - 2020

*Competitive program matching talented undergraduates with research mentors for 12 months*

- Trained three undergraduate students to independently clone, culture mammalian cells, and perform experiments related to T cell cytotoxicity, viability, proliferation, etc.

- Managed and directed research goals for all three mentees for a minimum of two years
- Two mentees were selected for selective Petit Scholars program and chose to extend research commitments until graduation once the program ended

## Publications

---

- **Miller, I. C.**, Sun, L., et al. Remote control of CAR T cell therapies by thermal targeting. *Under review*. Pre-print bioRxiv doi:10.1101/2020.04.26.062703.
- Tadros, A., Romanyuk, A., **Miller, I.C.**, et al. STAR particles for enhanced topical delivery of drugs to skin. *Nat. Med.*, 2020, 26, 341-347.
- Gamboa, L., Phung, E.V., Li, H., Meyers, J.P., Hart, A., **Miller, I.C.**, Kwong, G.A. Heat-triggered remote control of CRISPR-dCas9 for tunable transcriptional modulation. *ACS Chem. Biol.*, 2020, 15, 2, 533-542.
- **Miller, I. C.**, et al. Remote control of mammalian cells with heat-triggered gene switches and photothermal pulse trains. *ACS Synth. Biol.*, 2018, 7, 1167–1173.
- Petty, J. T., Giri, B., **Miller, I. C.**, et al. Silver clusters as both chromophoric reporters and DNA ligands. *Anal. Chem.*, 2013, 85, 2183-2190.

## Patents

---

- Kwong, G. A., **Miller, I.C.**, Gamboa Castro, M. 2017. Remote control of engineered T cell therapies. International application No. PCT/US18/53962, filed October 2, 2018.

## Conference Abstracts and Presentations

---

- **Miller, I.C.**, et al., February, 2020. Thermal control of CAR T cell therapies. Keystone Symposia: Emerging Cellular Therapies, Banff, AB. (poster)
- **Miller, I.C.**, et al. October, 2019. Remote Control of CAR T Cells Using Thermal Cues. Biomedical Engineering Society Annual Meeting, Philadelphia, PA. (oral)
- **Miller, I.C.**, et al. October, 2019. Remote Control of Adoptive T cell Therapies. Fred Hutchinson Cancer Research Center Graduate Student Symposium, Seattle, WA. (oral)
- **Miller, I.C.**, et al., October, 2018. Remote Control of Engineered T Cells Using Photothermal Pulses. American Institute of Chemical Engineers Annual Meeting, Pittsburgh, PA. (oral)
- **Miller, I.C.**, et al., February, 2018. Engineering therapeutic T cells that activate by photothermal triggers. Career, Research, and Innovation Development Conference, Georgia Institute of Technology, Atlanta, GA. (poster)
- **Miller, I.C.**, et al., October, 2017. Engineering Therapeutic T Cells that Activate by Photothermal Triggers. Immunoengineering Seminar Series, Atlanta, GA. (oral)

- **Miller, I.C.**, et al. October, 2016. Engineering Therapeutic T cells that Activate by Photothermal Triggers. Biomedical Engineering Society Annual Meeting, Minneapolis, MN. (oral)
- **Miller, I.C.**, et al., November, 2012. Size Exclusion Chromatography Studies of Silver Clusters Conjugated with DNA. Southeast Regional Meeting of the American Chemical Society, Raleigh, NC. (poster)